

Climate change and migration: the case of Africa*

Bruno Conte[†]

October 2023

Abstract

How will future climate change affect rural economies like sub-Saharan Africa (SSA) in terms of migration and welfare losses? How can policy enhance SSA's capacity to adapt to this process? I answer these questions with a quantitative framework that, coupled with rich spatial data and forecasts for the future, estimates millions of climate migrants and sizeable and unequal welfare losses in SSA. Investigating migration and trade policies as mitigating tools, I find a trade-off associated with the former: reducing SSA migration barriers to the European Union (EU) standards eliminates aggregate welfare losses at the cost of more climate migration and high regional inequality. Reducing tariffs to the EU levels attenuates this cost.

Keywords: Climate change, migration, economic geography.

JEL Codes: O15, Q54, R12.

*I am indebted to my advisors Hannes Mueller and Dávid Nagy for their constant support, guidance, and patience. I am also thankful to Gabriel Ahlfeldt, Clare Balboni, Paula Bustos, Donald Davis, Klaus Desmet, Remi Jedwab, Gabriel Kreindler, David Lagakos, Ishan Nath, Heitor Pellegrina, Giacomo Ponzetto, Esteban Rossi-Hansberg, Silvia Sarpietro, Sebastian Sotelo, Jaume Ventura, Giulio Zanella, and Yanos Zylberberg for useful comments and rich discussions along different stages of this project. Audiences at numerous seminars and conferences provided valuable feedback, to which I am also grateful. Julie Albigot provided excellent research assistance. All errors are my own.

[†]Università di Bologna and CESifo. Email: b.conte@unibo.it. Web: brunoconteleite.github.io.

1 Introduction

One of the most concerning potential consequences of climate change is population displacement, recently coined as the *Great Climate Migration* (Lustgarten, 2020). Subsistence rural economies, like the sub-Saharan African (SSA henceforth) countries, lie at the center of this issue. They are agriculture-dependent economies whose populations are expected to increase remarkably during the next decades (United Nations and Social Affairs, 2019). Understanding how these rural economies would adjust to a climate-changing world, with potentially different crop yields, is crucial for identifying how this growing population will reallocate geographically.

Assessing the potential decisions of SSA economic agents when adapting to climate change is challenging. Changing agricultural yields could lead farmers to switch production towards alternative crops, yet remaining in the agricultural sector. Alternatively, they could sort out of agriculture, potentially moving geographically. Trade frictions would determine how much specialization between agriculture and non-agriculture is feasible. Migration barriers would discipline the capacity of factors to reallocate geographically, potentially limiting sectoral reallocation. Understanding how these forces (production switching, trade, and migration) respond to climate change is key to evaluating its impact on the economy.

In this paper, I develop a spatial model that accounts for these forces and can be used to quantify how their response to climate change translates into migration and welfare losses. I link the model to a rich, high-resolution spatial dataset that I assemble, covering 42 countries of SSA. By simulating it for a future scenario by the end of the century, I estimate the aggregate and distributional impacts of climate change in terms of migration flows, welfare losses, and sectoral and spatial reallocation of production. I also show that trade and migration are important for adaptation, and investigate the mitigating capacity of real-world trade and migration policies.

I begin my analysis with three empirical facts on SSA's exposure to future changes in the climate and the margins and frictions for economic adaptation. The first documents that the expected impacts in SSA agriculture will be heterogeneous across space and, within locations, heterogeneous across crops. Hence, local producers could respond to this uneven shock by switching production across crops and sectors. The second fact argues that trade barriers would limit this margin, documenting a weaker degree of sectoral specialization in trade than specialization in production across countries in the SSA economy. Then, I establish a third, novel fact on migration as another margin, showing that past changes in the climate positively correlate with internal and international migration flows in the past decades in SSA, though limited by geographical mobility barriers.

Informed by this evidence, I develop a multi-sector spatial model that accommodates these mechanisms and frictions in general equilibrium. In the model, trade and migration between locations are costly. In each location, farmers produce goods from multiple agricultural sectors (crops) and firms produce non-agricultural goods. Differences in sectoral total factor productivities and market access across locations generate trade, shaping the spatial pattern of sectoral specialization. Relative sectoral prices and real income determine sectoral expenditure shares, generating endogenous structural transformation through substitution and income effects.¹

My framework takes the perspective of subnational locations, so that trade and migration happen both within and across countries in SSA.² The intensity of the spatial frictions depends primarily on the distance between locations over the transportation network. However, they are also determined by country-level institutional factors. In particular, frictions for international trade are subject to tariffs. Likewise, international migration is subject to an additional mobility cost related to barriers to foreign migrants at the destination country. Therefore, I map my setting into real-world trade and migration policies, which allows me to investigate their role on the resulting climate change effects and the efficiency of alternative policy schemes.

To quantify the model, I assemble a high-resolution spatial dataset on, among others, population, transportation infrastructure, international trade, crop prices, internal and international migration, and agricultural production and suitability in SSA. Following [Costinot et al. \(2016\)](#), I model climate change as a shock to the suitability for growing crops. In practice, I draw on the [GAEZ \(IIASA and FAO, 2012\)](#) estimates of crop-specific potential yields for several grain crops in recent, past, and future (under IPCC's business-as-usual scenario for climate change) periods. These potential yields reflect only local natural characteristics (e.g. topographic and climatic) and thus provide a measure of geographical natural advantages for growing a specific crop.^{3,4}

I link the data to my model in three steps. First, I use the potential yields for 2000 as the fundamental productivity of crops. Second, I use transportation data to build an optimal trade network between all location pairs in SSA. Third, I quantify the remaining fundamentals and parameters, like sectoral productivities, amenities, migration costs, and trade frictions, by embedding standard quantification methods

¹I model preferences over agricultural and non-agricultural goods as nonhomothetic and assume the former to be a necessity (subsistence) good. Thus, my model features key aspects of structural change; in particular a downward sloping demand for agricultural goods with respect to income.

²I do not consider migration and trade with the rest of the world in my baseline because about 75% of international migrants from SSA by the early 21st century moved within the continent. However, I extend my setting by adding trade and migration with the rest of the world in Section 6.4.

³Hereafter, I refer to these potential yields as fundamental productivities/advantages indistinctly.

⁴To focus on subsistence agriculture, I consider only the main staple crops produced and consumed in the region (cassava, maize, millet, rice, sorghum, and wheat; see Table D.2). They account for 80% of the agricultural production, as of 2000, and 50% of the caloric intake in SSA ([Porteous, 2019](#)).

for spatial models into a GMM estimation. The richness of my data is a crucial input in this step. For instance, I can carefully separate the role of tariffs and geographical distances when determining trade frictions by exploiting, respectively, variation from international trade flows and the spatial distribution of prices.⁵ The method I design for that is innovative relative to standard approaches, as it requires data on local prices rather than on spatial price wedges (as in [Donaldson, 2018](#)).

With the quantified model in hand, I perform a backcasting exercise that validates it. Using past crop suitabilities, I simulate the model back in time for 1975 and contrast the results with observable data. The model predicts well the grid cell-level changes in population between 2000 and 1975, reassuring its capacity to provide similar numbers for the future. An additional overidentification test shows that the model identifies closely the degree of specialization in agriculture across countries.

My main counterfactual exercise consists of simulating a climate-changed SSA by the end of the century. I draw the estimates for crop productivities in 2080 with climate change and simulate the model with them, keeping all other fundamentals unchanged.⁶ The results show that climate change displaces about 14 million individuals in SSA. Most of the climate migrants move out of the Western Sahel and DR Congo, regions severely hit by climate change, into nearby countries like South Africa or Tanzania. Damaged countries also experience large internal migration flows, and overall the population in country capitals increases. Importantly, the welfare effects, measured as changes in real income per capita, are small in aggregate terms.⁷ However, they are very heterogeneous across space: the bottom and top deciles of the welfare changes across countries are -10 and 3 percent, respectively, and some countries experience losses of up to 27 percent.

Analogously, climate change does not affect SSA aggregate sectoral employment, but does so in distributional terms. The median country increases agricultural employment by about one percentage point, and the distribution of sectoral employment changes is fairly skewed. This happens because I model crops to be subsistence goods. Thus, affected economies respond to the reduced crop yields by allocating more labor into that sector. Nonetheless, this effect is spatially heterogeneous, and the direction of sectoral specialization roughly follows the relative changes in sectoral productivity (i.e. affected countries specialize out of agriculture, and the opposite for the least damaged). Interestingly, however, the resulting welfare effects across countries go in several directions and depend on a rich interaction between the forces driving migra-

⁵Analogously, I carefully separate the role of geographical distances and national policies against migrants when determining migration costs (with, respectively, internal and international migration).

⁶These simulations also account for the estimated future population growth with fertility rates taken exogenously from data by demographers. I endogenize it as of robustness in [Section 6.4](#).

⁷[Section 6.3](#) shows the qualitative equivalence of the results if using alternative welfare measures.

tion, sectoral specialization, and trade.

I highlight the role of these forces with additional simulations centered on the main mechanisms of my framework. I start with bilateral migration frictions: eliminating them in the counterfactuals increases total climate migration to 87 million individuals, remarkably close to estimates from studies that disregard these barriers (e.g., 90 million from [Rigaud et al., 2018](#)). Moreover, welfare losses reverse in this frictionless setting (aggregate welfare increases by 8 percent). That happens because lower mobility barriers boost the push-aspect of climate change, reallocating labor out of unproductive rural regions and permitting a welfare-improving process of structural transformation. Importantly, these aggregate gains hide an underlying cost: the distribution of welfare changes across countries remains remarkably wide and skewed. Thus, reducing mobility frictions as a policy poses a trade-off of reverting aggregate losses at the expense of more climate migration and high regional inequality.

Next, I analogously investigate the role of two additional mechanisms: trade and crop-switching. For the former, I find that trade openness reduces migration and the inequality in the welfare changes by providing more room for sectoral specialization. For the latter, I show that the capacity of producers to reallocate production across crops is a crucial margin of adaptation for SSA farmers. Ignoring this margin overestimates the productivity and welfare losses of climate change by not considering that crop yields are differently affected within locations.

I close my investigation with a policy experiment that assesses the potential mitigating role of real-world migration and trade policies. I simulate a counterfactual scenario where migration and trade frictions in SSA drop to the levels of the European Union (EU). Doing so requires quantifying EU tariffs and country barriers to foreigners within the structure of the model (and using the result in the SSA simulations).⁸ Adopting the migration policy of the EU eliminates the aggregate welfare losses in SSA at the cost of more climate migration and high regional inequality. However, setting tariffs to EU levels on top of the migration policy attenuates that. In particular, the policy mix increases the efficiency of the allocation of factors across sectors and locations, which reduces welfare losses both in aggregate and distributional terms. This last result has important policy implications: by combining both tools, SSA policymakers would take advantage of the changes in the climate and allow the economy to structurally change, through trade and migration, in a less unequal manner.

This paper contributes to the current academic and policy research on future climate migration. Several policy institutions produced results to guide policymakers in this matter, such as the Pulitzer Center ([Lustgarten, 2020](#)) and the World Bank

⁸More specifically, I build a likewise rich spatial dataset for the EU in 2000. I then link it to my model (with the same quantification procedure), retrieve the EU policy-related parameters (tariffs and country barriers to foreigners), and use them in the SSA simulations. See section 6.3 for details.

(Rigaud et al., 2018). They use partial equilibrium frameworks that disregard several mechanisms of my framework, like migration barriers. Other studies are Benveniste et al. (2020) and Burzyński et al. (2022), who model migration responses to global warming and coastal flooding. I complement these studies by modeling the spatial links behind the adaptation decisions and providing policy-relevant results that are informative about the reach and interplay of migration and trade policies. Relatedly, by accounting for the general equilibrium forces driving future climate migration, I add to the rich empirical literature on the causal link between past climate shocks, migration, and urbanization in developing rural economies.⁹

I also contribute to the general equilibrium literature on the welfare benefits of reducing migration barriers in rural economies (Bryan et al., 2014; Pellegrina and Sotelo, 2021; Meghir et al., 2021; Lagakos et al., 2023) by investigating these gains in the context of adaptation to climate change. Moreover, my central finding on the aggregate versus inequality welfare trade-off associated with migration policy speaks to studies that infer heterogeneous effects of similar policies in developing economies (Bryan and Morten, 2019; Morten and Oliveira, 2018; Imbert et al., 2023). Besides, my findings on the attenuating role of trade policy (and the innovative method I propose to quantify trade frictions) enrich a large literature on the importance of market integration for development (Atkin and Donaldson, 2015; Donaldson, 2018; Asturias et al., 2019; Sotelo, 2020; Pellegrina, 2022; Nagy, 2023).

Lastly, I contribute to a literature that studies the consequences of climate change with quantitative spatial models (Redding and Rossi-Hansberg, 2017).¹⁰ My contribution is to incorporate, into a unified framework, a threefold set of features that are crucial to model climate migration in rural developing economies. First, by allowing for labor mobility within and across countries in Costinot et al. (2016)'s framework, I account for the cross-crop heterogeneity of the climate shock and show that this dimension matters for understanding the migration and welfare consequences of climate change in SSA. Second, I allow for the subsistence aspect of agriculture to limit structural change as adaptation, as in Nath (2022) and Cruz (2021), but show that migration is a margin that attenuates this issue. Third, I account for realistic trade and migration policies and show how they interact with sectoral specialization, structural change, and the aggregate and distributional welfare effects of climate change.¹¹

⁹These studies empirically estimate the causal link between past weather shocks and migration (e.g., Baez et al., 2017; Gröger and Zylberberg, 2016; Cai et al., 2016; Albert et al., 2021) and urbanization (e.g., Barrios et al., 2006; Castells-Quintana et al., 2021; Henderson et al., 2017) in SSA, Asia, and Latin America. Their results are informative about the strength of short-term climate shocks as a determinant of migration, but cannot be extrapolated for the understanding of future climate migration.

¹⁰This literature focuses on, among others, global warming (Desmet and Rossi-Hansberg, 2015, 2023; Conte et al., 2021, 2022; Cruz and Rossi-Hansberg, 2023; Bilal and Rossi-Hansberg, 2023; Rudik et al., 2021) and coastal flooding (Desmet et al., 2021; Balboni, 2021; Hsiao, 2022).

¹¹Naturally, there are aspects of this literature that my paper does not feature. One is endogenous cli-

The paper is organized as follows. Section 2 describes the main data sources, and Section 3 documents a number of empirical facts related to the potential impact of climate change on SSA economy. Section 4 presents the theoretical framework. Section 5 details quantification of the model, and Section 6 the results of the climate change counterfactuals, policy experiments, and robustness checks. Section 7 concludes.

2 Data

I collect and aggregate several sources of geographical data within $1^\circ \times 1^\circ$ grid cells (about 100 km^2 at the equator), the empirical unit of observation. The set of cells covering 42 countries of SSA contains 2,007 cells. The data sources, collection, and aggregation follow below; see Appendix A for details.

GDP. Grid cell-level data on GDP per capita in US\$ PPP (2000) comes from the Global Gridded Geographically Based Economic Data v4 (G-Econ, Nordhaus et al., 2006).

Population. The G-Econ database also provides the population count at the grid cell-level for 1990 and 2000, which is complemented with grid cell-level 1975 population data from the Global Human Settlement Project (GHSP, Florczyk et al., 2019). Finally, country-level projections for the future population at the end of the century were taken from United Nations and Social Affairs (2019).

Agricultural suitability. I construct a spatial and time-varying dataset of crop-specific suitabilities using the Food and Agriculture Organization’s Global Agro-Ecological Zones database (GAEZ, IASA and FAO, 2012). This data is generated by an agronomic model that combines geographic characteristics (e.g. soil, elevation, etc.) with yearly climatic conditions to produce high-resolution estimates of potential yields for different crops and periods.¹² I collect and aggregate the potential yields for the 6 crops of interest for 1975, 2000, and 2080.¹³

Agricultural production. Grid cell-level crop production comes from two sources: grid cell-level production data (in tonnes) for 2000 from GAEZ and country-level crop production (in current US\$) for 2000-2010 from FAO-STAT. I convert current US\$ to US\$ PPP using their ratio on the G-Econ data.

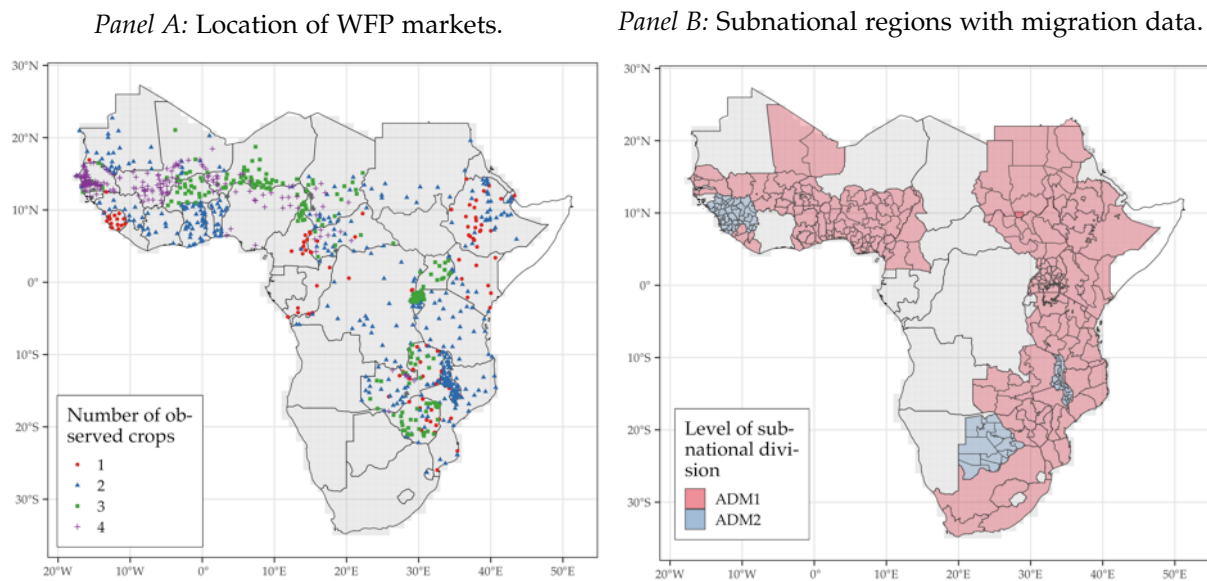
Crop prices. I retrieve spatially disaggregated crop price data from the Vulnerability Assessment and Mapping program of the World Food Programme (WFP-VAM),

mate, which is reasonable given the small SSA contribution to global emissions. Another is dynamics, whose absence is motivated by the static feature of the GAEZ data. Section 6.4 elaborates on that.

¹²These potential yields refer to the yield that a certain cell would obtain, on average, if its surface was fully devoted to a specific crop.

¹³The 2080 yields refer to a climate-changed world under the business-as-usual scenario RCP 8.5.

Figure 1: Spatial coverage of crop prices and internal (within-country) migration data



Notes: Panel A shows the locations (markets) with crop price data from the WFP-VAM project. Panel B shows the subnational locations with within-country migration data from [IPUMS \(2020\)](#).

which has been monitoring crop prices in more than 900 markets across SSA since the early 1990s. I focus on prices for maize, millet, sorghum, and rice – the crops with higher temporal and spatial coverage. Figure 1 Panel A shows the wide spatial coverage within and across countries of this data, as well as a rich within-market coverage of prices for different crops (i.e. many markets with data for more than one crop).

Transportation network. I build up a network connecting all grid cells of SSA by combining the Global Roads Open Access Data Set (gROADS, [CIESIN, 2013](#)) with the friction surface from the Accessibility to Cities project ([Weiss et al., 2018](#)).

Bilateral trade. I extract bilateral crop trade flows (in current US\$, scaled to PPP as above) between SSA country pairs from the International Trade and Production Database (ITPD-E, [Borchert et al., 2021](#)). It is a benchmark source of trade data due to its large geographical, sectoral, and temporal (2000 to 2016) coverage.

Internal and international migration flows. I obtain bilateral gross migration flows between SSA countries from [Abel and Cohen \(2019\)](#)'s database (a comprehensive source of migration data that covers about 200 countries and 25 years). Moreover, I built a matrix of internal (i.e. within countries) migration at the grid cell pair-level from census data (from [IPUMS, 2020](#)) by aggregating individual-level migration data at the subnational level for 24 countries and 40 years (since the 1970s to the early 21st century). Figure 1 Panel B shows the high coverage and granularity of this data, with migration between regional (ADM1) and provincial (ADM2) units.

3 Motivating facts

This section documents three facts about the potential impact of climate change in SSA. It establishes that (i) these effects are expected to be strong and heterogeneous and, as such, (ii) potentially determinant in the future organization of the SSA economy and (iii) future migration flows. Overall, these facts provide empirical support for the channels I embed in the model.

Fact 1: Climate change is expected to bring about substantial and spatially heterogeneous changes in agricultural suitability in SSA.

I use the GAEZ estimates of agro-climatic potential yields for 2000 and 2080 to show the expected degree of severity and heterogeneity in climate change's impact.¹⁴ I define ΔA_i^k as the changes in the yields of crop k (in tonnes/ha) in location (i.e. grid cell) i between the two periods, and ΔA_i as the average change within locations.

Panel A of Figure 2 illustrates the high level of heterogeneity in the average climate change shock to agricultural yields. In terms of levels, several locations will become less suitable for agriculture, with average yields declining by 3 tonnes/ha (50 percent of average yields) or more. However, other locations will become more suitable and to a similar extent. This finding contradicts a general view of climate change as a spatially homogeneous shock.

To illustrate the heterogeneity across crops, Panel B of Figure 2 documents the dispersion of climate change effects at the cell level (in standard deviations of ΔA_i^k). The changes in yields are not homogenous across crops, differentially shifting the relative ranking of crop suitabilities within cells. Hence, climate change will affect agricultural comparative advantages heterogeneously across both space and crops.

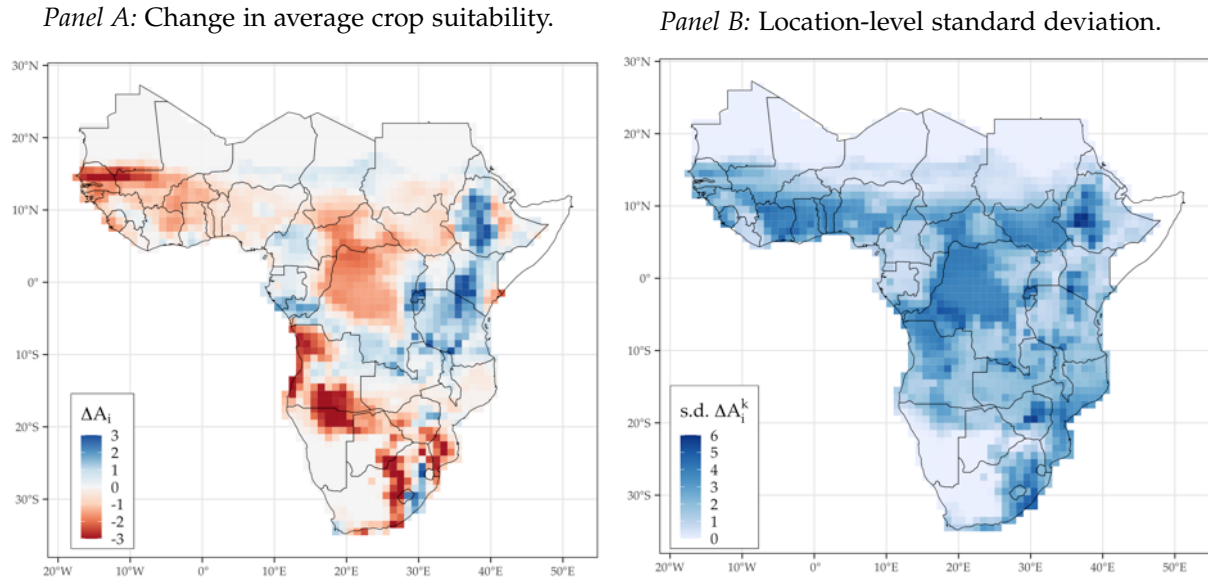
Thus, adjusting crop choices is a potential coping margin for affected farmers in SSA. However, the extent to which such Ricardian production adjustments can take place in SSA depends on the strength of these natural comparative advantages in shaping effective agricultural production. The next empirical fact provides evidence that such a mechanism indeed exists and emphasizes the importance of embedding it in my theoretical framework.

Fact 2: Natural crop suitability explains to a large degree the patterns of crop specialization across SSA, but not as much the trade patterns between countries.

Figure 3 Panel A documents a positive correlation between observed production and the GAEZ yields in 2000. It plots the linear fit of effective crop production on average crop yields at the country level, both in logs and net of crop and country fixed

¹⁴The 2080 GAEZ forecasts are calculated assuming a hypothetical scenario for the future evolution of the world's climate. Appendix A describes how I chose the scenario from which to draw the data in order that the results refer to the Representative Concentration Pathway (RCP) 8.5.

Figure 2: Expected impact of climate change on average crop yields (left) and the standard deviation of crop-yield changes (right) in SSA between 2000 and 2080



Notes: Panel A shows the level changes in average potential yields between 2000 and 2080. Panel B shows the standard deviation of the crop-level yield changes within cells. See Section 2 and Appendix A for details, and Figure B.5 for Panel A in relative changes.

effects. The strong, positive correlation (elasticity of 0.73) is evidence of specialization in production, with countries producing the crops that they are more suitable for.¹⁵

Furthermore, Panel A documents a weaker degree of specialization in trade: the slope of bilateral trade on exporter-importer relative yields is about 40 percent lower.¹⁶ Notably, this pattern remains if controlling for the distance between exporter-importer capitals (a component of trade costs; see Appendix D.1), suggesting that other resistance elements (e.g., tariffs) could be the reason for the weaker specialization in trade.

Hence, to align with these empirical patterns, my model will take the perspective of subnational locations (and countries) that specialize in (and trade, but costly) crops based on comparative advantage. As such, it will consider how climate change, in general equilibrium, will reshuffle production and trade in SSA in the next decades.

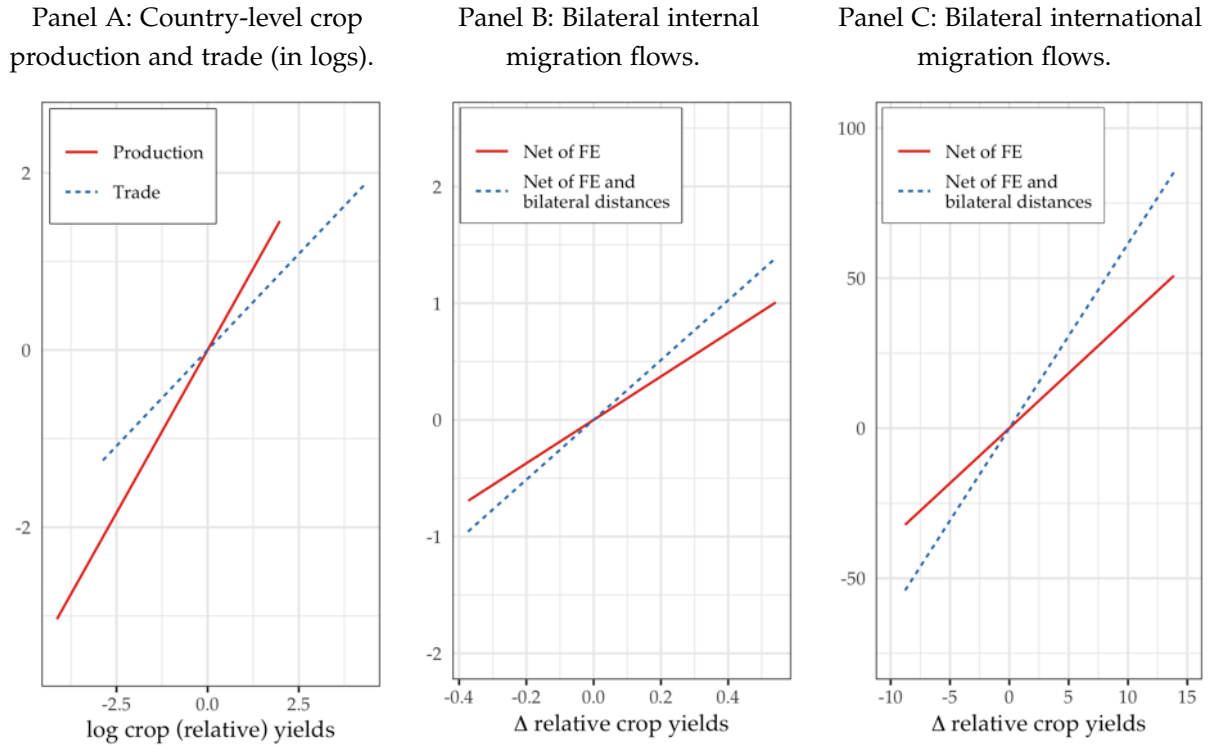
Fact 3: Changes in crop suitability positively correlate with past internal and international migration flows in SSA.

Panels B and C of Figure 3 show that changes in crop suitabilities between 1975 and 2000 explain migration choices, within and across countries, in SSA. For that, they plot the linear fit of bilateral migration flows on the change in the relative yields

¹⁵Appendix D.1 discusses more formally these correlations, documents the associated regression results, and documents additional facts, e.g., evidence for within-country specialization in production.

¹⁶The trade slope refers to the linear fit of bilateral crop trade on exporter-importer relative crop yields, in logs, and net of importer-exporter and crop fixed effects.

Figure 3: Comparative advantage and the organization of the SSA economy: relationship between crop yields (changes) and effective production, trade, and migration



Notes: Panel A plots, with the solid line, the correlation between GAEZ potential yields and country-level effective production from FAOSTAT. The dashed line plots the correlation between country-pair relative GAEZ potential yields and bilateral trade flows from ITPD-E. Panel B plots the correlation between internal (within-country) migration and changes in relative potential yields over time (and if controlling for bilateral distances). Panel C plots analogous correlations to B but for international migration (between countries). All the correlations shown are net of fixed effects that make cross-country (and cross-crop) relationships comparable; see appendix D.1 for details.

between subnational locations (i.e., regions or provinces) or countries.¹⁷ A positive relationship is evidence of relative yields as a push factor of migration over time, with larger bilateral flows for the pairs whose destination-origin relative yields increased.

This is the case for both internal and international migration. Moreover, this relationship is stronger for location pairs (subnational regions or countries) that are geographically closer: controlling for bilateral distances increases the estimated slopes for both types of migration flows. This shows that migration costs, like geographical distance, limited the capacity of agents migrating to locations that became relatively better off in the past decades. Hence, my model will incorporate these mobility barriers in general equilibrium, limiting the capacity of migration as an adaptation response to future climate change.

¹⁷The relative yield changes refer to the percentual changes, between 2000 and 1975, in the relative average yields between location pairs. Moreover, the migration flows refer to thousands of migrants between origin and destination per thousand population at the origin in 1975 (which is equivalent to controlling for the initial population at origin). See Appendix D.1 for details.

4 Model

This section presents a static quantitative spatial model that quantifies the general equilibrium impacts of future climate change. It provides a tractable framework to account for the role of geographical heterogeneity along several dimensions (i.e. sectoral productivities, market access, and migration barriers, among others) in determining the spatial distribution of economic activity and population.¹⁸

4.1 Environment

The economy S is composed by N locations, denoted by i, j , or s . Each i belongs to a country $c(i) \in \{1, \dots, C\}$, has a surface $H_i \in \{H_i\}_{i \in S} \equiv \mathcal{H}$, and is initially populated by $L_i^0 \in \{L_i^0\}_{i \in S} \equiv \mathcal{L}$ of workers who supply their labor inelastically. There are K sectors $k \in \{1, \dots, K\}$ in the economy: $K - 1$ crops and a non-agricultural composite K sector. Locations can produce a horizontally differentiated variety ω of each sector's goods. Each location has a sector-specific fundamental productivity $A_i^k \in \mathcal{A} = \{A_1^1, \dots, A_N^K\}$ that partially drives the degree of sectoral comparative advantage across space. Moreover, workers residing in i enjoy an amenity value $u_i \in \{u_i\}_{i \in S} \equiv \mathcal{U}$.

Goods and labor units are mobile in S , subject to frictions. In particular, $\mathcal{T} = \{\tau_{ij}\}_{i,j \in S}$ is the bilateral trade friction matrix where $\tau_{ij} = \tau_{ji} \geq 1$ is the iceberg cost of trading between i and j . Frictions migration depend on an analogous mobility cost $\bar{m}_{ij} \in \mathcal{M}$ and on an idiosyncratic taste shock to the migration choices of agents.

The geography of the economy is $\mathcal{G}(S) = \{\mathcal{L}, \mathcal{H}, \mathcal{A}, \mathcal{U}, \mathcal{T}, \mathcal{M}\}$: the set of spatial fundamentals that interact with the economic forces of the economy and determine the spatial distribution of the economic activity, explained next.

Technology and Market Structure. In every i , a continuum of firms produces an ω variety of sector k goods with labor $L_i^k(\omega)$ and land $H_i^k(\omega)$ in:

$$q_i^k(\omega) = z_i^k(\omega) \times L_i^k(\omega)^{\alpha_k} H_i^k(\omega)^{1-\alpha_k}, \text{ where} \quad (1)$$

$z_i^k(\omega)$ is a Hicks-neutral productivity shifter that firms draw independently from:

$$z_i^k(\omega) \sim F_i^k(\omega) = e^{-\omega^{-\xi_k} \times (b_i^k A_i^k)}. \quad (2)$$

F_i^k 's shape parameter ξ_k determines the dispersion of firms' productivity draws (hence, their ex-post heterogeneity) around the scale parameter $(b_i^k A_i^k)$. Thus, they depend on A_i^k (i.e., i 's fundamental characteristics) and b_i^k , a location-sector efficiency shifter that represents other determinants of firms' productivity (e.g. technology).

¹⁸Refer to Appendix B for further details and derivations of the model.

The output can be locally consumed or traded with other locations in a perfectly competitive, full information framework. Thus, the final price of the sector k variety ω produced in i and shipped to j is:

$$p_{ij}^k(\omega) = \left(\bar{c}^k w_i^{\alpha_k} r_i^{1-\alpha_k} / z_i^k(\omega) \right) \times \tau_{ij}, \quad (3)$$

where \bar{c}^k is a constant and w_i and r_i are factor prices (wages and land rents).

Preferences. Each location i is initially populated by a continuum of workers who decide where to live and how much to consume. In particular, a worker n initially living in location i who decides to migrate to j enjoys

$$U_{ij}(n) = C_j \times \bar{m}_{ij}^{-1} \times \varepsilon_j(n), \quad (4)$$

where C_j is the utility obtained from consumption in j , \bar{m}_{ij} is the mobility cost of migrating to j , and $\varepsilon_j(n)$ is a destination taste shock that disciplines workers' (ex-post) heterogeneous taste with respect to their preferred destination.

Consumption choice. Workers in a location j decide how much to consume of all possible ω varieties from all K sectors goods, $c_j^k(\omega)$. Their preferences feature love for varieties, which is modeled using a sectoral tier with CES $\eta_k > 1$:

$$C_j^k = \left(\int c_j^k(\omega)^{\frac{\eta_k-1}{\eta_k}} d\omega \right)^{\frac{\eta_k}{\eta_k-1}}. \quad (5)$$

Workers at j enjoy per capita income $v_j = w_j + r_j H_j / L_j$. Following [Eaton and Kortum \(2002\)](#), the share of j 's spending on sector k goods is:

$$\lambda_{ij}^k = b_i^k A_i^k \left(\Gamma^k \bar{c}^k w_i^{\alpha_k} r_i^{1-\alpha_k} \tau_{ij} / P_j^k \right)^{-\xi_k}, \text{ where} \quad (6)$$

$$P_j^k = \Gamma^k \left(\sum_{i \in \mathcal{S}} b_i^k A_i^k \left(\bar{c}^k w_i^{\alpha_k} r_i^{1-\alpha_k} \tau_{ij} \right)^{-\xi_k} \right)^{-1/\xi_k} \quad (7)$$

is the price index of sector k at j . Thus, workers expend a larger share on the cheapest suppliers (i.e., with the lowest price vis-à-vis sectoral price index P_j^k). ξ_k determines the extent to which this occurs, being the sectoral trade elasticity in the economy.

Worker choices across the $K - 1$ crops also feature love for varieties. All crop C_j^k composites are aggregated into the following agricultural CES tier:

$$C_j^a = \left(\sum_{k \neq K} \left(C_j^k \right)^{\frac{\gamma_a-1}{\gamma_a}} \right)^{\frac{\gamma_a}{\gamma_a-1}}. \quad (8)$$

$\gamma_a > 1$ is the CES between crops which drives their degree of substitutability. Hence, j 's share of expenditure on crop k relative to total crop expenditure is:

$$\Xi_j^k = (P_j^k / P_j^a)^{1-\gamma_a}, \text{ where} \quad (9)$$

$$P_j^a = \left(\sum_{k \neq K} (P_j^k)^{1-\gamma_a} \right)^{\frac{1}{1-\gamma_a}} \quad (10)$$

is the price index of the aggregate agricultural sector a . Therefore, workers substitute crops based on their relative prices. Larger values of γ_a imply more consumption of the locally cheapest crop and a stronger degree of specialization in crop consumption across locations.

Finally, the consumption choice between agricultural and non-agricultural goods is modeled with a further nonhomothetic CES tier in the spirit of [Comin et al. \(2021\)](#). In particular, the utility from consuming goods, C_j , is implicitly determined from:

$$\sum_{k \in \{a, K\}} \left(\Omega^k \right)^{1/\sigma} (C_j)^{\epsilon_k/\sigma} \left(C_j^k \right)^{(\sigma-1)/\sigma} = 1, \quad (11)$$

where $\sigma > 0$ is the CES between the a and K aggregate sectors, ϵ_k is their nonhomothetic elasticity of substitution, and Ω_k are sectoral preference shifters. Utility maximization implies that total consumption equals real income, $C_j = v_j / P_j$, and that aggregate price indexes and expenditure shares at j are respectively determined as:

$$P_j = \left(\sum_{k \in \{a, K\}} \left(\Omega^k (P_j^k)^{1-\sigma} \right)^{\frac{1-\sigma}{\epsilon_k}} \times \left(\mu_j^k v_j^{1-\sigma} \right)^{\frac{\epsilon_k - (1-\sigma)}{\epsilon_k}} \right)^{\frac{1}{1-\sigma}}, \text{ and} \quad (12)$$

$$\begin{aligned} \mu_j^k &= P_j^k C_j^k / v_j \\ &= \underbrace{\Omega^k \times \left(P_j^k / P_j \right)^{1-\sigma}}_{\text{substitution}} \times \underbrace{\left(v_j / P_j \right)^{\epsilon_k - (1-\sigma)}}_{\text{nonhomotheticity}} \quad \forall k \in \{a, K\}. \end{aligned} \quad (13)$$

Equation (13) shows that workers' choices between agricultural and non-agricultural goods are more complex than within agriculture. The reasons are two: first, it contains a substitution component analogous to eq. (9) that nevertheless permits a lower degree of substitutability between sectors ($\sigma < 1$). That makes it possible for changes in sectoral expenditures to be relatively lower (in magnitude) than the changes in relative prices. Second, it features a nonhomothetic component that maps changes in real income onto changes in sectoral expenditure shares – essentially, an income effect. The elasticities ϵ_k determine this relation: if $\epsilon_k < 1 - \sigma$, then sector k goods are a necessity whose expenditure decreases with income (and the opposite if $\epsilon_k > 1 - \sigma$).

Note that if $\epsilon_k = 1 - \sigma$ for all k , then the nonhomothetic component vanishes and eqs. (12) and (13) become isomorphic to eqs. (9) and (10).¹⁹

In equilibrium, j 's per capita demand for sector k goods produced in i is $\lambda_{ij}^k \Xi_j^k \mu_j^a v_j$ for crops and $\lambda_{ij}^K \mu_j^K v_j$ for the K^{th} sector. Hence, the total bilateral expenditure X_{ij} is:

$$\begin{aligned} X_{ij} &= \sum_{k \in \mathcal{K}} X_{ij}^k = \sum_{k \neq K} \lambda_{ij}^k \Xi_j^k \mu_j^a v_j L_j + \lambda_{ij}^K \mu_j^K v_j L_j \\ &= \sum_{k \neq K} b_i^k A_i^k \left(\Gamma^k \bar{c}^k w_i^{\alpha_k} r_i^{1-\alpha_k} \tau_{ij} / P_j^k \right)^{-\zeta_k} \left(\frac{P_j^k}{P_j^a} \right)^{1-\gamma_a} \Omega^a \left(\frac{P_j^a}{P_j} \right)^{1-\sigma} \left(\frac{v_j}{P_j} \right)^{\epsilon_a - (1-\sigma)} v_j L_j + \\ &+ b_i^K A_i^K \left(\Gamma^K \bar{c}^K w_i^{\alpha_K} r_i^{1-\alpha_K} \tau_{ij} / P_j^K \right)^{-\zeta_K} \Omega^K \left(\frac{P_j^K}{P_j} \right)^{1-\sigma} \left(\frac{v_j}{P_j} \right)^{\epsilon_K - (1-\sigma)} v_j L_j. \end{aligned} \quad (14)$$

Location choice. Workers choose where to live in order to maximize utility. In particular, worker n initially living in i chooses a destination j in order to solve:

$$\max_j U_{ij}(n) = (w_j / P_j) \times \bar{m}_{ij}^{-1} \times \varepsilon_j(n). \quad (15)$$

Therefore, workers will prefer locations with higher real income, although subject to the bilateral migration cost \bar{m}_{ij} and the destination taste shock $\varepsilon_j(n)$. Formally, the former is modeled as

$$\bar{m}_{ij} = m_{ij} \times m_{c(j)} \text{ if } c(i) \neq c(j), \text{ and } \bar{m}_{ij} = m_{ij} \text{ otherwise,} \quad (16)$$

where m_{ij} and $m_{c(j)} \geq 1$. Thus, mobility costs depend on m_{ij} (which accounts for bilateral characteristics like distance) and potentially $m_{c(j)}$. The latter matters only if the location choice requires workers to switch countries. Hence, it captures country-specific characteristics of destination j in terms of national barriers to foreigners.

I assume that the taste shock is drawn independently from an extreme-value distribution with shape parameter $\theta > 0$ and scale parameter $u_i(L_i / H_i)^{-\beta}$:

$$\varepsilon_j \sim G_j(z) = e^{-z^{-\theta} \times u_i(L_i / H_i)^{-\beta}}. \quad (17)$$

The parameter θ drives workers' heterogeneity with respect to their location tastes (and, to some extent, the dispersion forces in the economy). A higher θ makes agents more homogeneous and their location decisions more dependent on real income v_j / P_j . That drives down the dispersion forces in the economy. In contrast,

¹⁹Such a demand structure is required in order to account for the necessity (subsistence) aspect of agricultural goods when endogenizing sectoral shifts from agriculture to non-agriculture (i.e. structural change). This is what Gollin et al. (2007) refer to as the food problem and what Nath (2022) shows to be a limitation of structural change as a response to climate change. I discuss this further in Section 4.2.

a lower θ implies greater heterogeneity among agents who are more likely to draw higher values of taste shocks for every location. In that case, dispersion forces increase. Moreover, the scale parameter $u_i(L_i/H_i)^{-\beta}$ determines the average of the preference draws; u_j stands for the fundamental amenity of destination j ; and $\beta > 0$ determines the extent to which population density diminishes quality of life.

Analogously to eq. (2), the distributional assumption on taste preferences allows for a closed-form solution to the share of workers initially in i migrating to j :

$$\Pi_{ij} = \mathbb{P}\left(W_j(v) \geq \max\{W_s(v)\}_{s \neq j}\right) = \frac{(v_j/P_j)^\theta \bar{m}_{ij}^{-\theta} u_j (L_j/H_j)^{-\beta}}{\sum_{s \in S} (v_s/P_s)^\theta \bar{m}_{is}^{-\theta} u_s (L_s/H_s)^{-\beta}}. \quad (18)$$

Therefore, the total number of workers that choose to live in destination j is:

$$L_j = \sum_{i \in S} \Pi_{ij} \times L_i^0. \quad (19)$$

This is an intuitive result: locations with higher real income (v_j/P_j) and/or density-adjusted amenities $u_j(L_j/H_j)^{-\beta}$ will have a higher population in equilibrium. The magnitude of this effect is partially driven by θ , which is the elasticity of the location choice with respect to real income and to bilateral migration costs.

Spatial equilibrium. Given the geography $\mathcal{G}(S)$ and the exogenous parameters $\Theta \equiv \{\Omega_k, \eta_k, \gamma_a, \epsilon_k, \alpha_k, \xi_k, \sigma, \theta, \beta\}$, a spatial equilibrium is a vector of factor prices and labor allocations $\{w_j, r_j, L_j\}_{j \in S}$ such that eqs. (7), (10), (12) to (14) and (19) hold, and markets for goods clear. Formally, market clearing requires trade-balancing, such that each j 's income equals total exports to and total imports from all locations $i \in S$.²⁰

$$w_j L_j + r_j H_j = \sum_{i \in S} X_{ji} = \sum_{i \in S} X_{ij}. \quad (20)$$

4.2 Illustration and discussion of the underlying mechanisms

I illustrate how changes in the fundamentals shape the geographical distribution of economic activity and population by representing it as a line with a discrete number of locations. By doing so, I emphasize the effect of the model's underlying mechanisms on the agent's mobility decisions in response to a climate shock to the economy.

The locations $i \in \{1, \dots, N\}$ are distributed over a line and are homogeneous with respect to amenities, efficiency shifters, and initial population ($u_i = u$, $b_i^k = b$, and $L_i^0 = l \forall i, k$). The economy is composed of two countries, where the ten left-

²⁰Appendix B.3 documents the non-linear system of $7 \times N$ equations that characterize the spatial equilibrium, the iterative algorithm used to solve it, and aspects related to its existence and uniqueness.

most locations stand for country 1. I initially set $K = 2$, so that the agricultural a sector consists of one crop only. I assume that the distribution of sectoral fundamental productivities is increasing in the right-most locations and that every location is more productive in the K^{th} sector. I also set bilateral trade and mobility frictions to be proportional to the bilateral distances and make it costly to migrate to country 2. In terms of preferences, I assume that the agricultural crop is a necessity good and the opposite for the K^{th} sector. For simplicity, I disregard land \mathcal{H} .²¹

Panel A of Figure 4 plots the equilibrium distributions of $\{L_i^k\}$ as dashed lines (baseline). Overall, the economy produces more non-agricultural goods, which is the most productive sector. In distributional terms, the rightmost locations in each country have a higher level of economic activity and a larger population. The discontinuity at the country boundaries ($i = 10$) illustrates the role of country migration barriers (i.e. $m_2 > 1$). There is a higher population density on country 1's side due to the inability of workers to cross into country 2, where productivities and real wages are higher.

Subsequently, I simulate a climate shock by reducing country 1's crop productivities even further. The result is shown in Panel A of Figure 4 using solid lines (Δ). Country 1 changes its patterns of sectoral specialization by increasing its relative employment in agriculture. This is driven by the necessity aspect of agricultural goods. Climate change reduces crop productivity in country 1, which reacts by increasing agricultural employment so to produce the needed quantity of crops. This reduces real income in that country, increasing its share of expenditure on crops. Country 2, if anything, gets benefitted. Its population and non-agricultural employment increase due to the climate migrants from country 1.

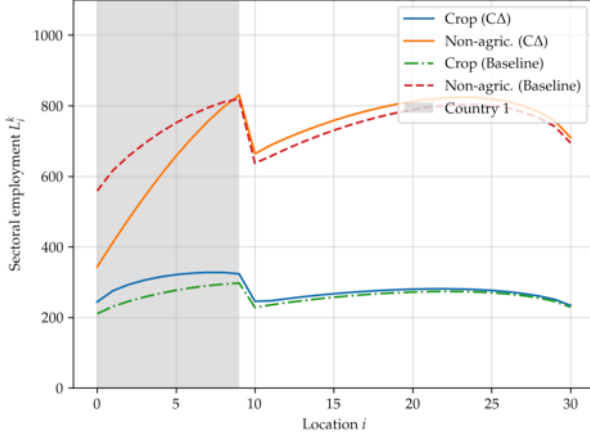
This simple exercise illustrates the limitations of structural transformation as a response to climate change. As rightly argued by Nath (2022), economies will switch production out of affected sectors only if capable of importing subsistence goods from unaffected regions. He refers to this as the food problem, inspired by previous studies of structural change and development (Gollin et al., 2007; Herrendorf et al., 2014). Panel B of Figure 4 provides further quantitative evidence of how this mechanism works in my model. When facing lower trade frictions, country 1 switches production out of agriculture, since it can now outsource crops from the nearest locations in country 2 (which shifts its production towards agriculture).

The novelty of my framework lies in the addition of two dimensions that further interact with the mentioned adaptation mechanisms. The first is migration barriers, whose role is illustrated in Panel C of Figure 4 (the climate change scenario without country migration barriers, i.e. $m_c = 1$ for all c). The results are intuitive: instead

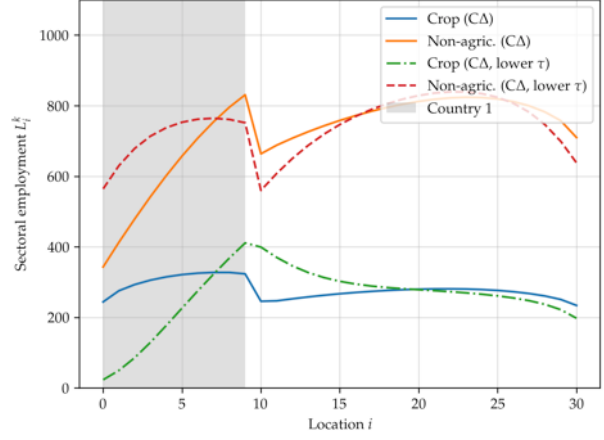
²¹That is, $\alpha_k = 1 \forall k$, $\epsilon_a < 1 - \sigma$ (and the opposite for $k = K = 2$), $m_1 = 1$, $m_2 = 1.5$, $\tau_{ij} = m_{ij} = e^{\tau \times |i-j|}$, and $A_i^k = a_k \times i$, where $\tau = 0.05$ and $a_2 > a_1$. See Appendix B.5 for details.

Figure 4: Equilibrium values of $\{L_i^1, L_i^2\}_{i \in S}$ for an economy represented on a line

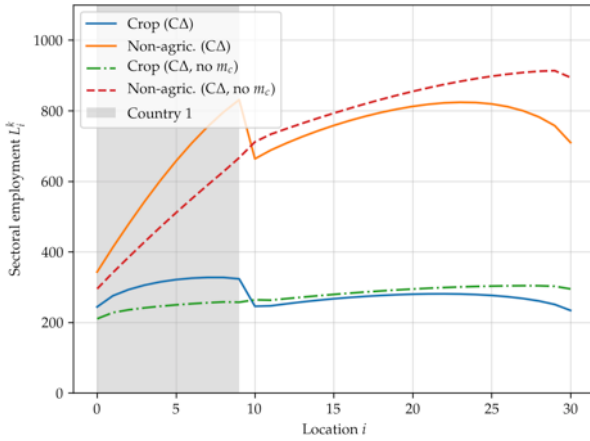
Panel A: Migration barriers, sectoral specialization, and CA.



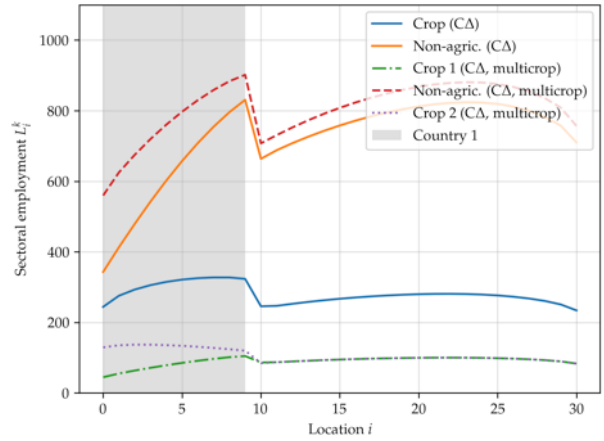
Panel B: CA, the food problem, and the role of trade frictions.



Panel C: CA and migration barriers.



Panel D: CA and crop switching.



Notes: Equilibrium labor allocations for the model described in Section 4.2. Panel A describes the equilibrium of the baseline and climate change simulations (country 1 becomes less suitable for crops). Panel B, C, and D plot the results of the climate change scenario with, respectively, lower trade frictions (a reduction in τ), no migration barriers between countries ($m_c = 1$ for all c) and multiple crops ($K = 3$).

of reacting to the food problem, workers in country 1 migrate to country 2. Overall, workers enjoy higher real wages and spend lower income shares on agricultural goods, making climate change less of a problem. Thus, migration can have a welfare-improving role as a response to climate change. It permits individuals to move out of unproductive rural regions, allowing for a more efficient sectoral spatial sorting of workers. This echoes the insights obtained from research on spatial structural change (Eckert and Peters, 2018) and on the gains from lowering migration barriers in rural economies (Bryan and Morten, 2019; Pellegrina and Sotelo, 2021; Lagakos et al., 2023).

The second additional dimension is the multi-crop aspect of the agricultural sector. Crops are partial substitutes as subsistence, and Section 3 shows that climate change is expected to alter their yields heterogeneously within locations. Thus, a potential

response of farmers in affected locations would be to switch production towards less-affected crops. The role of this margin is shown in Panel D of Figure 4. Dashed lines represent the outcomes of a simulation with two crops, where only crop 1 is affected in country 1. As a result, locations in that country switch production towards (unaffected) crop 2. This increases non-agricultural employment, real wages and welfare. Country 2 remains qualitatively unaffected, and overall the economy is better off relative to the one-crop scenario.

5 Bringing the model to the SSA data

I quantify the model to match SSA data by the early 21st century. To do so, I use a mix of quantification methods that map Θ and $\mathcal{G}(S)$ to observable features of SSA. Tables 1 and 2 document the methods and sources used, and Section 5.5 the results of overidentification tests that validate the calibrated model.²²

5.1 Parameters from the literature

I draw the values for $\{\eta_k, \gamma_a, \epsilon_k, \alpha_k, \zeta_k, \sigma, \theta, \beta\}$ from the related literature. I set the lower-tier CES as $\eta_k = 5.4$ for crops and $\eta_K = 4$ (as in Costinot et al., 2016; Desmet et al., 2018, respectively), and the mid-tier CES as $\gamma_a = 2.5$ as in Sotelo (2020). As for the upper-tier nonhomothetic CES, I follow Comin et al. (2021) and set $\sigma = 0.26$, $\epsilon_a = 0.2$, and $\epsilon_K = 1$. Therefore, agricultural goods in my framework are a necessity, as opposed to non-agricultural K goods. I obtain the factor shares $\alpha_k = 0.39$ and $\alpha_K = 0.58$ from Fajgelbaum and Redding (2022) and the trade elasticities $\zeta_k = 5.66$ and $\zeta_K = 6.63$ from Pellegrina (2022). Finally, I set $\theta = 3$ and $\beta = 0.32$ following Morten and Oliveira (2018) and Desmet et al. (2018), respectively.

5.2 Transportation and trade networks

I follow the related literature (e.g. Allen, 2014; Donaldson, 2018; Pellegrina, 2022) by assuming that trade frictions are proportional to the travel distance between locations:

$$\tau_{ij} = \text{distance}(i, j)^\delta \times \tau_{ij}^F, \quad (21)$$

where $\text{distance}(i, j)$ is the shortest distance between the location pair (in kilometers) and $\tau_{ij}^F \geq 1$ is an additional tariff-like trade friction. That is, $\tau_{ij}^F > 1$ only if $c(i) \neq c(j)$.

²²In addition, Appendix B.6 describes the data used and the numerical algorithms implemented, while Appendix B.8 discusses the implications of the parameter values drawn from the literature.

Table 1: Preference and technology parameters borrowed from the related literature

Parameters	Description	Source
<i>Panel A: Demand parameters</i>		
$\eta_k = 5.4$	Lower-tier CES ($k \neq K$, crops)	Costinot et al. (2016)
$\eta_K = 4$	Lower-tier CES (non-agriculture)	Desmet et al. (2018)
$\gamma_a = 2.5$	Mid-tier CES (across crops)	Sotelo (2020)
$\sigma = 0.26$	Upper-tier CES	Comin et al. (2021)
$\epsilon_a = 0.2$	Non-homothetic CES (agriculture)	Comin et al. (2021)
$\epsilon_K = 1$	Non-homothetic CES (non-agriculture)	Comin et al. (2021)
<i>Panel B: Supply parameters</i>		
$\zeta_k = 5.66$	Sectoral trade elasticity ($k \neq K$, crops)	Pellegrina (2022)
$\zeta_K = 6.63$	Sectoral trade elasticity (non-agriculture)	Pellegrina (2022)
$\alpha^k = 0.39$	Crop labor share ($k \neq K$)	Fajgelbaum and Redding (2022)
$\alpha^K = 0.58$	Non-agricultural labor share	Fajgelbaum and Redding (2022)
<i>Panel C: Location choice parameters</i>		
$\theta = 3$	Migration elasticity $\in [2, 4]$	Morten and Oliveira (2018)
$\beta = 0.32$	Congestion to population density	Desmet et al. (2018)

I retrieve $\text{distance}(i, j)$ for all location pairs by feeding the road network and friction surface data to a pathfinding algorithm that calculates the shortest routes and respective distances between all neighboring cells. Then, I use the Dijkstra algorithm to calculate the shortest distance between all pairs. Finally, I map these distances onto \mathcal{T} with a GMM that estimates $\delta = 0.168$ and $\tau_{ij}^F = 7.8$. This last step is done simultaneously with the calibration of other fundamentals, as explained in Section 5.3.

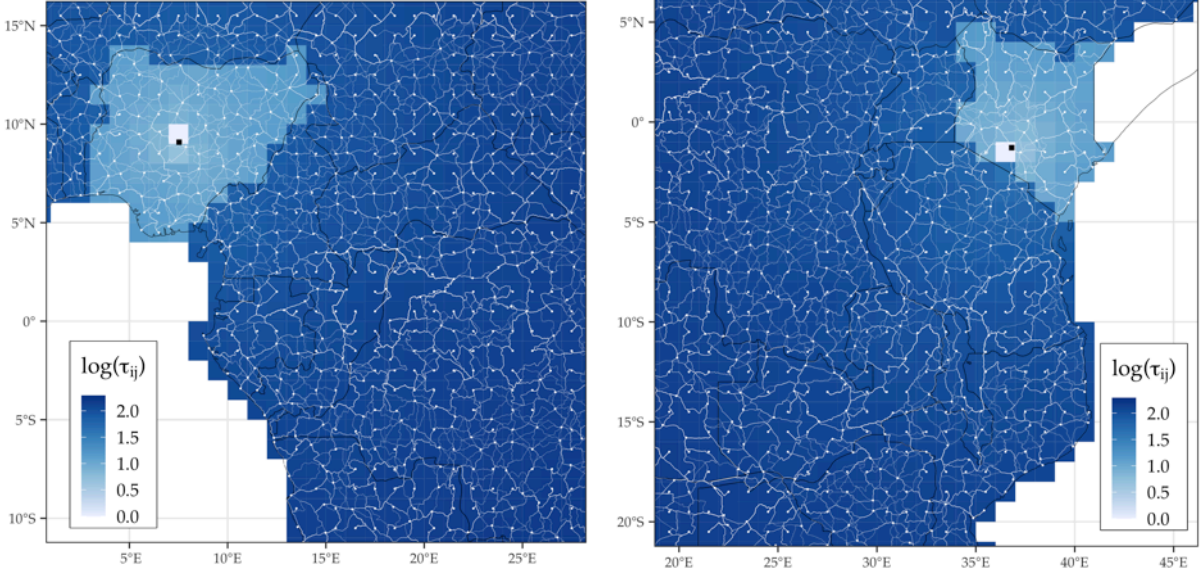
Figure 5 illustrates subsamples of the quantified \mathcal{T} . It shows the complexity of the trade network, which replicates well the existing transportation infrastructure both within and across countries. As expected, trade frictions increase with distance. Moreover, the discontinuity of the gradient is evidence of the additional cost of international trade captured by τ_{ij}^F .

5.3 Productivities, sectoral shifters, land endowments, and trade costs

The set of fundamentals and parameters $\{\mathcal{H}, \mathcal{A}, b_i^k, \Omega_k, \tau_{ij}^F, \delta\}_{i,j,k}$ are quantified as follows. First, I set \mathcal{H} as each cell's land area in square kilometers. Subsequently, I follow Costinot et al. (2016) and use the agro-climatic yields from GAEZ as the fundamental productivities of crops $\{A_i^k\}_{i \in S, k \neq K}$.²³ The underlying rationale is that the GAEZ data

²³To be consistent with the SSA rural context in 2000, I use the agro-climate potential yields calculated for rain-fed agriculture with low usage of modern inputs. See Appendix A for details.

Figure 5: Estimated trade network for SSA – Western and Eastern Africa



Notes: Notes: Estimated trade network for Western Africa (left) and Eastern Africa (right). The network is built by finding the shortest path between all neighboring cells over the road infrastructure. τ_{ij} represents the estimated iceberg trade costs with respect to the capital of Nigeria (left) and the capital of Kenya (right), both represented by a black dot. See Section 5.2 for details.

provides potential yields and is thus informative about the productivity variation across location-crops that is driven exclusively by differences in natural characteristics, including the climate. The variation in effective productivity across locations, conditional on the former, is embedded in $\{b_i^k\}_{i,k}$.

To quantify the remaining elements $\mathbf{t} \equiv \{\tau_{ij}^F, \delta\}$ and $\mathbf{T} \equiv \{\{A_i^K\}_i, \{b_i^k\}_{i,k}, \{\Omega_a, \Omega_K\}\}$, I implement a two-stage procedure. In the first stage (inner loop), I guess values for \mathbf{t} and quantify \mathbf{T} by inverting the general equilibrium conditions of the model. Then, the second stage (outer loop) estimates $\hat{\mathbf{t}}$ with a GMM that targets model-generated moments to their data counterparts conditional on the first stage. In what follows, I concisely describe this two-stage approach, leaving further details to Appendix B.6.

Model inversion (inner loop). This step calibrates \mathbf{T} by inverting the spatial equilibrium so that the model reproduces, in general equilibrium, the spatial distribution of GDP, the spatial distribution of sectoral production, and the relative a and K aggregate expenditure shares. I represent this solution of this inner loop, conditional on a guess for \mathbf{t} , as $z(\mathbf{T}; \mathbf{t}) = 0$.

Importantly, the model inversion identifies the product $\{b_i^K A_i^K\}_i$ (since its two elements cannot be separated), and pins down $\{b_i^k\}_{k \neq K}$ in relative terms within locations. Therefore, the latter is identified using within-crop variation in observed production across locations, conditional on the fundamental productivities of \mathcal{A} . The former,

conditional on the latter, is identified using spatial variation in GDP.

Estimation (outer loop). This step estimates \mathbf{t} with a GMM that exploits moments related to international trade flows and prices. Specifically, I design the first moment $m_1 = \sum_c \sum_{c'} \sum_{i \in c} \sum_{j \in c'} \sum_k X_{ij}^k$, that is, the aggregate exports between all country pairs in SSA. It provides variation to identify $\tau_{ij}^F = \tau^F$ given the (intuitive) decreasing relationship between tariffs and international trade flows in the economy.²⁴

Then, I take an innovative approach that identifies δ using spatial variation in crop prices. Rather than using bilateral price (wedges), as in the literature, I read my crop price data as sectoral prices P_i^k and use its dispersion to identify δ with $m_2 \equiv$ standard deviation(P_i^k).²⁵ Intuitively, the identification relies on the positive relationship between trade frictions and price dispersion: the lowest the former, the more homogeneous are price indexes across space (hence, less dispersion). Appendices B.6 and B.7 elaborate on identification aspects and discuss data-related aspects, such as the mapping between time-varying prices with the static framework of my model.

My approach is innovative for two reasons. First, it provides a novel method that quantifies bilateral trade costs with an empirical counterpart that is much more accessible (especially for developing economies): local prices rather than bilateral prices. Second, it pins down the differential role of geography (δ) and tariffs (τ^F) when determining trade costs, thus allowing for experiments along this dimension.

For the estimation, I define $\mathbf{m} = [m_1, m_2]$ and $g(\mathbf{t}) = [\mathbf{m}(\mathbf{t}) - \mathbf{m}^{\text{data}}]$ and solve for $\hat{\mathbf{t}}$ which, based on $\mathbb{E}[g(\mathbf{t})] = 0$, satisfies:

$$\hat{\mathbf{t}} = \arg \min_{\mathbf{t}} g(\mathbf{t})' W g(\mathbf{t}) \text{ subject to } z(\mathbf{T}; \mathbf{t}) = 0,$$

where W is the weighting matrix. The estimates $\hat{\mathbf{t}} = \{7.8, 0.168\}$ (with bootstrapped standard errors of $\{0.357, 0.012\}$) have meaningful economic implications. First, $\hat{\tau}^F = 7.8$ suggests barriers for international trade in SSA that are substantially larger than developed economies (such as $\tau^F = 2.375$ for the US from Antràs et al., 2022). Second, my δ estimate is about half of what Moneke (2020) estimates using only Ethiopian data. That stresses the importance of using cross-country data for continental-scale applications like mine: assuming a higher δ would underestimate $\hat{\tau}^F$.²⁶

²⁴In practice, m_1 is aggregated over the set of country-pair-crop combinations covered by the ITPD-E trade data. In fact, its relative sparsity (in terms of observed trade flows for SSA by the early 2000s) is the main reason behind the modeling of $\tau_{ij} = \tau^F$, that is, a common tariff for all country pairs in SSA.

²⁵I take this approach because the WFP-VAM data do not specify the location of production of the crops. Hence, it should not be interpreted as bilateral prices (as in, for instance, Donaldson, 2018), but rather as local crop prices in different locations in SSA (i.e., crop prices indexes as in Equation (7)).

²⁶My estimated trade costs lie also within other estimates that use different functional formats (e.g., Donaldson, 2018; Pellegrina, 2022, for India and Brazil, respectively); see Appendix B.9 for details.

Table 2: Quantified fundamentals and parameters, data sources, and matched moments

Fundamentals	Subset	Description	Data source / Moment matched
\mathcal{L}	-	SSA's initial population	Population data in 2000 and 1990
$\{b_i^k\}_{i \in S}$	-	Productivity shifters	Matched to location-sector production data
$\{\Omega_k\}_{a,K}$	$\Omega_a = 1$ $\Omega_K = .16$	Sectoral preference shifters	Matched to aggregate sectoral expenditure
\mathcal{H}	-	Land endowments	Grid cell land areas
\mathcal{A}	$\{A_i^k\}_{i \in S, k \neq K}$	Agricultural productivities	GAEZ data
	$\{A_i^K\}_{i \in S}$	Non-agricultural productivities	Matched to GDP data
\mathcal{U}	-	Amenities	Matched to population data
\mathcal{T}	dist(i,j)	Bilateral travel distance	Transportation data
	$\delta = 0.168$ (0.012)	Distance elasticity of τ	Matched to spatial dispersion of sectoral prices
	$\tau_{ij}^F = 7.8$ (0.357)	Tariff-like trade friction	Matched to aggregate trade flows
\mathcal{M}	dist(i,j)	Bilateral travel distance	Transportation data
	$\phi = 0.46$ (0.025)	Distance elasticity of m_{ij}	Matched to total internal migration (from census data)
	$\{m_c\}_{c=1}^C$	Country migration barriers	Matched to country migration data (from bilateral flows)

Notes: Values in parenthesis stand for bootstrapped standard errors; refer to Appendix B.6 for details.

5.4 Migration frictions and amenities

As with τ_{ij} , I set the bilateral component of migration frictions to be proportional to distance, i.e. $m_{ij} = \text{distance}(i, j)^\phi$. Thus, the remaining elements to be quantified are $\{\phi, m_c, u_i\}_{i,c}$, which are solved for with an analogous two-stage procedure.

Inner loop. It uses the quantified elements in Section 5.3 to solve for prices and real income in the economy. Then, starting with a guess for ϕ , it inverts the spatial equilibrium for $\{m_c\}_c$ and $\{u_i\}_i$ such that the model replicates, respectively, the gross

migration flows at the country level and the spatial distribution of the population.²⁷ The separate identification of $\{m_c\}_c$ and $\{u_i\}_i$ is possible because they are additively separable in the denominator of eq. (18). That provides within-country variation in terms of potential origins from which the migration cost is or is not scaled by $\{m_c\}_c$, and allows for a separate identification conditional on $\{u_i\}_i$.²⁸ The latter, conditional on the former, is identified with spatial variation in population.²⁹

Outer loop. It consists of a similar GMM that estimates $\hat{\phi} = 0.46$ (with bootstrapped standard errors of 0.025) by matching the total internal migration observed in the census data.³⁰ It conveys evidence of large mobility barriers in SSA: the resulting (median) $\{m_{ij}\}_{i,j}$ is about 20 percent higher than the estimates for Indonesia (from Bryan and Morten, 2019), and three and four times larger than those for Brazil and the US (respectively from Morten and Oliveira, 2018; Allen and Donaldson, 2022).³¹

5.5 Validating the model

Before using the quantified model to simulate the future, I first check the reasonability of the quantified fundamentals. They align well with the mechanisms in the model. I find high non-agricultural productivities in highly productive locations, high migration barriers in countries with (relative) little migration, high amenities in denser locations with (relative) low real income, and preference shifters that match the SSA context (and are close to estimates from related studies; see Appendix B.10 for details).

Next, I test the capacity of the model to replicate observed moments with a back-casting exercise that solves for the spatial equilibrium in 1975 using the GAEZ agricultural productivities and population endowments in that year. The result illustrates the extent to which the model is able to replicate the population changes in SSA between 1975 and 2000 using the observed changes in the climate during that period.³²

²⁷Importantly, the international migration data from Abel and Cohen (2019) provides cross-country gross flows between 1990 (the earliest year available) and 2000. Thus, my estimation requires a measure of the initial population in 2000, i.e. $\{L_i^0\}_i$. I calculate it by scaling the distribution of the population in 1990 to the levels of SSA population in 2000, while accounting for the observed natural population growth rates (fertility minus mortality) across countries during the period. Intuitively, this represents the population distribution in SSA if there had been no mobility during that period.

²⁸Intuitively, the additive separation holds because, for each destination, there are several origins of migrants, some of them being other countries and others not.

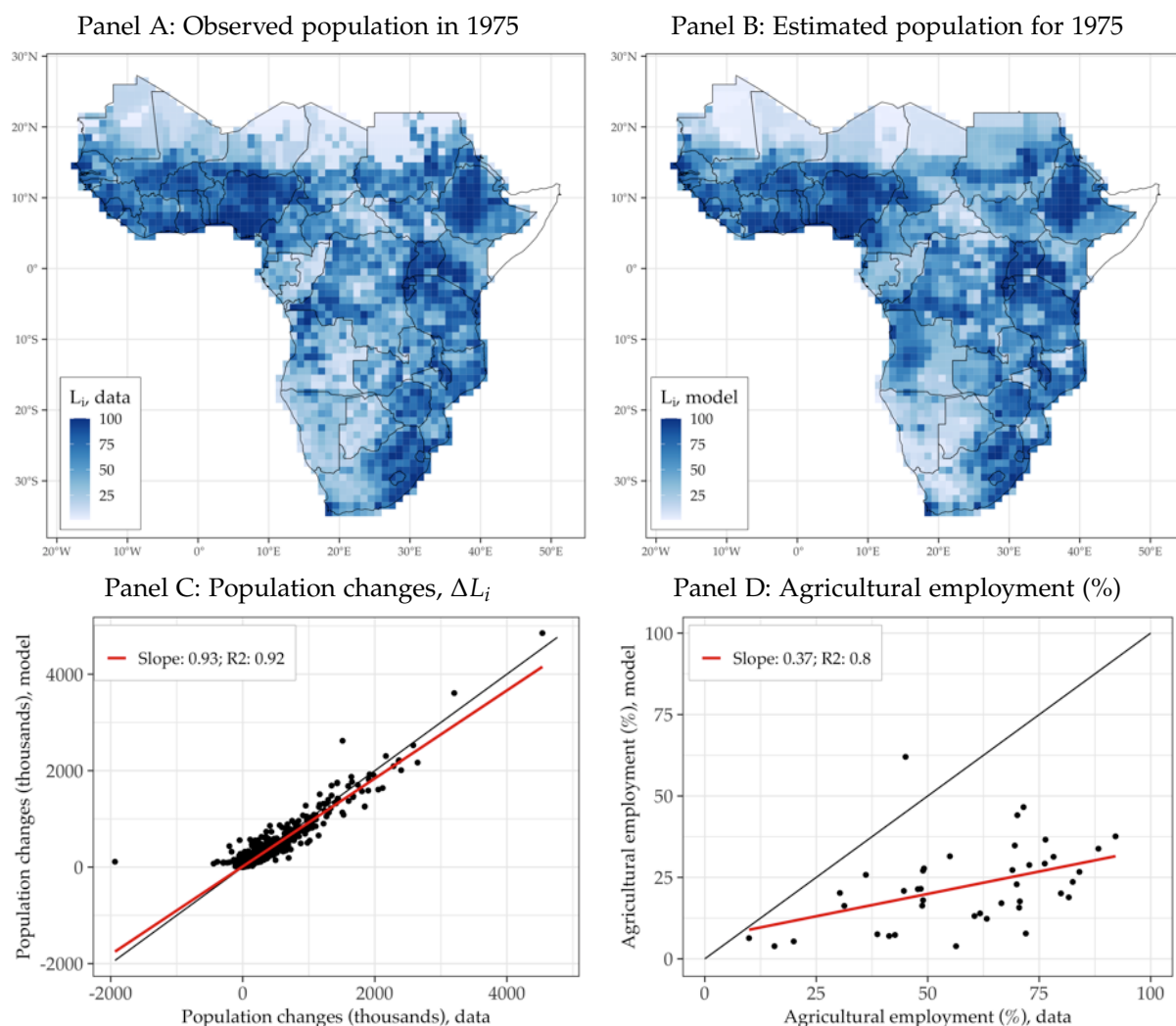
²⁹Therefore, amenities stand as a structural residual of my model: it rationalizes all location choices observed in the data that cannot be explained by differences in real wages and migration frictions.

³⁰To be consistent other data, I use internal migration flows between 1990 and the early 2000s.

³¹As with trade costs, the estimates from these sources are not directly comparable to my $\hat{\phi}$ due to different functional formats and/or units (e.g., travel time rather than distance). Appendix B.9 discusses their equivalence in detail and the reasons for (and benefits of) my specification.

³²The data source for the 1975 population (GHSP) differs from that used in the calibration (G-Econ). I check their compatibility using the correlation between them for the population in 2000 (available in both datasets) at the grid-cell and country level. Furthermore, in order to have an initial population for

Figure 6: Validation of the calibrated model in levels and differences



Notes: Panels A shows the observed 1975 population distribution in SSA while Panel B shows the distribution produced by the model. The values are shown in percentiles, where 1 (100) stands for the bottom (top) percentile of each sample. Panel C plots the model fit in terms of population change (between 1975 and 2000, in thousands) while Panel D plots the model fit for country-level agricultural employment in 2000 (in percentage points).

Panels A and B of Figure 6 report the results in levels. The model closely replicates the spatial distribution of the population in 1975 both within and across countries. Moreover, Panel C shows that the results closely fit the population changes between 1975 and 2000, with a slope and R² of about 0.9. Importantly, the major change in this backcasting exercise is on the agricultural suitabilities, i.e. $\{A_i^k\}_{i,k \neq K}$. According to the GAEZ estimates, about 75 percent of the locations in SSA experienced a decline in crop yields between 2000 and 1975. Thus, the fact that using this variation in the model can explain the changes in population during the period confirms the model's

solving the model for 1975 – i.e. $\{L_i^0\}_i$ – I project the 2000 population distribution onto the 1975 levels. Appendix B.11 discusses that in detail.

capacity to provide reliable forecasts of the future using the GAEZ estimates.³³

As an additional overidentification test, in Panel D I compare country-level agricultural employment shares (for all crops) generated by the model for 2000 against World Bank data. The model closely replicates the ranking of countries with respect to agricultural employment shares, though it underestimates their levels. In aggregate, the model predicts about a 25 percent share of employment in agriculture as compared to 58 percent in the data. The main reason for this discrepancy is that I include only a subset of the crops produced in SSA.

6 Climate change and migration: the 2080 forecast

I quantify potential climate migration in SSA by performing a series of counterfactual simulations. The benchmark exercise consists of solving for the spatial equilibrium in 2080 with and without climate change. By comparing the two, I quantify the impact of climate change on population reallocation, welfare losses, and other outcomes. Subsequently, I study the role of the model’s mechanisms and conduct a policy experiment that investigates the impact of climate change if SSA becomes as frictionless as the EU (in terms of migration and trade barriers). I conclude with robustness checks.

6.1 Benchmark counterfactual

I solve for the spatial equilibrium in 2080 by inserting the 2080 forecasts of the initial population \mathcal{L} and crop productivities \mathcal{A} into the calibrated model. The former is obtained by scaling the observed population of 2000 using the estimates of country-level population increase from the Population Prospects of [United Nations and Social Affairs \(2019\)](#) for 2080.³⁴ The latter, in contrast, is taken directly from the GAEZ data. For the climate change simulations, I use the estimates of potential crop productivities in 2080 based on the business-as-usual scenario.³⁵ The simulations with no climate change assume no changes in \mathcal{A} and thus capture only the increase in population \mathcal{L} .³⁶

³³A complementary explanation for the good fit in this exercise is path dependence (i.e. the densest locations in 1975 are also the densest in 2000). That is, in a context of high mobility frictions, such as in SSA, the geography of the economy needs extreme shocks to its fundamentals in order to generate dramatic changes in this kind of counterfactual. As shown in Figure B.5, the changes between 1975 and 2000 are not as dramatic as the ones expected by 2080.

³⁴These estimates project the observed country-level natural rates of population growth (fertility minus mortality without migration) at the beginning of the 21st century onto subsequent years. Hence, I assume that fertility is exogenous. Section 6.4 shows how the results change if fertility is endogenized.

³⁵Specifically, I draw the GAEZ data that assumes the business-as-usual future scenario, that is, the Representative Concentration Pathway (RCP) 8.5; see Appendix A for details.

³⁶Note that the spatial distribution of outcomes in the no-climate-change simulations differs from the observed distribution for 2000 due to dispersion forces driven by θ and β .

I quantify climate migration, ΔL_i , using the differences between the equilibrium populations of the two simulations – with and without climate change. Hence, it measures migration pressure in each location i net of the potential migration inflows and outflows. Similarly, I infer the changes in sectoral specialization from the differences in non-agricultural employment ΔL_i^K (in percentage points) and the welfare changes from the percentage change in real income per capita, $\Delta v_i / P_i$.

Figure 7 shows the results on a map. At the country level, Panel A shows large climate migration flows – on the order of a million individuals or more – from Western Sahelian countries like Mauritania and Senegal to nearby countries (e.g. Mali, Ivory Coast, and Burkina Faso) and from DR Congo and other South African countries to Tanzania and South Africa. Panel B, which presents grid-cell-level results, shows a high degree of within-country heterogeneity. Countries experiencing large migration outflows, such as Senegal and DR Congo, also experience a high level of internal migration. There are large movements from their central locations, which are highly affected by climate change, to their relatively less affected south(western) locations. Overall, countries heterogeneously hit by climate change experience large internal migration flows and large population increases in their capitals.³⁷

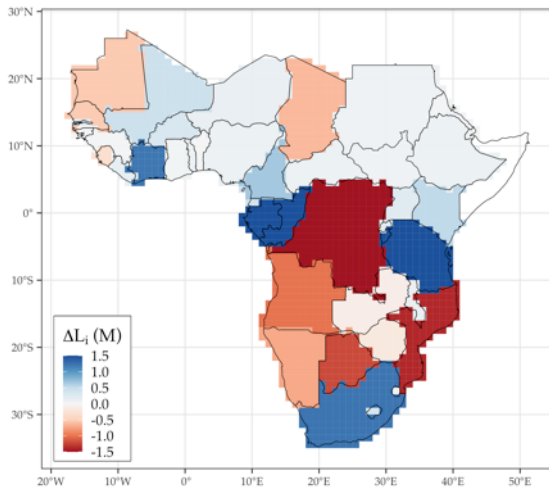
Panels C to F show the results in terms of structural change and real income per capita. The countries that benefit from climate change, such as Tanzania, Rwanda, and Kenya, specialize into agriculture (Panel C). This occurs because such an increase in comparative advantage transforms them into the new agricultural powerhouses of SSA. As a consequence, their real income increase (Panel E), which attracts migrants from nearby countries, such as DR Congo and Mozambique. Panel D and F illustrate the richness of these results in terms of within-country heterogeneity. Even within countries that benefit from climate change, there is substantial variation in terms of sectoral specialization and welfare effects.

Nevertheless, some countries forcedly shift towards agriculture in a non-welfare-improving way. Western African countries like Guinea and Sierra Leone are an example: compared to the no climate change scenario, they need to produce higher crop quantities to supply food to nearby countries that, being much more affected by climate change, specialize out of agriculture (e.g. Mauritania and Senegal). This shows that the necessity aspect of crops limits the Western African economies to adapt to climate change (through structural change) and forces them into a climate change-driven poverty trap. Interestingly, the opposite holds for DR Congo. Climate change pushes individuals from its poorest regions either abroad or to its more productive south. As it stands among the poorest SSA countries in the no climate change scenario, such a

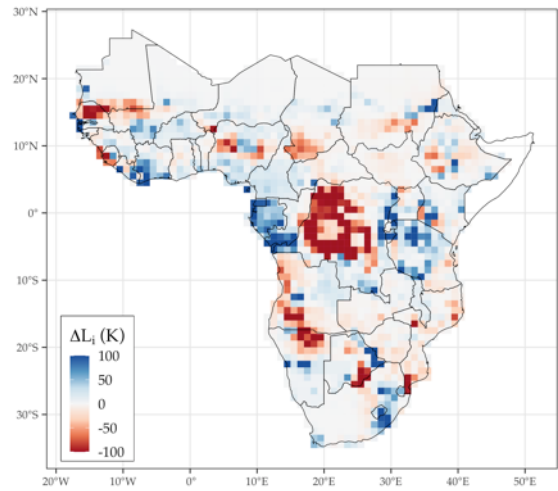
³⁷See Table D.3 for details. Note that the large estimated increase in the populations of capital cities is consistent with the findings in the empirical literature on the high urbanization rates associated with climate change (e.g. Henderson et al., 2017; Peri and Sasahara, 2019; Castells-Quintana et al., 2021).

Figure 7: Counterfactual results for a climate-changed SSA in 2080

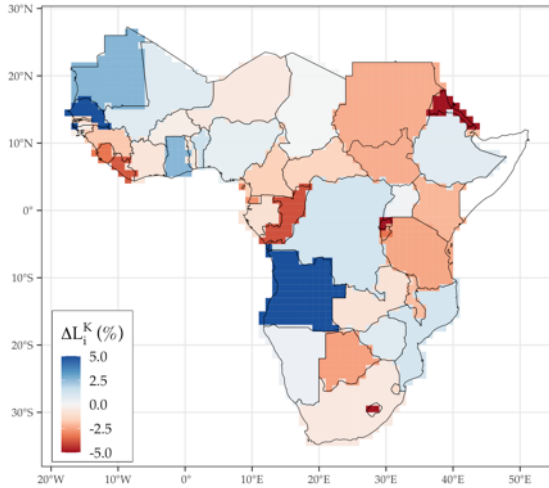
Panel A: Climate migration - country level



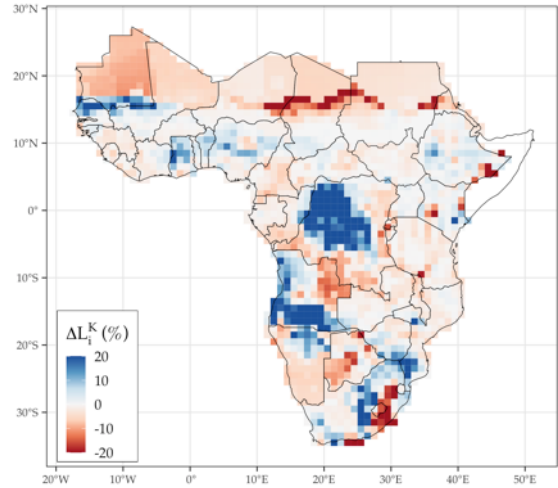
Panel B: Climate migration - grid cell level



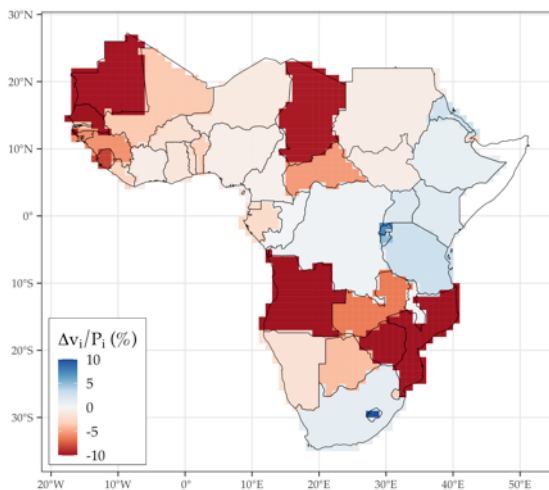
Panel C: Non-agric. employment - country level



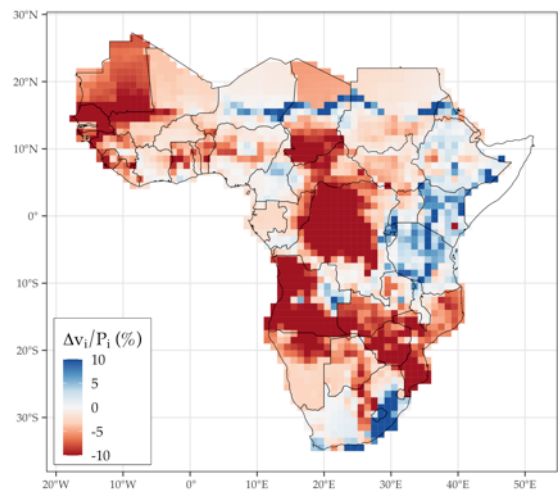
Panel D: Non-agric. employment - grid cell level



Panel E: Real GDP pc - country level



Panel F: Real GDP pc - grid cell level



Notes: Panel A and B plot the results of climate migration in thousands of individuals. Panel C and D describe the results in terms of non-agricultural employment, in percentage points. Panel E and F present the welfare results in terms of percentage changes in real GDP per capita.

productivity-improving reallocation slightly increases real income in relative terms.

In aggregate, the estimated climate migration flows in SSA total about 14 million individuals (Panel A of Table 3 column 1). This is much lower than Rigaud et al. (2018)'s estimates of 90 million climate migrants in SSA by 2050. This discrepancy is explained by the migration frictions that I account for and estimate using actual migration data. Without them, my estimates of climate migration increase to 87 million individuals, surprisingly close to these studies.³⁸ I explore this result in detail, together with other aspects of the role of migration barriers, in Sections 6.2 to 6.4.

Table 3 also shows that climate change barely affects aggregate welfare. However, this seemingly null effect hides a large degree of heterogeneity. At the country level, the bottom and top deciles of welfare changes are about -10 percent and 3 percent, respectively (Panel B). Thus, climate change will lead to unequal consequences across SSA, generating some winners and many losers (see Figure 7 Panel E). This final outcome depends on several mechanisms that interact with each other, such as migration barriers and the heterogeneous forces driving sectoral specialization and structural change. I investigate the welfare importance of these mechanisms in Section 6.2.

Furthermore, climate change hardly affects aggregate sectoral employment. In distributional terms, however, this effect is also heterogeneous and negatively skewed: the top and bottom deciles of the country-level changes in non-agricultural employment are about -4 percentage points and 1.5 percentage points, respectively, and the median country experiences a decrease in non-agricultural employment of about one percentage point. This happens because, with climate change, more labor needs to be employed in agriculture to produce the necessary quantity of crops (making these countries poorer and increasing their agricultural expenditure share).³⁹

6.2 Investigating the underlying channels

I investigate the extent to which the model's underlying channels (migration frictions, trade, and crop-switching) affect the estimated climate migration flows and the associated welfare and sectoral specialization effects. To do so, I perform additional simulations centered on each of the channels.

³⁸This pattern is with consistent related findings that show that large mobility frictions in developing economies may have an inhibiting effect on future climate migration and thus may exacerbate welfare losses (e.g. Peri and Sasahara, 2019; Benveniste et al., 2020; Burzyński et al., 2022).

³⁹This result is consistent with related findings in the literature. For instance, Nath (2022) estimates an increase in agricultural expenditure shares of about 2.7 percentage points in the world's poorest quartile of countries, whereas Cruz (2021) estimates an increase in global agricultural employment of about 2 percent. The main channel explaining the differences in magnitude between those estimates and my own (0.83, median) is the multi-crop feature of my framework. By not taking into consideration the potential production reallocation within agriculture (i.e. across crops), the consumption specialization effect of climate change is overestimated. I discuss this extensively in Section 6.2.

Table 3: Aggregate and disaggregate results of the climate change counterfactuals

	(1) Baseline	(2) No mig. fric. ($\bar{m}_{ij} = 1$)	(3) No tariffs ($\tau^F = 1$)	(4) Agriculture as one crop
<i>Panel A - Aggregate effects:</i>				
Climate migration ¹	14.33	87.15	1.04	10.27
Δ Real income pc (%)	-0.07	8.08	-0.18	-2.44
ΔL_i^K (non-agric. employment, %)	-0.10	0.81	-0.21	-1.23
<i>Panel B - Country-level effects:</i>				
Median Δ population ¹	0.09	-0.86	0	0.05
Bottom/top deciles	[-0.72; 1.23]	[-3.97; 0.38]	[-0.06; 0.12]	[-0.57; 0.64]
Median Δ Real income pc (%)	-1.87	0.97	-0.31	-0.62
Bottom/top deciles	[-9.8; 2.61]	[-1.48; 4.98]	[-2.01; 1.36]	[-9.53; 3.9]
Median ΔL_i^K (%)	-0.88	0.61	0	-1.08
Bottom/top deciles	[-3.78; 1.42]	[-2.54; 5.63]	[-5.39; 2.8]	[-3.78; 2.78]

Notes: Column 1 shows the baseline results, column 2 shows the results with no migration frictions ($m_{ij} = 1$ for all i, j), column 3 shows the results with no tariffs to international trade ($\tau^F = 1$), and column 4 shows the results when assuming a single crop. ¹Climate migration in million individuals.

Migration frictions. I study the role of migration costs with an experiment that eliminates them (i.e. $m_{ij} = 1$ for all i, j ; results in column 2 of Table 3).⁴⁰ As expected, aggregate migration flows increase substantially – by about 70 million climate migrants. Perhaps surprisingly, the aggregate welfare consequences of climate change are reversed: real income per capita increases by 8 percent.

What explains this welfare-improving role of migration as adaptation? The answer lies in its interaction with sectoral specialization. Facing reduced mobility barriers, workers in affected areas can migrate to farther-away, more productive regions, which improves the efficiency of the SSA economy in terms of sectoral comparative advantage. In the climate change scenario, this means that agricultural production reallocates to the climate-change-benefitted regions, while non-agricultural production moves to the most developed countries in SSA. This efficiency gain increases real income in SSA and reduces the demand for agricultural goods and employment in that sector. Thus, migration allows SSA to benefit from the push-aspect of climate change by permitting individuals to move out of unproductive rural regions and allowing the economy to go through a welfare-improving process of structural transformation.

Table 3 Panel B provides quantitative evidence of this result. The distribution

⁴⁰This exercise eliminates mobility frictions in the simulations with and without climate change. Thus, the comparison of the two isolates the climate change effect and shows how they compare with the baseline in the absence of these barriers. The same applies to the counterfactuals below.

of non-agricultural employment changes across countries shifts rightwards without mobility frictions, thus confirming that more countries specialize out of agriculture in this scenario. Hence, my results corroborate the well-established potential of reducing migration barriers in rural economies (e.g., Bryan et al., 2014; Bryan and Morten, 2019; Lagakos et al., 2023), but in the context of adaptation to climate change.

The role of trade. Table 3 Column 3 presents the results of a counterfactual without tariffs (i.e., $\tau^F = 1$). On aggregate, climate migration flows decrease dramatically, by about 90 percent. This occurs because lower trade frictions permit the economy to adapt through sectoral specialization, thus discouraging migration (as in Conte et al., 2021). This is evident in Panel B: the distributional changes in sectoral employment centers around zero and widens remarkably, meaning that relatively benefitted countries specialize even more in agriculture (and the opposite for damaged countries).

In terms of aggregate welfare effects, removing tariffs seems not as efficient as removing migration barriers. However, it is much more efficient in distributional terms: columns 2 and 3 of Table 3 Panel B show that the distribution of real income changes is relatively wider in the case of relaxed migration. That is, while migration allows SSA to adapt to climate change in an aggregate welfare-improving manner, it makes the individuals remaining in the most-affected regions relatively worse off.⁴¹ Therefore, the results imply that mitigating climate change by reducing migration barriers poses a trade-off between aggregate gains and higher inequality (and climate migration), if compared to eliminating tariffs. In Section 6.3, I explore this in detail with a set of experiments centered at realistic migration and trade policies.

Crop switching. To investigate the importance of the multi-crop feature of my framework, I perform a counterfactual exercise in which agriculture is comprised of a single crop (results in Table 3 column 4).⁴² Compared to the baseline, climate migration decreases only slightly. However, aggregate welfare losses and agricultural employment increase dramatically. This is explained by the heterogeneity of the expected crop yield changes within locations (Figure 2). Affected producers can, in a multi-crop setting, reallocate agricultural production to the less-affected crop (but not in the case of a single crop). Hence, assuming a single crop overestimates the impact of climate change on agricultural productivity and amplifies the necessity for the economy to allocate, on aggregate, more labor into agriculture. Thus, accounting for this margin is key in correctly predicting the impact of climate change on subsistence rural economies like those in SSA.

⁴¹Note that eliminating migration frictions \bar{m}_{ij} does not remove the congestion forces in the economy. The heterogeneity of agents with respect to their location choice (disciplined by θ and β) still works as a dispersion force, thus preventing all agents from moving to the best locations in the economy.

⁴²I assume a representative crop whose spatial distribution of potential yields is the cross-crop average within a location. See Appendix C.1 for details.

6.3 Policy experiment - SSA as frictionless as the EU

One of the key takeaways from Section 6.2 is the trade-off that migration policy poses: it allows SSA to be better off when adapting to climate change at the expense of higher regional inequality and migration (if compared to trade policy). In what follows, I further investigate this trade-off with a realistic set of policy experiments. Specifically, I quantify the consequences of climate change for SSA in the hypothetical scenario where migration and trade frictions are reduced to the levels prevailing in the EU.

Doing so requires the quantification of the migration and trade frictions in the EU within the structure of the model. I do that by mapping the country migration barriers $\{m_c\}_c$ and tariffs τ_{ij}^F onto EU migration and trade policies. Focusing on these parameters is particularly convenient because they reflect the institutional characteristics of the EU in terms of trade and migration policies. In other words, they are more tangible and realistic, as policy tools, than the elasticity parameters ϕ or δ .⁴³

In practice, I quantify $\{m_c\}_c$ and τ_{ij}^F by bringing the model to the EU data using the procedure described in Section 5.⁴⁴ The estimated EU frictions are substantially lower than those in the SSA. For trade, I estimate $\tau_{ij}^F = 2.6$, which is a third of SSA's and remarkably close to estimates for the US ($\tau^F = 2.375$ from Antràs et al., 2022). Figure 8 shows that: the discontinuity in bilateral frictions for cross-country trade is barely visible. It also shows that the estimated EU country migration barriers are much less stringent. The average $\{m_c\}_c$ is 60 percent lower than in the SSA case, and its distribution is shifted far more to the left (Panel B).

Armed with that, I perform counterfactual simulations that replace the trade and migration barriers with the EU values. Table 4 Column 2 shows the results for trade policy only. Reducing tariffs to EU levels reduces climate migration flows by a tenth and widens the distribution of sectoral employment changes. It also narrows and shifts rightwards the distribution of welfare changes (i.e., the median country experiences losses of about one percent). As in Section 6.2, the underlying channel is the higher adaptive capacity achieved through sectoral specialization, which reduces the inequality on the climate change impacts. Thus, trade policy can be a powerful tool for a policymaker interested in reducing migration flows while attenuating the distributional impacts of climate change.

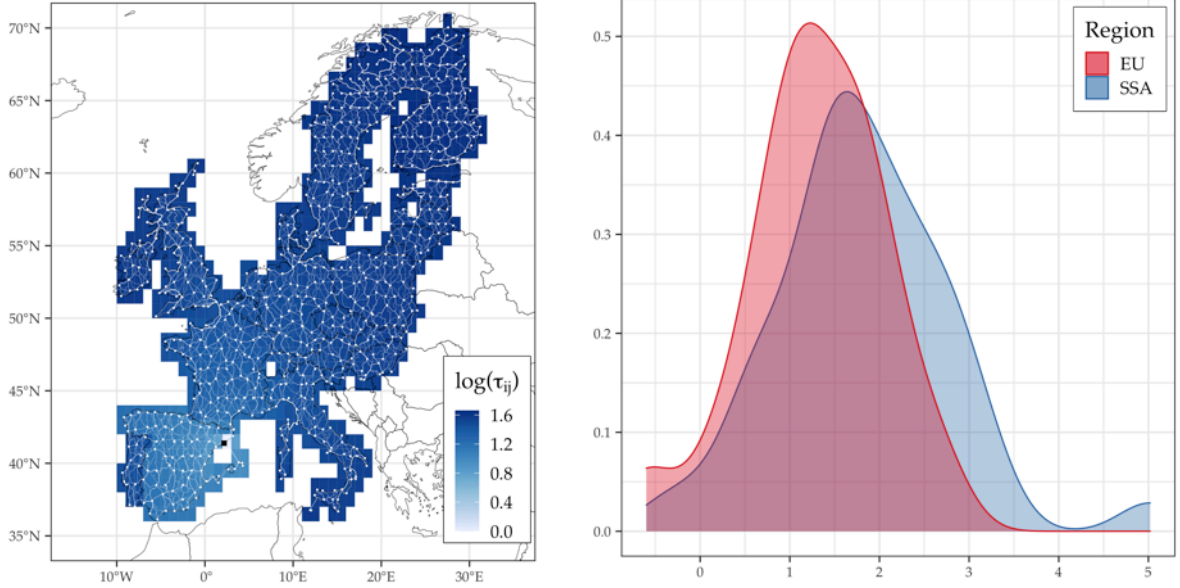
I next conduct an analogous exercise that instead reduces country migration bar-

⁴³Moreover, a comparison to the EU provides results that are more policy-relevant: equating the parameters to EU levels reflects tangible policy actions with a real-world connection. This is less the case with arbitrary changes, as in Section 6.2.

⁴⁴This requires data for the same period and therefore the estimated values for the EU are also for 2000. Importantly, I focus on isolating the variation in the observed trade and migration flows within the EU. Thus, the values of the preference parameters and the bilateral elasticities δ and ϕ remain as described in Table 2. See Appendix B.12 for details.

Figure 8: Estimated trade and migration frictions in the European Union

Panel A: Tariff-like trade frictions τ_{ij}^F in the EU Panel B: Country migration barriers $\{m_c\}_c$ (in logs)



Notes: Panel A presents trade frictions in the EU as was done for SSA in Figure 5 (in this context, trade frictions are relative to Barcelona (Spain), represented by the black dot). Panel B plots the distribution of country migration barriers $\{m_c\}_c$ (in logs, x-axis) in SSA and the EU.

riers to EU levels (column 3).⁴⁵ In line with previous results, there is an increase in climate migration (Panel A) that sets off the migration-induced process of structural change described in Section 6.2. The magnitude of the results is not as stark as in that case. Yet, they do show that by reducing country migration barriers to EU levels, a policy maker in SSA can eliminate the aggregate losses due to climate change, although at the cost – as before – of more climate migration and regional inequality. Figure 9 Panel A documents visually the inequality aspect of migration policy, and shows that the same pattern holds if using alternative measures of welfare (Panel B).⁴⁶

Then, I combine both policies (column 4) and find that the policy mix reduces climate migration by about 90 percent. Moreover, it drastically attenuates the inequality effect of the migration policy alone. The distribution of welfare changes narrows and centers much closer to zero, and the mass of countries experiencing substantial welfare losses drastically reduces (Figure 9). The importance of this policy experiment cannot be overstated: by combining both tools, a policymaker can take advantage of climate change by enabling SSA to structurally change and adapt, through trade and migration, more efficiently and less unequally.

⁴⁵I match the EU $\{m_c\}_c$ values to the SSA countries by deciles (i.e. scaling the barriers of the SSA countries to the value of their respective decile in the EU distribution). See Appendix B.12 for details.

⁴⁶Panel B documents the analogous changes for an alternative measure: weighted expected welfare $W_i = \omega_i \sum_{j \in S} (v_j/P_j)^\theta \bar{m}_{ij}^{-\theta} u_j (L_j/H_j)^{-\beta}$, where $\omega_i \equiv L_i/\mathcal{L}$ (i 's initial population share). It accounts for other components of utility in eq. (4), like amenities, congestion, and migration costs.

Table 4: Aggregate and distributional results of the policy experiments

	(1) Baseline	(2) EU trade frictions	(3) EU mig. barriers	(4) EU trade + mig. barriers
<i>Panel A - Aggregate effects:</i>				
Climate migration ¹	14.33	1.35	18.89	2.41
Δ Real income pc (%)	-0.07	-0.79	2.29	-0.61
ΔL_i^K (non-agric. employment, %)	-0.10	-0.40	0.03	-0.48
<i>Panel B - Country-level effects:</i>				
Median Δ population ¹	0.09	0	0	0
Bottom/top deciles	[-0.72; 1.23]	[-0.11; 0.12]	[-1.1; 0.74]	[-0.25; 0.11]
Median Δ Real income pc (%)	-1.87	-1.55	-1.09	-1.54
Bottom/top deciles	[-9.8; 2.61]	[-4.43; 1.1]	[-9.7; 2.85]	[-4.42; 1.17]
Median ΔL_i^K (%)	-0.88	0	-0.76	0
Bottom/top deciles	[-3.78; 1.42]	[-3.66; 2.09]	[-3.11; 2.72]	[-3.69; 1.94]

Notes: Column 1 presents to the baseline results, while columns 2 to 4 present the results of policy experiments in which frictions are equated to EU levels: in column 2, SSA adopts the same level of tariffs as the EU; in column 3 it adopts the same migration policy, and in column 4 it combines both policies. ¹Climate migration in million individuals.

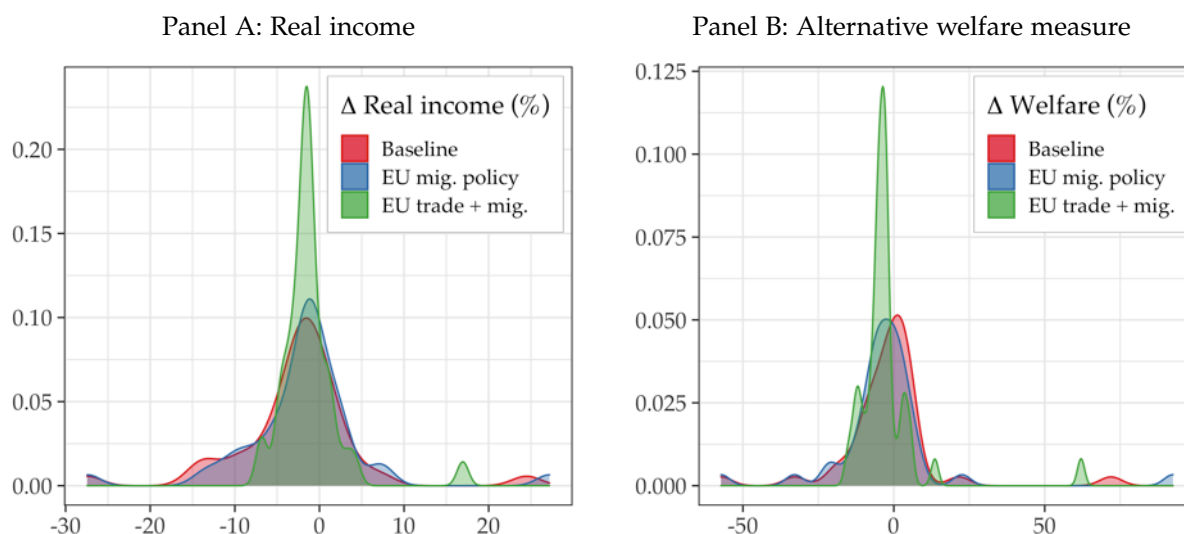
6.4 Robustness checks and discussions

In what follows, I check the robustness (or discuss the importance) of the previous results in several dimensions: the addition of the rest of the world, the migration barriers, the climate change data used in the simulations, and various model's assumptions. Tables 5 and 6 show the results and Appendix C provides further details.

Rest of the world. I introduce trade and migration with the rest of the world (ROW) by augmenting my setting with an additional R representative location.⁴⁷ Table 5 documents the results of several climate change simulations under this setting. Starting with an analogous baseline exercise but with the ROW (column 2), I find that the interaction with the ROW attenuates remarkably climate migration (about 5 million individuals) and the distributional effects of climate change (i.e., lower median welfare losses with a narrower distribution). That happens because now SSA increases crop imports from the ROW and switches specialization as a response to the agricultural losses. In fact, aggregate non-agricultural employment increases, and the distribution of non-agricultural employment changes shifts drastically to the right.

⁴⁷I introduce R as a representative location whose fundamentals and observed economic outcomes are aggregates of the ROW (e.g., land endowments, population, income, migration flows). Appendix C.2 elaborates on that and documents the quantification method for this setting.

Figure 9: Welfare effects of climate change for the baseline and different EU policies



Notes: Panel A and B plot the distributions of country-level changes in welfare in three different policy scenarios for SSA: baseline, EU migration policy, and EU trade and migration policy. Panel A refers to the baseline welfare measure (real income per capita). Panel B refers to an alternative welfare measure that also account for mobility barriers and congestion (see footnote 46).

Perhaps surprisingly, column 2 documents no climate migration from SSA to the ROW under the baseline setting. That happens because of the remarkably high m_R that my model quantifies relative to $\{m_c\}_{c \neq R}$.⁴⁸ Column 3 elaborates on that: removing these barriers ($m_R = 1$) increases aggregate migration, but towards the ROW (of about 1.7 million individuals). Moreover, under this setting, the SSA is better off both on aggregate and distributional terms, which shows the potential of removing barriers from SSA to developed economies as a mitigating policy tool.

Subsequently, column 4 performs an exercise that removes tariffs between SSA and the ROW, τ^R . In line with Nath (2022), this setting amplifies the capacity of crop imports as adaptation. Specifically, there are major migration flows to highly productive regions (and countries) in non-agriculture that acquire crops through imports and specialize in non-agriculture. In fact, almost all SSA countries have now higher non-agricultural employment as a consequence of climate change. Finally, column 5 shows that combining both policies amplifies this effect, allowing more people to migrate both within and across SSA, increasing its specialization in non-agriculture, and considerably reversing welfare losses.

Country migration barriers. I also check the sensitivity of my baseline results to

⁴⁸Specifically, the quantified migration barriers to the ROW exceed those to SSA countries in the order of dozens of thousands. This is not a farfetched result: the observed migration flows, while large in magnitude, are in relative terms drastically lower than the real income differences between the ROW and SSA (which, through the lens of my model, is interpreted as high m_R). Importantly, this null effect on climate migration does not mean that there is no migration between SSA and the ROW, but rather that this number does not change in the presence of climate change.

Table 5: Aggregate and disaggregate results of the climate change counterfactuals accounting for trade and migration with the rest of the world (ROW)

	(1) Baseline	(2) Baseline + ROW	(3) ROW + no barriers m_R	(4) ROW + no tariffs τ^R	(5) ROW + no tariffs/barriers
<i>Panel A - Aggregate CΔ effects:</i>					
Climate migration ¹	14.33	4.79	4.29	19.61	17.65
(of which to the ROW) ¹		0.00	1.67	0.00	11.93
Δ GDP pc (%)	-0.07	-0.70	2.00	1.31	3.50
ΔL_i^K (non-agric. employment, %)	-0.10	0.82	0.04	1.58	0.36
<i>Panel B - Country-level CΔ effects:</i>					
Median Δ population ¹	0.09	0.02	0.09	0	-0.03
Bottom/top deciles	[-0.72; 1.23]	[-0.04; 0.31]	[-0.19; 1.33]	[-0.03; 0.45]	[-0.53; 0.66]
Median Δ GDP pc (%)	-1.87	-0.51	-2.22	-0.01	-0.56
Bottom/top deciles	[-9.8; 2.61]	[-3.01; 2.75]	[-6.94; 5.34]	[-1.47; 1.5]	[-3.21; 6]
Median ΔL_i^K (%)	-0.88	0.46	0	0.39	0
Bottom/top deciles	[-3.78; 1.42]	[-1.51; 4.39]	[0; 2.97]	[-2.61; 7.63]	[0; 7.99]

Notes: Column 1 presents the baseline results, while columns 2 to 5 present the results of extensions with the ROW: column 2 is analogous to the baseline but where trade and migration also take place between SSA and the ROW, column 3 eliminates migration barriers into the ROW ($m_r = 1$), column 4 eliminates tariffs for trading between SSA and the ROW ($\tau^R = 1$), and column 5 eliminates both barriers. ¹Climate migration in million individuals.

potential changes in country barriers over time. There are two reasons for that. First, the time frame of migration choices in my setting is of about a decade, whereas the time interval of my counterfactuals is of almost a century (during which agents could become less sensitive to the decade-specific migration barriers). Second, restrictive countries could become even stricter to foreign migrants over time. I account for these two potential patterns by increasing or decreasing $\{m_c\}_c$ (results in Table 6 Panel A).⁴⁹ The changes in the results are consistent with the findings of Table 3 column 2, but with lower magnitudes (and in the opposite direction if increasing m_c).

Homothetic preferences. I now show that the nonhomotheticity feature of the preferences for agricultural goods and non-agricultural goods is a key driver of climate change's welfare consequences. Table 6 Panel B shows the results of a counterfactual that assumes homothetic preferences (see Appendix C.3 for details). There is almost no aggregate climate migration in this framework, and the welfare losses are dramatically centered around zero. This occurs because, by disregarding the subsistence aspect of agricultural goods, agents replace agricultural goods with non-agricultural

⁴⁹In particular, I alter the distribution of country barriers with $(m_c)^\iota$, where ι is 1.25 (0.75) in the increasing (decreasing) case. I choose the monotonic transformation (instead of scaling them up or down) because the barriers $\{m_c\}_c$ matter in the location choice (Equation (18)) up-to-scale.

goods. This intensifies the patterns of sectoral specialization (i.e. more production and consumption of non-agricultural goods takes place in the most affected regions), increasing non-agricultural employment on aggregate and distributional terms.

Endogenous fertility. I perform a simple exercise that illustrates how the results change if fertility is allowed to be endogenous to climate change. To do so, I adjust the estimates for population growth taken from the Population Prospects of [United Nations and Social Affairs \(2019\)](#) using a damage function that depends on the average change in potential crop yields.⁵⁰ This reduces the initial population \mathcal{L} assumed in the counterfactuals for 2080, particularly in the most affected countries. Table 6 Panel B shows that the baseline results are unresponsive to this dimension: aggregate climate migration and related effects remain around the same magnitude.

Economic growth. I also allow the non-agricultural sector to grow by increasing sector K 's TFP over time (using each i 's average country growth in the first decades of the century). My results remain qualitatively robust to this extension. This happens because the quantified $\{b_i^K A_i^K\}_i$ has remarkable spatial differences in levels. Thus, even if accounting for uneven growth across countries, the results remain unaffected.⁵¹

Climate damage to non-agriculture. My baseline counterfactual assumes no effects of climate change on the non-agricultural sector. The advantage of that is isolating the consequences of the effects on agriculture, the most relevant push factor of migration for subsistence rural economies like SSA. However, I also check how the results change if allowing the K^{th} sector to be also affected. To do that, I scale the quantified productivities of that sector by the equivalent sectoral damage function from [Conte et al. \(2021\)](#).⁵² Table 6 Panel C shows that the baseline results remain unchanged if so, for the same reason if allowing for economic growth (see footnote 51).

Climate damage on amenities. Analogously, the baseline counterfactuals assume that amenities $\{u_i\}_i$ remain constant and unaffected by climate change. I relax this assumption using the damage function of temperature on amenities by [Cruz and Rossi-Hansberg \(2023\)](#).⁵³ The baseline results remain robust (Table 6 Panel C) due to

⁵⁰In particular, I assume that the rate of net population growth changes by 50 percent of the change in average potential yield in each location. Appendix C.4 provides further details and documents additional results with alternative scaling rules. Importantly, I adopt this approach for simplicity, rather than the more realistic approaches in the literature ([Delventhal et al., 2021](#); [Cruz and Rossi-Hansberg, 2023](#)), due to the static feature of my model.

⁵¹Specifically, the observed real income differences (in levels) across SSA are remarkably high, yielding level $\{b_i^K A_i^K\}_i$ differences across locations in the order of thousands or more. Hence, allowing for uneven, country-level growth does not affect drastically its distribution, which explains the little sensitivity of my results to this extension. Appendix C.5 discusses that in detail.

⁵²The damage function depends on the deviations from the optimal temperature for the non-agricultural sector. Thus, to conduct this experiment, I also use the forecasts of temperature for 2080 from [Conte et al. \(2021\)](#) and match them to the locations of SSA. See Appendix C.6 for details.

⁵³I use their estimated $\Lambda^b(T_i)$ damage function for the global economy; see Appendix C.7 for details.

Table 6: Robustness of the benchmark results with respect to trade and migration frictions, model assumptions, and climate change scenarios

	(1)	(2)	(3)
	Climate migration (million individuals)	Δ Real income per capita (%)	Δ Non-agricultural employment (%)
Baseline results	14.33 [0.09]	-0.07 [-1.87]	-0.1 [-0.88]
<i>Panel A: Robustness to country barriers</i>			
Higher country barriers m_c	11.67 [0.04]	-0.54 [-1.99]	-0.09 [-0.86]
Lower country barriers m_c	18.32 [0.06]	1.25 [-1.72]	-0.07 [-0.86]
<i>Panel B: Robustness to model assumptions</i>			
Homothetic preferences	0.38 [0]	0.03 [-0.25]	0.69 [0.62]
Endogenous fertility	13.8 [0.09]	-0.08 [-1.85]	-0.1 [-0.88]
Non-agricultural prod. growth	14.28 [0.09]	-0.3 [-1.96]	-0.13 [-0.84]
<i>Panel C: Robustness to $C\Delta$ damages or scenarios</i>			
$C\Delta$ damages to non-agriculture	14.27 [0.09]	-0.07 [-1.86]	-0.1 [-0.86]
$C\Delta$ damages to amenities	14.35 [0.09]	-0.05 [-1.87]	-0.1 [-0.88]
RCP 4.5 $C\Delta$ scenario	8.18 [0.01]	-0.04 [-0.52]	-0.15 [-0.35]

Notes: Panel A presents the aggregate effect of climate change for different levels of trade and migration frictions, driven by the parameters δ and ϕ , respectively. Panel B presents the results of the benchmark simulation when (separately) assuming homothetic preferences between agriculture and non-agriculture, endogenous fertility, and a less severe climate change scenario.

the large spatial dispersion of the quantified amenities.⁵⁴

Assumption of climate change scenario. I also check the sensitivity of the results to the severity of the underlying climate change scenario, by switching to the RCP 4.5 scenario (which assumes that carbon emissions will peak by mid-century and decrease thereafter). I simulate the model with the suitability data for this scenario (Table 6 Panel C). As expected, all climate change effects are attenuated in this setting.

Endogenous climate and dynamics. The static nature of my model excludes, naturally, dynamic mechanisms such as climate-economy feedback (as in Conte et al., 2021; Cruz and Rossi-Hansberg, 2023) and forward-looking agents (like Balboni, 2021; Takeda, 2022; Allen and Donaldson, 2022; Castro-Vincenzi, 2023; Kleinman et al., 2023; Bilal and Rossi-Hansberg, 2023). The reason for the former is that Africa emits about 3 percent of global emissions, which makes it reasonable to assume exogenous climate change. The reason for the latter is data-driven: the GAEZ data provides estimates for specific points in time, rather than a time-varying function to feed a dynamic setting.

⁵⁴Analogously to the above (footnote 51), this is due to the large observed real income differences across space that map into large level differences in $\{u_i\}_i$ across locations. See Appendix C.7 for details.

7 Conclusion

The main message of this paper is that climate change must not lead to bad outcomes if rural economies like SSA can adapt to it. If mobility barriers can be reduced, climate change can encourage the shift of population out of poor, low-productivity rural locations and set off a process of structural change. Openness to trade determines the aggregate and distributional welfare effects of this process, by allowing affected economies to switch production to less-affected sectors. The interaction of these – and other – mechanisms in general equilibrium is complex and interconnected. I model that with a transparent framework that I develop and connect to SSA data.

I identify that a high degree of frictions in SSA that inhibit the welfare-improving process just described. My estimates suggest sizeable welfare losses of climate change and migration flows in many orders of magnitude smaller than reduced-form estimates from the literature. However, a policy experiment shows that, by becoming as frictionless as the EU, SSA adaptation to climate change could increase welfare both in aggregate and distributional terms. My climate migration estimates when relaxing migration frictions approach those from other studies that disregard these barriers.

My results deliver important contributions to the literature and the policy debates. I connect the findings from the literature on the gains from incentivizing migration in developing economies with those from the literature on the importance of sectoral specialization and trade in adapting to climate change. I also deliver a policy-relevant message on the potential role of real-world trade and migration policies in adapting to climate change.

References

- Abel, Guy J and Joel E Cohen**, “Bilateral international migration flow estimates for 200 countries,” *Scientific data*, 2019, 6 (1), 1–13.
- Albert, Christoph, Paula Bustos, and Jacopo Ponticelli**, “The Effects of Climate Change on Labor and Capital Reallocation,” Technical Report, National Bureau of Economic Research 2021.
- Allen, Treb**, “Information frictions in trade,” *Econometrica*, 2014, 82 (6), 2041–2083.
- **and Costas Arkolakis**, “Trade and the Topography of the Spatial Economy,” *The Quarterly Journal of Economics*, 2014, 129 (3), 1085–1140.
- **and Dave Donaldson**, “Persistence and path dependence in the spatial economy,” 2022.

- Antràs, Pol, Teresa C Fort, Agustín Gutiérrez, and Felix Tintelnot**, “Trade Policy and Global Sourcing: An Efficiency Rationale for Tariff Escalation,” Working Paper 30225, National Bureau of Economic Research July 2022.
- Asturias, Jose, Manuel García-Santana, and Roberto Ramos**, “Competition and the welfare gains from transportation infrastructure: Evidence from the Golden Quadrilateral of India,” *Journal of the European Economic Association*, 2019, 17 (6), 1881–1940.
- Atkin, David and Dave Donaldson**, “Who’s getting globalized? The size and implications of intra-national trade costs,” Technical Report, National Bureau of Economic Research 2015.
- Baez, Javier, German Caruso, Valerie Mueller, and Chiyu Niu**, “Heat Exposure and Youth Migration in Central America and the Caribbean,” *American Economic Review*, 2017, 107 (5), 446–50.
- Balboni, Clare Alexandra**, “In Harm’s Way? Infrastructure Investments and the Persistence of Coastal Cities,” 2021.
- Barrios, Salvador, Luisito Bertinelli, and Eric Strobl**, “Climatic change and rural–urban migration: The case of sub-Saharan Africa,” *Journal of Urban Economics*, 2006, 60 (3), 357–371.
- Benveniste, Hélène, Michael Oppenheimer, and Marc Fleurbaey**, “Effect of border policy on exposure and vulnerability to climate change,” *Proceedings of the National Academy of Sciences*, 2020, 117 (43), 26692–26702.
- Bernard, Andrew B, Jonathan Eaton, J Bradford Jensen, and Samuel Kortum**, “Plants and productivity in international trade,” *American economic review*, 2003, 93 (4), 1268–1290.
- Bilal, Adrien and Esteban Rossi-Hansberg**, “Anticipating Climate Change Across the United States,” Technical Report, Working Paper 2023.
- Borchert, Ingo, Mario Larch, Serge Shikher, and Yoto V Yotov**, “The international trade and production database for estimation (ITPD-E),” *International Economics*, 2021, 166, 140–166.
- Bryan, Gharad and Melanie Morten**, “The aggregate productivity effects of internal migration: Evidence from Indonesia,” *Journal of Political Economy*, 2019, 127 (5), 2229–2268.

- , **Shyamal Chowdhury, and Ahmed Mushfiq Mobarak**, “Underinvestment in a profitable technology: The case of seasonal migration in Bangladesh,” *Econometrica*, 2014, 82 (5), 1671–1748.
- Burzyński, Michał, Christoph Deuster, Frédéric Docquier, and Jaime De Melo**, “Climate Change, Inequality, and Human Migration,” *Journal of the European Economic Association*, 2022, 20 (3), 1145–1197.
- Cai, Ruohong, Shuaizhang Feng, Michael Oppenheimer, and Mariola Pytlikova**, “Climate variability and international migration: The importance of the agricultural linkage,” *Journal of Environmental Economics and Management*, 2016, 79, 135–151.
- Castells-Quintana, David, Melanie Krause, and Thomas KJ McDermott**, “The urbanising force of global warming: the role of climate change in the spatial distribution of population,” *Journal of Economic Geography*, 2021, 21 (4), 531–556.
- Castro-Vincenzi, Juanma**, “Climate hazards and resilience in the global car industry,” Technical Report, Technical report, Working Paper 2023.
- CIESIN**, “Global roads open access data set, version 1 (gROADSv1),” *Palisades, NY: NASA Socioeconomic Data and Applications Center (SEDAC)*, 2013.
- Comin, Diego, Danial Lashkari, and Martí Mestieri**, “Structural change with long-run income and price effects,” *Econometrica*, 2021, 89 (1), 311–374.
- Conte, Bruno, Klaus Desmet, and Esteban Rossi-Hansberg**, “On the Geographic Implications of Carbon Taxes,” Technical Report, National Bureau of Economic Research 2022.
- , – , **Dávid Krisztián Nagy, and Esteban Rossi-Hansberg**, “Local sectoral specialization in a warming world,” *Journal of Economic Geography*, 2021, 21 (4), 493–530.
- Costinot, Arnaud, Dave Donaldson, and Cory Smith**, “Evolving comparative advantage and the impact of climate change in agricultural markets: Evidence from 1.7 million fields around the world,” *Journal of Political Economy*, 2016, 124 (1), 205–248.
- Cruz, Jose Luis**, “Global Warming and Labor Market Reallocation,” 2021.
- Cruz, José-Luis and Esteban Rossi-Hansberg**, “The Economic Geography of Global Warming,” *forthcoming, Review of Economic Studies*, 2023.
- Delventhal, Matthew J, Jesús Fernández-Villaverde, and Nezih Guner**, “Demographic transitions across time and space,” Technical Report, National Bureau of Economic Research 2021.

- Desmet, Klaus and Esteban Rossi-Hansberg**, “On the spatial economic impact of global warming,” *Journal of Urban Economics*, 2015, 88, 16–37.
- and – , “Climate Change Economics over Time and Space,” 2023.
- , **Dávid Krisztián Nagy**, and **Esteban Rossi-Hansberg**, “The geography of development,” *Journal of Political Economy*, 2018, 126 (3), 903–983.
- , **Robert E. Kopp**, **Scott A. Kulp**, **Dávid Krisztián Nagy**, **Michael Oppenheimer**, **Esteban Rossi-Hansberg**, and **Benjamin H. Strauss**, “Evaluating the Economic Cost of Coastal Flooding,” *American Economic Journal: Macroeconomics*, April 2021, 13 (2), 444–86.
- Donaldson, Dave**, “Railroads of the Raj: Estimating the impact of transportation infrastructure,” *American Economic Review*, 2018, 108 (4-5), 899–934.
- Eaton, Jonathan and Samuel Kortum**, “Technology, geography, and trade,” *Econometrica*, 2002, 70 (5), 1741–1779.
- Eckert, Fabian and Michael Peters**, “Spatial structural change,” *Unpublished Manuscript*, 2018.
- Fajgelbaum, Pablo and Stephen J Redding**, “Trade, Structural Transformation, and Development: Evidence from Argentina 1869–1914,” *Journal of Political Economy*, 2022, 130 (5), 1249–1318.
- Florczyk, AJ, C Corbane, D Ehrlich, S Freire, T Kemper, L Maffenini, M Melchiorri, M Pesaresi, P Politis, M Schiavina et al.**, “GHSL Data Package 2019,” *Luxembourg. EUR*, 2019, 29788.
- Gollin, Douglas, Stephen L Parente, and Richard Rogerson**, “The food problem and the evolution of international income levels,” *Journal of Monetary Economics*, 2007, 54 (4), 1230–1255.
- Gröger, André and Yanos Zylberberg**, “Internal labor migration as a shock coping strategy: Evidence from a typhoon,” *American Economic Journal: Applied Economics*, 2016, 8 (2), 123–53.
- Henderson, J Vernon, Adam Storeygard, and Uwe Deichmann**, “Has climate change driven urbanization in Africa?,” *Journal of development economics*, 2017, 124, 60–82.
- Herrendorf, Berthold, Richard Rogerson, and Akos Valentinyi**, “Growth and structural transformation,” *Handbook of economic growth*, 2014, 2, 855–941.

- Hsiao, Allan**, “Sea Level Rise and Urban Adaptation in Jakarta,” Technical Report, Mimeo, 2022.[6] 2022.
- IIASA and FAO**, “Global Agro-Ecological Zones (GAEZ v3. 0),” 2012.
- Imbert, Clément, Joan Monras, Marlon Seror, and Yanos Zylberberg**, “Floating Population: Migration With (Out) Family and the Spatial Distribution of Economic Activity,” *Work in progress*, 2023.
- IPCC**, “IPCC Special Report,” 2000.
- , *Managing the risks of extreme events and disasters to advance climate change adaptation: special report of the intergovernmental panel on climate change*, Cambridge University Press, 2012.
- IPUMS**, “Integrated Public Use Microdata Series, International: Version 7.3 [dataset],” Technical Report, Minnesota Population Center, Minneapolis, MN: IPUMS 2020.
- Kleinman, Benny, Ernest Liu, and Stephen J Redding**, “Dynamic spatial general equilibrium,” *Econometrica*, 2023, 91 (2), 385–424.
- Lagakos, David, Ahmed Mushfiq Mobarak, and Michael E Waugh**, “The welfare effects of encouraging rural–urban migration,” *Econometrica*, 2023, 91 (3), 803–837.
- Lustgarten, Abrahm**, “The Great Climate Migration Has Begun,” *The New York Times*, Jun 2020.
- Meghir, Costas, A Mushfiq Mobarak, Corina Mommaerts, and Melanie Morten**, “Migration and Informal Insurance: Evidence from a Randomized Controlled Trial and a Structural Model,” *The Review of Economic Studies*, 04 2021, 89 (1), 452–480.
- Moneke, Niclas**, “Can big push infrastructure unlock development? evidence from ethiopia,” *STEG Theme*, 2020, 3, 14–15.
- Morten, Melanie and Jaqueline Oliveira**, “The effects of roads on trade and migration: Evidence from a planned capital city,” *NBER Working Paper*, 2018, 22158, 1–64.
- Nagy, Dávid Krisztián**, “Hinterlands, City Formation and Growth: Evidence from the U.S. Westward Expansion,” *The Review of Economic Studies*, 01 2023, p. rdad008.
- Nath, Ishan B**, “The Food Problem and the Aggregate Productivity Consequences of Climate Change,” Technical Report 2022.

- Nordhaus, William, Qazi Azam, David Corderi, Kyle Hood, Nadejda Makarova Victor, Mukhtar Mohammed, Alexandra Miltner, and Jyldyz Weiss**, “The G-Econ database on gridded output: methods and data,” *Yale University, New Haven*, 2006, 6.
- of Economic United Nations, Department and Population Division Social Affairs**, “World Population Prospects 2019: Highlights,” 2019.
- Pellegrina, Heitor S**, “Trade, productivity, and the spatial organization of agriculture: Evidence from Brazil,” *Journal of Development Economics*, 2022, p. 102816.
- **and Sebastian Sotelo**, “Migration, Specialization, and Trade: Evidence from Brazil’s March to the West,” Technical Report, National Bureau of Economic Research 2021.
- Peri, Giovanni and Akira Sasahara**, “The impact of global warming on rural-Urban migrations: Evidence from global big data,” Technical Report, National Bureau of Economic Research 2019.
- Porteous, Obie**, “High trade costs and their consequences: An estimated dynamic model of African agricultural storage and trade,” *American Economic Journal: Applied Economics*, 2019, 11 (4), 327–66.
- Redding, Stephen J and Esteban Rossi-Hansberg**, “Quantitative spatial economics,” *Annual Review of Economics*, 2017, 9, 21–58.
- Rigaud, KK, B Jones, J Bergmann, V Clement, K Ober, J Schewe, S Adamo, B McCusker, S Heuser, and A Midgley**, “Groundswell: Preparing for Internal Climate Migration (Washington, DC: World Bank),” 2018.
- Rudik, Ivan, Gary Lyn, Weiliang Tan, and Ariel Ortiz-Bobea**, “The Economic Effects of Climate Change in Dynamic Spatial Equilibrium,” 2021.
- Sotelo, Sebastian**, “Domestic trade frictions and agriculture,” *Journal of Political Economy*, 2020, 128 (7), 2690–2738.
- Takeda, Kohei**, “The Geography of Structural Transformation: Effects on Inequality and Mobility,” 2022.
- Veronese, N and H Tyrman**, “MEDSTATII: Asymmetry in Foreign Trade Statistics in Mediterranean Partner Countries,” Technical Report, Eurostat Methodologies Working Papers 2009.

Weiss, D, A Nelson, HS Gibson, W Temperley, S Peedell, A Lieber, M Hancher, E Poyart, S Belchior, N Fullman et al., "A global map of travel time to cities to assess inequalities in accessibility in 2015," *Nature*, 2018, 553 (7688), 333.

Appendix

Appendix A provides more details about the data sources mentioned in Section 2 and other data sources not mentioned therein. Appendix B documents theoretical derivations that support the main results of Section 4. Appendix C describe alternative models used in the robustness. Appendix D contains additional figures and tables.

A Data Appendix

Table A.1 below documents all data sources used and their temporal coverage. Next, I provide further detail on the data choices and aggregation.

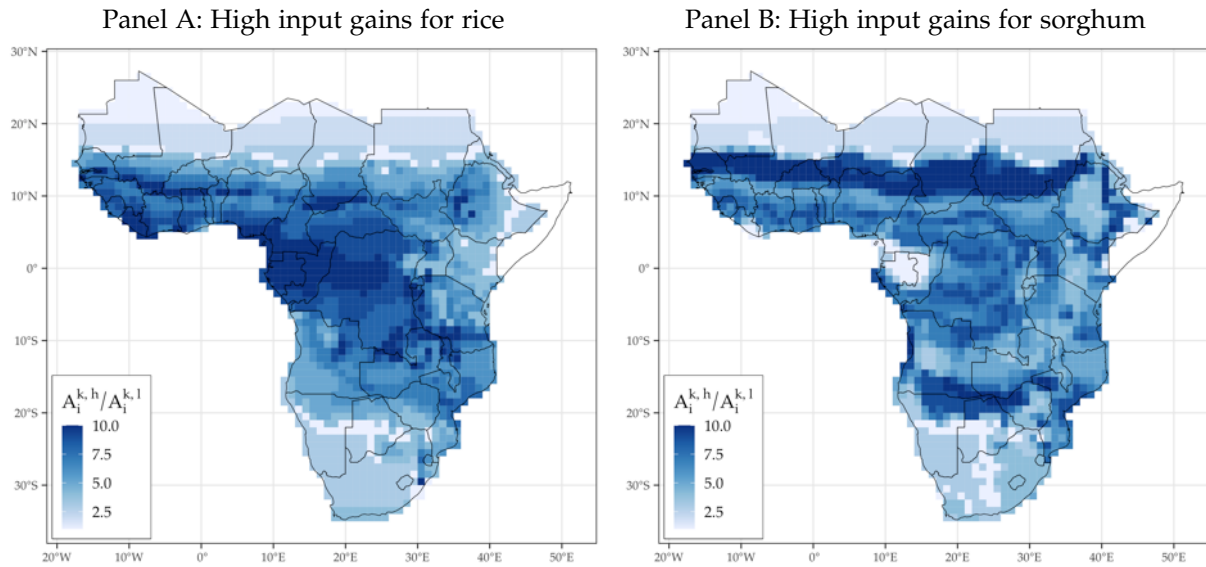
Table A.1: Main data sources

Type of data	Coverage	Source
GDP and Population	2000	G-Econ Project v4.0 (Nordhaus et al., 2006)
Population	1975, 2000	Global Human Settlements Project (Florczyk et al., 2019)
Population projections	2021 – 2100	United Nations and Social Affairs (2019)
Agric. Productivities	1960–2000	GAEZ v3.0 (IIASA and FAO, 2012)
Climate Δ projections	2020, 2050, 2080	GAEZ v3.0 (IIASA and FAO, 2012)
Transportation data	2000	gROADS project (CIESIN, 2013)
Friction transportation surface	2000	Accessibility to Cities' project (Weiss et al., 2018)
Bilateral crop international trade	1995–2005	ITPD-E (Borchert et al., 2021)
Bilateral international migration	1990–2000	Abel and Cohen (2019)
Bilateral internal migration	1970–2015	Census data from IPUMS (2020)
Crop prices	1990–2015	VAM project, World Food Program

GAEZ agro-climatic yields. The GAEZ's database provides estimates of agricultural potential yields for several crops, in different time periods, and for different degrees of technology usage in agriculture. As my interest in subsistence agriculture setup of SSA, I aim at building a time varying dataset of potential yields over the entire sub-continent, for several crops, at low usage of modern inputs: with rainfed water access, labor intensive techniques, and no application of nutrients, no use of chemicals for pest and disease control and minimum conservation measures.

A challenge, however, is that the time varying potential yields from GAEZ are available only for high usage of modern inputs (based on improved high yielding varieties, fully mechanized with low labor intensity techniques, and usage of optimum applications of nutrients and chemical pest, disease and weed control). The estimates for different input levels are only available for the long-run estimates (averages between 1960-1990).

Figure A.1: Yield gains from adoption of high inputs in agriculture vis-à-vis low inputs for selected crops.



Notes: Panels A and B show the ratio of high/low input usage yields for growing two selected crops according to GAEZ long-run estimates. The values are shown in deciles; 1 (10) stands for the bottom (top) decile of each sample.

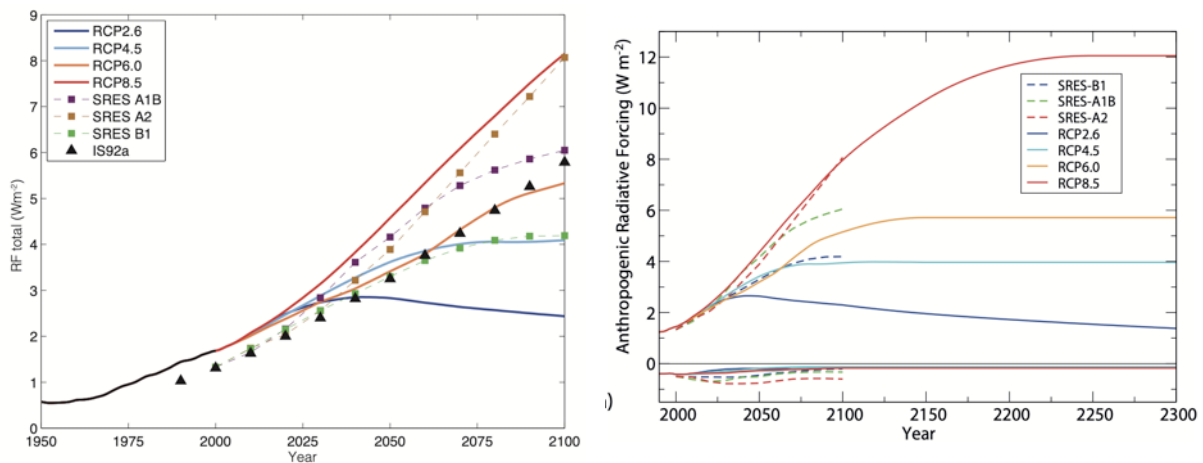
Therefore, to obtain a time varying dataset of the agro-climatic yields at low input usage, I first use the long-run values to calculate the GAEZ-implied ratio between high inputs ($A_i^{k,h}$) / low inputs ($A_i^{k,l}$) yields for each crop. This procedure reveals how the gains from adopting higher input levels differ across locations and crops – Figure A.1 illustrates the results for two selected crops in deciles. I use the calculated ratios to scale down the time varying estimates for high inputs that I collect.

Armed with the location-crop technology scales, I collect the time varying estimates of agro-climatic yields for high input usage. For the estimates in the past, retrieve those for 1971-1975 and 1996-2000. I average out the 5 years' blocks so to avoid year-specific outliers. The reason is to capture long term changes, which could be contaminated if a certain year faces unusual climate conditions.

The yield estimates for future periods require another parametrical selection: the underlying scenario for which the data is produced and with which climatic (general circulation) model (GCM) the data is produced. As carefully discussed by Costinot et al. (2016), the GAEZ v3.0 database provides such estimates produced with four main GCM, and for several future scenarios. The latter is of key importance: it contains the underlying assumption on how the global carbon emissions are going to evolve in the future so to produce the changes in the climate.

I choose the scenario A1 from the GAEZ database, which is the baseline scenario of Costinot et al. (2016) that matches closely the current standard of severe evolution

Figure A.2: Equivalence between long and longer-run estimates of radiative forcing (proportional to carbon emissions) between SRES and RCP scenarios.



Source: IPCC (2012), chapter 1, Figure 1.15 (left) and Chapter 12, Figure 12.3 (right).

of the global climate for the future: the RCP 8.5.⁵⁵ This scenario assumes a steady increase in carbon stocks in the atmosphere throughout the 21st and 22nd centuries, becoming stable by mid-23rd century. A milder scenario that I use for my robustness checks is the B1, which is similar to the nowadays-standard RCP 4.5. It assumes that the global stock of carbon will peak by late 21st century, becoming stable thereafter.

Agricultural production data. To build a dataset for agricultural production at the location-crop level for 2000, I combine the GAEZ data of production (in tonnes) with the FAOSTAT agricultural production data (country-crop level) and World Bank country GDP data (both in current US\$). First, I use the GAEZ data at the cell-crop level to calculate the share that each cell is observed to produce, of each crop, over its country's total production. Second, I obtain with the FAOSTAT and WB data the share of each country crop production for the years of 2000 to 2010. I average out such shares and multiply them by the country GDP implied by the G-Econ data, so that the unit is consistent with the monetary unit of the model (US\$ PPP). Finally, I multiply the country-crop PPP values by the location-crop shares. For very few locations, the outcome exceeds their total GDP: I then trim the value by 99.99% of its GDP.

Crop price data. The Vulnerability and Assessment Program from the WFP (WFP-VAM) has been collecting prices at various markets (locations within cities) across the developing world since the early 1990s at the monthly basis; I retrieved the prices for all SSA markets from the earliest dates to early 2019. When doing so, I focus on

⁵⁵The GAEZ v3.0 forecasts are based on the Special Report on Emission Scenarios (SRES; see IPCC, 2000). The SRE Scenarios were later updated by IPCC as the RCP scenarios, which are now the standards in the climate community (IPCC, 2012). Figure A.2 illustrates the equivalence between the SRES and RCP scenarios.

Table A.2: Summary statistics of the WFP-VAM price data

	Obs.	Mean	St. Dev.	Min	Pctl(25)	Median	Pctl(75)	Max
<i>All Sample</i>								
Year	173,101	2,012.006	4.578	1,992	2,009	2,013	2,016	2,019
Maize	173,101	0.376	0.484	0	0	0	1	1
Millet	173,101	0.216	0.411	0	0	0	0	1
Sorghum	173,101	0.218	0.413	0	0	0	0	1
Rice	173,101	0.191	0.393	0	0	0	0	1
<i>Market-Crop</i>								
Lenght of Series	2,516	68.800	60.627	1	20.8	53	107	329
Min(Year)	2,516	2,010.331	4.824	1,992	2,007	2,011	2,014	2,018
Max(Year)	2,516	2,016.914	2.070	2,006	2,016	2,018	2,018	2,019
Average crop price (USD)	2,516	0.437	0.243	0.035	0.284	0.377	0.541	2.244
<i>Market</i>								
# Crops	978	2.573	0.940	1	2	2	3	4
<i>Country</i>								
Number of Markets	31	31.548	23.511	1	13.5	25	46	87

maize, millet, sorghum, and rice (the set of crops with the largest temporal and spatial coverage). I geocode each market with Google Maps to subsequently link them to the grid cells by overlaying the former on the latter. Figure 1 shows the wide spatial coverage of the WFP-VAM data for SSA.

Besides, Table A.2 documents summary statistics. The whole data consists of about 173 thousand data points, of which about 37 percent of maize prices (and about 20 percent of the other crops). The data contain about 2,500 market-crop series, on average covering 5 years (68 months) during the 2010s (on average, starting at 2011 and ending at 2018). The data provides crop prices for 978 markets (for about 2 crops, on average) across 31 countries. On average, countries have about 30 markets surveyed.

ITPD-E international trade data. The trade data used in this paper is obtained from the ITPD-E database (Borchert et al., 2021). I collect all available bilateral trade flows, in current US\$, for all country-crops combinations of my study. Consistent with good practice with trade data, I collect import flows rather than exports.⁵⁶ Then, I transform the trade data to monetary unit of my study (US\$ PPP from G-Econ) as follows. First, I calculate the share of trade flows, at the importer-exporter-crop-year levels, over the GDP of of the importing country in each year, in current values. Next, I average out the shares over the 2000-2010 period, so to avoid outliers in the year of

⁵⁶The reason for that is the usual discrepancy between total import and exports at the country-pair-product level. While import flows are registered between country of production and final country of shipment, export data usually register intermediate countries on the trade chain as final destination, biasing the trade flows (Veronese and Tyrman, 2009).

Table A.3: Census waves for SSA countries available from IPUMS

Country	1960s	1970s	1980s	1990s	2000s	2010s
Benin		1979		1992	2002	2010
Botswana			1981	1991	2001	2011
Burkina Faso			1985	1996	2006	
Cameroon		1976	1987		2005	
Ethiopia			1984	1994	2007	
Ghana			1984		2000	2010
Guinea			1983	1996		2014
Kenya	1969	1979	1989	1999	2009	
Lesotho				1996	2006	
Liberia		1974			2008	
Malawi			1987	1998	2008	
Mali			1987	1998	2009	
Mozambique				1997	2007	
Rwanda				1991	2000	2012
Senegal			1988		2002	2013
Sierra Leone					2004	2015
South Africa				1996	2001/07	2011/16
Sudan ¹					2008	
Tanzania			1988		2002	2012
Togo	1960	1970				2010
Uganda				1991	2002	2014
Zambia				1990	2000	2010
Zimbabwe						2012

¹Sudan stands for both Sudan and South Sudan, as both countries were the same in the baseline period of 2000. The IPUMS data for these countries are available for the same year of 2008.

2000. Finally, I multiply the shares at the importer-exporter-crop level by the importer GDP of G-Econ for the year of 2000.

International migration data. I obtain bilateral gross migration flows between SSA countries from [Abel and Cohen \(2019\)](#)'s database. It is a comprehensive source of data on gross migration flows between about 200 x 200 country pairs during 5-years intervals from 1990 to 2015; I filter it for all SSA country pairs for 1990 to 2000.

Internal (within-country) migration data. I construct a bilateral matrix of internal migration flows using census data obtained from the IPUMS International Project from [IPUMS \(2020\)](#). Table [A.3](#) documents the set of country-census waves available. For each of these, I retrieve individual-level data on migration status and location of origin (within the same country). The whole data set, of about 17 million data points, is then aggregated at the subnational region pair level. I use the "Geography & GIS" supplementary data sources in IPUMS to obtain the time consistent boundaries of the subnational regions (or provinces, depending on the country – see [fig. 1](#)). That allows me to calculate long-term changes in potential yields for each of these regions (for [fig. 3](#)) or to match them to grid cells (to obtain total internal migration for [Section 5.4](#)).

Main populated places. I collect the coordinates of the main populated places of SSA from the Populated Places data set from Natural Earth. It consists of a geo-referenced

dataset with the coordinates of about 90 percent of all cities, towns and settlements in the World. I use it to set coordinates for each of the cells of SSA. If a certain cell contains more than one location, I pick the one with the highest population. If another does not have any location to obtain the coordinates, I set them to be the cell's centroid. If any of the centroids are not located in the mainland (e.g., ocean), I set it to be the closest coordinate to the centroid that is on the mainland.

B Theory Appendix

B.1 The producer problem, shipping prices, trade probabilities, price indexes, and consumption shares

Producers in the economy face a perfect competition. Hence, taking all prices as given, a firm/farmer in i produce variety ω of sector k choosing inputs $L_i^k(\omega)$ and $H_i^k(\omega)$ that, subject to production function Equation (1), maximize profits

$$p_{ij}^k(\omega)q_j^k(\omega) - w_iL_i^k(\omega) - r_iH_i^k(\omega), \quad (\text{B.1})$$

where $p_{ij}^k(\omega)$ is the price at destination/consumption location j . This standard Cobb-Douglas producer problem, solved as a cost minimization problem, yields the following unit cost of producing variety ω in i :

$$p_i^k(\omega) = \frac{\bar{c}^k w_i^{\alpha_k} r_i^{1-\alpha_k}}{z_i^k(\omega)}, \quad (\text{B.2})$$

where $\bar{c}^k = \alpha^{-\alpha}(1-\alpha)^{\alpha-1}$. Hence, scaling Equation (B.2) with the bilateral iceberg trade costs between i and a buyer location j , τ_{ij} , yields the bilateral shipping prices between locations in Equation (3). Moreover, the bilateral sectoral trade shares of Equation (6) are equivalent to

$$\lambda_{ij}^k \equiv \mathbb{P} \left(p_{ij}^k \leq \min_{s \neq i} \{ p_{sj}^k \} \right), \quad (\text{B.3})$$

that is, the probability that i is the cheapest supplier of sector k goods to destination j .⁵⁷ The distributional assumptions on z_i^k that conditional trade probabilities for a

⁵⁷Note that sectoral varieties become symmetric conditional on productivities, which allows us to disregard the ω index and focus on the location pair-sector dimension.

given price p , $\lambda_{ij}^k(p)$, are also distributed extreme value:

$$\lambda_{ij}^k(p) = \mathbb{P} \left(p = p_{ij}^k \leq \min_{s \neq i} p_{sj}^k \right) = \prod_{s \neq i} \mathbb{P} \left(p_{sj}^k \geq p \right) = \prod_{s \neq i} \left[1 - G_{sj}^k(p) \right] = e^{\Phi_j^{k,-i} p^{-\zeta_k}}, \text{ where}$$

$$\Phi_j^{k,-i} = \sum_{s \neq i} b_s^k A_s^k \left(\bar{c}^k w_s^{\alpha_k} r_s^{1-\alpha_k} \tau_{sj} \right)^{-\zeta_k}$$

Following Eaton and Kortum (2002), integrating over $p \in \mathbb{R}_+$ yields λ_{ij}^k :

$$\begin{aligned} \lambda_{ij}^k &= \int_0^\infty \lambda_{ij}^k(p) d\mathbb{P} \left(p_{ij}^k \leq p \right) dp \\ &= \int_0^\infty e^{\Phi_j^{k,-i} p^{-\zeta_k}} \times e^{b_i^k A_i^k \left(\bar{c}^k w_i^{\alpha_k} r_i^{1-\alpha_k} \tau_{ij} \right)^{-\zeta_k} p^{-\zeta_k}} (-\zeta_k) p^{\zeta_k-1} b_i^k A_i^k \left(\bar{c}^k w_i^{\alpha_k} r_i^{1-\alpha_k} \tau_{ij} \right)^{-\zeta_k} dp \\ &= b_i^k A_i^k \left(\bar{c}^k w_i^{\alpha_k} r_i^{1-\alpha_k} \tau_{ij} \right)^{-\zeta_k} / \Phi_j^k, \text{ where} \end{aligned} \quad (\text{B.4})$$

$$\Phi_j^k = \sum_{i \in S} b_i^k A_i^k \left(\bar{c}^k w_i^{\alpha_k} r_i^{1-\alpha_k} \tau_{ij} \right)^{-\zeta_k}. \quad (\text{B.5})$$

Moreover, the CES utility over varieties with elasticity of substitution $\eta_k < 1 + \zeta_k \forall k$ yields sectoral price indexes at destination j as:

$$\begin{aligned} P_j^k &= \left(\int_0^1 p_j^k(\omega)^{1-\eta_k} d\omega \right)^{1/1-\eta_k} \\ &= \Gamma^k \left(\Phi_j^k \right)^{1/\zeta_k}, \text{ where} \\ \Gamma^k &= \left[\Gamma \left(\frac{1-\eta_k}{\zeta_k} + 1 \right) \right]^{1/1-\eta_k} \end{aligned} \quad (\text{B.6})$$

is a constant and $\Gamma(a)$ is the Gamma function. Note that Equation (B.6) is equivalent to Equation (7); plugging it into Equation (B.4) yields Equation (6).

Sectoral consumption shares. These follow standard CES properties. Starting with crops, workers at j maximize welfare with respect to crop consumption by solving:

$$\max_{\{C_j^k\}_k} C_j \quad \text{s. to} \quad \sum_{k \neq K} P_j^k C_j^k \leq \mu^a v_j, \quad ,$$

where C_j is (implicitly) defined in eq. (11), C_j^k are the sectoral CES composites in eq. (5), and μ^a is j 's expenditure share in agriculture (i.e., crops). Then, rearranging the first order conditions yields $C_j^k / C_j^{k'} = \left(P_j^k / P_j^{k'} \right)^{-\gamma^a}$. Then, by defining Ξ_j^k as the share of j 's agricultural expenditure on crop $k \neq K$ goods (and making use of the

$C_j^k/C_j^{k'}$ ratio), one obtains:

$$\Xi_j^k = \frac{P_j^k C_j^k}{\sum_{k' \neq k} P_j^{k'} C_j^{k'}} = \left(P_j^k / P_j^a \right)^{1-\gamma_a} \quad \forall i, j,$$

where the last equation takes advantage of the definition of the agricultural price index from eq. (10). Note that, for the upper CES nest (choice between agricultural and non-agricultural consumption bundles), the derivation is analogous but with the additional income effect following Comin et al. (2021).

B.2 Derivation of migration shares

Take the definition of the welfare attained by a worker v living in i and moving to j as $W_{ij}(v) = (w_j/P_j)\bar{m}_{ij}^{-1}\varepsilon_j(v)$, $\varepsilon_i \sim G_j(v) = e^{-v^{-\theta}u_jL_j^{-\alpha}}$. Following Eaton and Kortum (2002), one can obtain the distribution of the welfare from one specific location i as

$$A_{ij}(w) \equiv \mathbb{P}(W_{ij} \leq w) = G_j(wP_j\bar{m}_{ij}/w_j) = e^{-(wP_j\bar{m}_{ij}/w_j)^{-\theta}u_jL_j^{-\alpha}}.$$

Thus, the joint distribution of welfare of all destinations s from i can be derived as

$$A_i(w) = \prod_{s \in S} e^{-(wP_s\bar{m}_{is}/w_s)^{-\theta}u_sL_s^{-\alpha}} = e^{-\Phi_i \times w^{-\theta}}, \quad \text{where } \Phi_i = \sum_{s \in S} (P_s\bar{m}_{is}/w_s)^{-\theta}u_sL_s^{-\alpha}.$$

Now, recalling the share of workers moving from i to j is equivalent to the probability that the welfare attained by moving to j , w , is the highest among all other possible s destinations, one writes

$$\Pi_{ij}(w) = \mathbb{P}\left(W_{ij}(v) \equiv w \geq \max\{W_{is}(v)\}_{s \neq j}\right) = \prod_{s \neq j} \mathbb{P}(W_{is} \leq w) = e^{-\Phi^{-j} \times w^{-\theta}}.$$

With that, it is possible to obtain the unconditional probability Π_{ij} by integrating over all possible values of $w \in \mathbb{R}_+$, i.e.

$$\begin{aligned} \Pi_{ij} &= \int_0^\infty \Pi_{ij}(w) d\mathbb{P}(W_{ij} \leq w) dw \\ &= \int_0^\infty e^{-\Phi^{-j} \times w^{-\theta}} \times e^{(wP_j\bar{m}_{ij}/w_j)^{-\theta}u_jL_j^{-\alpha}} \times (-\theta)w^{-\theta-1}(P_j\bar{m}_{ij}/w_j)^{-\theta}u_jL_j^{-\alpha} dw \\ &= \frac{(w_j/P_j)^\theta \bar{m}_{ij}^{-\theta} u_j L_j^{-\alpha}}{\sum_{s \in S} (w_s/P_s)^\theta \bar{m}_{is}^{-\theta} u_s L_s^{-\alpha}}, \end{aligned}$$

which is the equivalent of eq. (18).

B.3 Spatial equilibrium

Given the geography $\mathcal{G}(S)$ and the parameters $\Theta \equiv \{\Omega_k, \eta_k, \gamma_a, \epsilon_k, \alpha_k, \zeta_k, \sigma, \theta, \beta\}$, a spatial equilibrium is a vector of factor prices and labor allocations $\{w_j, r_j, L_j\}_{j \in S}$ such that eqs. (7), (10), (12) to (14) and (19) hold, and markets for goods clear. Formally, market clearing requires trade-balancing, such that each j 's income equals total exports to and total imports from all locations $i \in S$, as in Equation (20). In fact, by using eq. (14) on (20), one characterizes the spatial equilibrium with the following system of $7 \times N$ equations and unknowns:

$$v_j L_j = \sum_{i \in S} \sum_{k \neq K} b_i^k A_i^k \left(\Gamma^k \bar{c}^k w_i^{\alpha_k} r_i^{1-\alpha_k} \tau_{ij} / P_j^k \right)^{-\zeta_k} \left(\frac{P_j^k}{P_j^a} \right)^{1-\gamma_a} \Omega^a \left(\frac{P_j^a}{P_j} \right)^{1-\sigma} \left(\frac{v_j}{P_j} \right)^{\epsilon_a - (1-\sigma)} v_j L_j +$$

$$+ \sum_{i \in S} b_i^K A_i^K \left(\Gamma^K \bar{c}^K w_i^{\alpha_K} r_i^{1-\alpha_K} \tau_{ij} / P_j^K \right)^{-\zeta_K} \Omega^K \left(\frac{P_j^K}{P_j} \right)^{1-\sigma} \left(\frac{v_j}{P_j} \right)^{\epsilon_K - (1-\sigma)} v_j L_j \quad (\text{B.7})$$

$$P_j = \left(\sum_{k \in \{a, K\}} \left(\Omega^k (P_j^k)^{1-\sigma} \right)^{\frac{1-\sigma}{\epsilon_k}} \left(\mu_j^k v_j^{1-\sigma} \right)^{\frac{\epsilon_k - (1-\sigma)}{\epsilon_k}} \right)^{\frac{1}{1-\sigma}} \quad (\text{B.8})$$

$$P_j^k = \Gamma^k \left(\sum_{i \in S} b_i^k A_i^k \left(\bar{c}^k w_i^{\alpha_k} r_i^{1-\alpha_k} \tau_{ij} \right)^{-\zeta_k} \right)^{-1/\zeta_k} \quad (\text{B.9}) \quad P_j^a = \left(\sum_{k \neq K} (P_j^k)^{1-\gamma_a} \right)^{\frac{1}{1-\gamma_a}} \quad (\text{B.12})$$

$$L_j = \sum_{i \in S} \frac{(v_j / P_j)^\theta \bar{m}_{ij}^{-\theta} u_j L_j^{-\alpha}}{\sum_{s \in S} (v_s / P_s)^\theta \bar{m}_{is}^{-\theta} u_s L_s^{-\alpha}} \times L_i^0 \quad (\text{B.10}) \quad v_j = w_j + (r_j H_j) / L_j \quad (\text{B.13})$$

$$\mu_j^k = \Omega^k \left(P_j^k / P_j \right)^{1-\sigma} \left(v_j / P_j \right)^{\epsilon_k - (1-\sigma)} \quad (\text{B.11})$$

Existence and Uniqueness. My model is not isomorphic to the general set up of [Allen and Arkolakis \(2014\)](#) and, as a consequence, the existence and uniqueness of the equilibrium cannot be guaranteed under their conditions for such. The reason for that is the additional non-linearity introduced by the middle- and upper-level CES structures. I address that by solving my model for several parametric choices, starting from many different initial guesses. The solution is invariant across all cases.

B.4 Numerical algorithm for solving the model

I find $\{w_j, r_j, L_j\}_{j \in S}$ that solves for the spatial equilibrium characterized by the system of equations (B.7) to (B.13) with an algorithm that nests three loops in one another.

Inner loop. I start with a guess for $\{w_j, r_j, L_j\}_j$ and solve for sectoral price indexes in eqs. (B.9) and (B.12). Then, with a guess for $\{P_j\}_j$, I iterate over eqs. (B.8) and (B.11)

to find a simultaneous solution for $\{P_j, \mu_j^k\}_{j,k}$. In particular, with the guess for $\{P_j\}_j$, I solve for $\{\mu_j^k\}_k$ in eq. (B.11), replace it on eq. (B.8) to update solve for $\{P_j\}_j$, and iterate until both solutions converge.

Middle loop. I use the solution for $\{P_j^k, P_j^a, P_j, \mu_j^k\}_{j,k}$ and the guesses for $\{w_j, r_j, L_j\}_j$ in eq. (B.13) and (B.7) to update $\{w_j, r_j\}_j$.⁵⁸

Outer loop. I use the solution of $\{w_j, r_j, P_j\}_j$ and the guess for $\{L_j\}_j$ in eq. (B.10) to obtain an update for $\{L_j\}_j$, iterating it until the solution converges.

I then replace the solutions for $\{w_j, r_j, L_j\}_j$ back in the inner loop and repeat the procedure above until all solutions converge to a fixed point.

B.5 Details of the economy represented as line

The illustration of the model mechanisms in Section 4.2 represents the economy as a line with a discrete number of locations. To make the exposition of these mechanisms the cleanest possible, I make the economy as homogeneous as possible in many fundamentals, like amenities and land endowments. For the latter, I take a further simplification step: I disregard land as a factor, which implies that labor (wages) is the only factor (rent) in the economy.⁵⁹ Hence, to make the consumption choices of agents consistent (and more transparent) with new setting, I change the lower CES tier to a pure Armington set-up where the CES for local varieties, η_k , disciplines the trade elasticity of the economy.⁶⁰

B.6 Model quantification

I quantify the parameters and fundamentals related to technology and location choice in two different steps, each consisting of a two-stage procedure.

B.6.1 Technology

Conditional on parameters from the literature and fundamentals observed from the data, this step quantifies $\mathbf{t} \equiv \{\tau_{ij}^F, \delta\}$ and $\mathbf{T} \equiv \{\{A_i^K\}_i, \{b_i^k\}_{i,k}, \{\Omega_a, \Omega_K\}\}$ with a two-stage procedure (with the inner stage nested on the outer). Specifically, the first stage (inner loop), guesses values for \mathbf{t} and quantify \mathbf{T} by inverting the general equilibrium conditions of the model. Then, the second stage (outer loop) estimates $\hat{\mathbf{t}}$ with a GMM

⁵⁸For that, I use the Cobb-Douglas fixed proportion of factor bills. For the case of labor rents, that implies $w_j L_j = \sum_k \alpha_k X_j^k$, which can be solved for w_j (X_j^k is the right-hand side of eq. (B.7)).

⁵⁹In practice, it implies weaker dispersion forces vis-à-vis the full-fledged model.

⁶⁰That is, $\lambda_{ij}^k = (p_{ij}^k / P_j^k)^{\eta_k} = (w_i^k \tau_{ij} / A_i^k P_j^k)^{\eta_k}$, while equations (B.7) to (B.13) remain nearly identical.

that targets model-generated moments to their data counterparts conditional on the first stage.

Inner loop. With a guess on $\hat{\mathbf{t}}$, it finds $\mathbf{T} \equiv \{\{A_i^K\}_i, \{b_i^k\}_{i,k}, \{\Omega_a, \Omega_K\}\}$ such that make the model perfectly match, respectively, the spatial distribution of nominal income $\{v_j L_j\}_j$, the spatial-sector distribution of production $\{X_j^k\}_{j,k}$, and the aggregate sectoral expenditure ratios X^K / X^a . The model counterpart of these moments are:

$$v_j L_j = \sum_{i \in S} \sum_{k \neq K} \lambda_{ji}^k \Xi_i^k \mu_i^a v_i L_i + \sum_{i \in S} \lambda_{ji}^K \mu_i^K v_i L_i \quad (\text{B.14})$$

$$X_j^k = \sum_{i \in S} \lambda_{ji}^k \Xi_i^k \mu_i^a v_i L_i \quad \forall k \neq K \quad (\text{B.15})$$

$$X_j^K = \sum_{i \in S} \lambda_{ji}^K \mu_j^K v_i L_i \quad (\text{B.16})$$

$$X_K / X^a = \frac{\sum_{j \in S} \sum_{i \in S} \lambda_{ji}^K \mu_i^K v_i L_i}{\sum_{k \neq K} \sum_{j \in S} \sum_{i \in S} \lambda_{ji}^k \Xi_i^k \mu_i^a v_i L_i}. \quad (\text{B.17})$$

Then, one can invert each of the equations above to obtain the expressions for the unobserved fundamentals of interest. For instance, for $\{A_j^K\}_j$, one inverts eq. (B.14) to obtain:

$$\begin{aligned} v_j L_j &= \sum_{i \in S} \sum_{k \neq K} \lambda_{ji}^k \Xi_i^k \mu_i^a v_i L_i + \sum_{i \in S} b_j^K A_j^K \left(\Gamma^K \bar{c}^K w_j^{\alpha_K} r_j^{1-\alpha_K} \tau_{ji} / P_i^K \right)^{-\xi_K} \mu_i^K v_i L_i \rightarrow \\ A_j^K &= \frac{v_j L_j - \sum_{i \in S} \sum_{k \neq K} \lambda_{ji}^k \Xi_i^k \mu_i^a v_i L_i}{\sum_{i \in S} b_j^K \left(\Gamma^K \bar{c}^K w_j^{\alpha_K} r_j^{1-\alpha_K} \tau_{ji} / P_i^K \right)^{-\xi_K} \mu_i^K v_i L_i}. \end{aligned} \quad (\text{B.18})$$

Importantly, I do not observe factor prices $\{w_i, r_i\}_i$ from the data, but rather nominal incomes $\{v_i\}_i$, sectoral production $\{X_i^k\}_{i,k}$, land endowments \mathcal{H} , and sectoral allocation of land $\{H_i^k\}_{i,k}$.⁶¹ With that, I obtain $\{w_i, r_i\}_i$ with:

$$\begin{aligned} X_i^K &= r_i H_i^K / (1 - \alpha_K) \rightarrow \\ r_i &= X_i^K \times (1 - \alpha_K) / H_i^K, \text{ and} \end{aligned} \quad (\text{B.19})$$

$$\begin{aligned} v_i L_i &= w_i L_i + r_i H_i \rightarrow \\ w_i &= v_i - (r_i H_i) / L_i, \end{aligned} \quad (\text{B.20})$$

where eq. (B.19) comes from the fixed factor proportion from the Cobb-Douglas pro-

⁶¹I measure sector-cell-level data on land usage $\{H_i^k\}_{i,k}$ also from GAEZ. Specifically, I retrieve harvested land for all crops of my setting by overlaying (and aggregating) my grid into the GAEZ harvested land data. Then, I obtain $H_i^K = H_i - \sum_{k \neq K} H_i^k \forall i$.

duction function.⁶² Then, analogous to eq. (B.18), I invert eqs. (B.15) to (B.17) with:

$$b_j^k = X_j^k \times \left[\sum_{i \in S} A_j^k \left(\Gamma^k \bar{c}^k w_j^{\alpha_k} r_j^{1-\alpha_k} \tau_{ji} / P_i^k \right)^{-\zeta_k} \Xi_i^k \mu_j^a v_i L_i \right]^{-1} \quad \forall k \neq K \quad (\text{B.21})$$

$$b_j^K = X_j^K \times \left[\sum_{i \in S} A_j^K \left(\Gamma^K \bar{c}^K w_j^{\alpha_K} r_j^{1-\alpha_K} \tau_{ji} / P_i^K \right)^{-\zeta_K} \mu_j^K v_i L_i \right]^{-1} \quad (\text{B.22})$$

$$\Omega_K / \Omega_a = \frac{X^K}{X^a} \times \frac{\sum_{k \neq K} \sum_{j \in S} \sum_{i \in S} \lambda_{ji}^k \Xi_i^k (P_i^a / P_i)^{1-\sigma} (v_i / P_i)^{\varepsilon_a - (1-\sigma)} v_i L_i}{\sum_{j \in S} \sum_{i \in S} \lambda_{ji}^K (P_i^K / P_i)^{1-\sigma} (v_i / P_i)^{\varepsilon_K - (1-\sigma)} v_i L_i}. \quad (\text{B.23})$$

The inversion algorithm finds $\{A_j^K, \{b_j^k\}_{j,k}, \Omega_K / \Omega_a\}$ such that eqs. (B.18) and (B.21) to (B.23) hold simultaneously. However, because $\{b_j^K\}_j$ and $\{A_j^K\}_j$ cannot be separated out in levels, I normalize the latter to one and identify their product in eq. (B.22). That also gives me tractability, as then eq. (B.18) is not needed anymore for inverting the spatial equilibrium.⁶³ To solve this high-dimensional problem, I proceed as follows: with a guess for $\{b_j^k\}_{j,k}$, I solve for Ω_K / Ω_a in eq. (B.23). I then plug the solution in eqs. (B.21) and (B.22) (embedded in $\{\mu_j^k\}_{j,k}$) to solve for $\{b_j^k\}_{j,k}$. I iterate it until all solutions converge; I represent it, conditional on a guess for \mathbf{t} , as $z(\mathbf{T}; \mathbf{t}) = 0$.

Outer loop. Conditional on $z(\mathbf{T}; \mathbf{t}) = 0$, I estimate $\mathbf{t} \equiv \{\tau_{ij}^F, \delta\}$ with a GMM. For that, I design moments that provide the identifying variation for the parameters of interest and that are observable in the data. Specifically, these are:

$$m_1 = \sum_c \sum_{c'} \sum_{i \in c} \sum_{j \in c'} \sum_k X_{ij}^k, \text{ and} \quad (\text{B.24})$$

$$m_2 = \left[\frac{\sum_{j,k \in \mathcal{D}} (P_j^k - \bar{P})^2}{N(\mathcal{D})} \right]^{1/2}, \quad (\text{B.25})$$

that is, aggregate export flows and the dispersion (standard deviation) of sectoral price indexes.⁶⁴ Note that m_1 provides the required variation for identifying due to the (intuitive) decreasing relationship between bilateral trade flows and tariffs τ^F (i.e., larger tariffs, less international trade). Moreover, the identification of δ relies on the positive relationship between trade frictions and price dispersion in m_2 . That is, the

⁶²Importantly, all monetary values, built from the data in US\$ PPP units (see Section 2), are further normalized to the wages of the first location w_1 . This is done as I am not able to pin down levels in my quantification, but instead the spatial distribution of fundamentals up to a normalization.

⁶³In particular, that equation holds by construction if eqs. (B.21) and (B.22) hold simultaneously.

⁶⁴Note that \mathcal{D} is the set of location-crop combinations for which the WFP-VAM data provide data for. Moreover, $N(\mathcal{D})$ and \bar{P} are the size and mean of this set, respectively. Analogously, m_1 is calculated with the country pair-crop combinations with export data available from the ITPD-E trade data.

lowest δ , the lower the degree of trade frictions in the economy and, as a consequence, the more homogeneous would price indexes be across space (hence, less dispersion). Importantly, the WFP-VAM price data provides time varying data between 2000 and 2018; I discuss how I decompose these location-crop time series so to match the static feature of my model (and thus, sectoral price indexes $\{P_j^k\}_{i,k}$) in Appendix B.7.

I estimate \mathbf{t} by defining $\mathbf{m} = [m_1, m_2]$ and $g(\mathbf{t}) = [\mathbf{m}(\mathbf{t}) - \mathbf{m}^{\text{data}}]$ and solving for $\hat{\mathbf{t}}$ that, based on $\mathbb{E}[g(\mathbf{t})] = 0$, satisfies:

$$\hat{\mathbf{t}} = \arg \min_{\mathbf{t}} g(\mathbf{t})' W g(\mathbf{t}) \text{ subject to } z(\mathbf{T}; \mathbf{t}) = 0, \quad (\text{B.26})$$

where W is the weighting matrix.⁶⁵ I solve for $\hat{\mathbf{t}}$ with a bidimensional grid search over τ^F and δ values and infer standard errors by bootstrapping it ten thousands iterations.⁶⁶ Table 2 documents the estimation results.

Besides, Figure B.1 Panel A plots the grid search results (with the log objective function $g(\mathbf{t})' W g(\mathbf{t})$ evaluated at different δ and τ^F pairs). It shows a non-linear relationship between the two parameters and the objective function, as well as a "valley-looking region" along the diagonal where the solution lies on.⁶⁷ Moreover, Panels C and D show slices of the objective function evaluated for a fixed δ or τ^F . They convey the relevance of the designed moments in terms of providing identifying variation for the parameters of interest. In particular, Panel D shows that, for a given τ^F , the objective function is U-shaped along the δ dimension (and hence that the relationship between δ and price dispersion is monotonic, as expected).

B.6.2 Location choice

I proceed with an analogous two-stage step where $\mathbf{T} \equiv \{u_i, m_c\}_{i,c}$ and $\mathbf{t} \equiv \phi$.

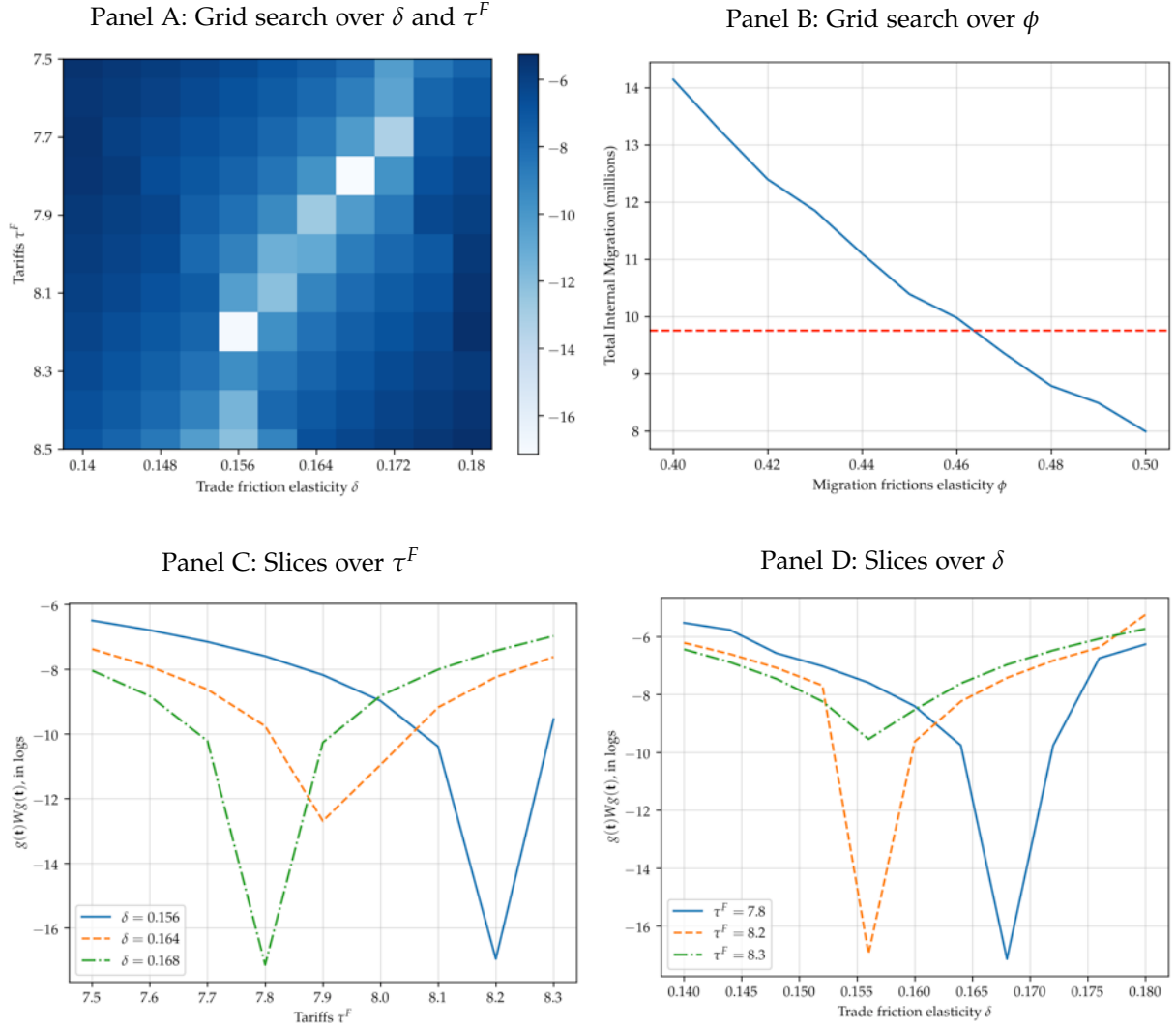
Inner loop. It solves for $\{u_i\}_i$ and $\{m_c\}_c$ conditional on all previously quantified parameters and fundamentals, a guess for \mathbf{t} , and the observed following endogenous variables: population $\{L_i\}_i$ and country-level total inflow of foreign migrants, $\{L_c\}_c$ (from Abel and Cohen, 2019, between 1990 and 2000, where 1990 is the earliest period available for SSA). In practice, I use eq. (19) to calculate L_c and invert it to obtain an expression for country barriers as a function of L_c and other endogenous variables

⁶⁵I choose W to be the identity matrix due to the high non-linearity of my moments (thus, the complexity of their Jacobian and Hessian matrices).

⁶⁶Grid search methods can easily lead to curse of dimensionality and global-local optima issues. However, my model requires that tariffs and trade costs are both non negative; which restricts the parametric space for the search. I also rule out global-local optima tradeoffs by running a coarse search over large intervals and then narrowing down the search within the minimum of this coarse search.

⁶⁷Importantly, it shows the result of a fine search around an area that, from a coarser search, is identified as the global optimum region (see footnote 66).

Figure B.1: Results of the outer loops that solve for τ^F , δ , and ϕ



Notes: Panel A: Grid search over δ (x-axis) and τ_{ij}^F (y-axis) with the colored evaluation of the objective function (in logs) for each of these pairs. Panel B: analogous grid search over ϕ and the resulting model-generated internal migration flows (the dashed red line stands for observed total internal migration flows from IPUMS data). Panel C (D) shows slices of A evaluated at fixed values δ (τ^F).

and fundamentals as follows:

$$L_c = \sum_{j \in c} \sum_{i \notin c} \frac{(v_j/P_j)^\theta m_{ij}^{-\theta} m_{c(j)}^{-\theta} u_j}{\sum_{s \in c(j)} (v_s/P_s)^\theta m_{is}^{-\theta} u_s + \sum_{s \notin c(j)} (v_s/P_s)^\theta m_{is}^{-\theta} m_{c(s)}^{-\theta} u_s} L_{i0} \rightarrow$$

$$m_c = \left[L_c^{-1} \times \sum_{j \in c} \sum_{i \notin c} \frac{(v_j/P_j)^\theta m_{ij}^{-\theta} u_j}{\sum_{s \in c(j)} (v_s/P_s)^\theta m_{is}^{-\theta} u_s + \sum_{s \notin c(j)} (v_s/P_s)^\theta m_{is}^{-\theta} m_{c(s)}^{-\theta} u_s} L_{i0} \right]^{1/\theta} \quad (\text{B.27})$$

Note that the denominator in the equations above is equivalent to eq. (19)'s – it separates the inter/intranational bilateral choices to illustrate the identification of parame-

ters later on. Analogously, I invert eq. (B.10) to pin down amenities $\{u_j\}_j$ as a function of population distribution and other endogenous variables and fundamentals:

$$u_j = L_j \times \left[\sum_{i \in \mathcal{C}(j)} \frac{(v_j/P_j)^\theta m_{ij}^{-\theta}}{\sum_{s \in \mathcal{C}(j)} (v_s/P_s)^\theta m_{is}^{-\theta} u_s + \sum_{s \notin \mathcal{C}(j)} (v_s/P_s)^\theta m_{is}^{-\theta} m_{c(s)}^{-\theta} u_s} L_{i0} + \sum_{i \notin \mathcal{C}(j)} \frac{(v_j/P_j)^\theta m_{ij}^{-\theta} m_{c(j)}^{-\theta}}{\sum_{s \in \mathcal{C}(j)} (v_s/P_s)^\theta m_{is}^{-\theta} u_s + \sum_{s \notin \mathcal{C}(j)} (v_s/P_s)^\theta m_{is}^{-\theta} m_{c(s)}^{-\theta} u_s} L_{i0} \right]^{-1} \quad (\text{B.28})$$

I solve eqs. (B.27) and (B.28) as follows: with a guess for $\{u_j\}_j$, I solve for $\{m_c\}_c$ in eq. (B.27), plug it in eq. (B.28) to solve for $\{u_j\}_j$, and iterate it until all solutions converge. Importantly, I am able to separate out $\{u_j\}_j$ from $\{m_c\}_c$ because location pairs can refer to either intra or international migration. That is, conditional on a guess of $\{u_j\}_j$, there are distinct origins s for which a destination j stand for one type of migration of the other (the denominator of eq. (B.27)), and thus where amenities multiplies or not the country migration barriers $\{m_c\}_c$. Considering all possible origins s and destinations j in S , there is at least one pair for which they do and do not multiply one another, which then allows me to separately identify them.

Outer loop. The outer loop estimates $\mathbf{t} \equiv \phi$ similarly to Equation (B.26) but finding $\hat{\phi}$ such that the model-generated internal migration flows, $L^D = \sum_{c \in \mathcal{C}} \sum_{j \in \mathcal{C}} \sum_{i \in \mathcal{C}} L_{ij}$, matches the observed internal migration flows between 1990 and 2000 from IPUMS.⁶⁸ Figure B.1 Panel B shows the results of the grid search, displaying the intuitive decreasing relationship between ϕ and internal migration in the economy.

B.7 Mapping the time-varying price data into the static model prices

A challenge to link the sectoral prices $\{P_j^k\}_{j,k}$ to their empirical counterpart from the WFP-VAM data is the "static-dynamic mismatch" between them: while the former is static (due to the static aspect of the model), the latter is time-varying (due to the long location-crop price series available for numerous locations across SSA). The most immediate approach to overcome it is restricting the price data within a time window that is the closest to the baseline period of my quantification, the year of 2000.

This approach implies two drawbacks. First, it restricts the data to a narrow subset with a poor geographical coverage. Second, and most importantly, it incorporates location-crop-time specific shocks at that specific period that could pollute the resulting aggregate price dispersion used in Appendix B.6.1.⁶⁹ To avoid that, I propose a

⁶⁸Hence, \mathcal{C} is the set of countries for which migration data is available in IPUMS.

⁶⁹For instance, spatially heterogeneous incidence of droughts by 2000 (or before) could inflate the

time series decomposition approach that, by exploiting the long longitudinal characteristic of each location-crop series, nets them out of these shocks and retrieves a time invariant, location-crop component that maps into $\{P_j^k\}_{j,k}$.

More specifically, I first aggregate the market-crop-level price series at the grid cell-crop level by averaging crop prices across markets that belong to the same grid cell. While in principle this could add noise to the data, in practice the observed prices across markets evolve quite homogeneously in levels and trends within grid cell-crop pairs. Figure B.2 Panels A and B illustrate that for markets located at a common grid cell, one in Mali and another in Malawi, respectively. I define these observed location-crop-time (year-month t) price series as $\tilde{P}_{j,t}^k$ and assume it evolves as:

$$\tilde{P}_{j,t}^k = a_{c(j)} \times t + b_{c(j) \times m(t)} + \overbrace{c_j^k}^{\equiv P_j^k} + \varepsilon_{j,t}^k, \quad (\text{B.29})$$

where $a_{c(j)} \times t$ is a set of country-specific time trends that account for secular evolution in crop prices that are common for all markets j in the same country $c(j)$. Moreover, $b_{c(j) \times m(t)}$ are country-month of the year (e.g., January or February) fixed effects that account for country-specific cyclicity on crop production and prices. Finally, $c_j^k \equiv P_j^k$ are location-crop fixed effects that absorb the common $j \times k$ component of the price series. Hence, it is the empirical counterpart of the theoretical prices $\{P_j^k\}_{j,k}$: it contains the time invariant, location-crop specific component of prices at each observed $j \times k$ combination (net of the shocks over their time series).⁷⁰

I estimate Equation (B.29) with the WFP-VAM price data and retrieve \hat{c}_j^k as the observed $\{P_j^k\}_{j,k}$. Figure B.2 Panels C and D illustrate the result for the two locations j in Mali and Malawi (from Panels A and B, respectively). They also contrast \hat{c}_j^k to a naive approach of averaging out prices along the grid cell-crop dimension ("Mean prices"). Because of the increasing trend in prices over time, averages are upward biased vis-à-vis \hat{c}_j^k (that account for this secular trends). In fact, some \hat{c}_j^k have negative values – while counterintuitive if thinking of negative prices, this makes sense for the purpose of my exercise (that aims at exploiting (spatial) within-country differences in prices). Hence, not accounting for the components in Equation (B.29) overestimates the magnitude of prices. That would, in turn, underestimate the aggregate dispersion of prices across space and, as a consequence, the estimated δ .

observed price dispersion, hence underestimating δ .

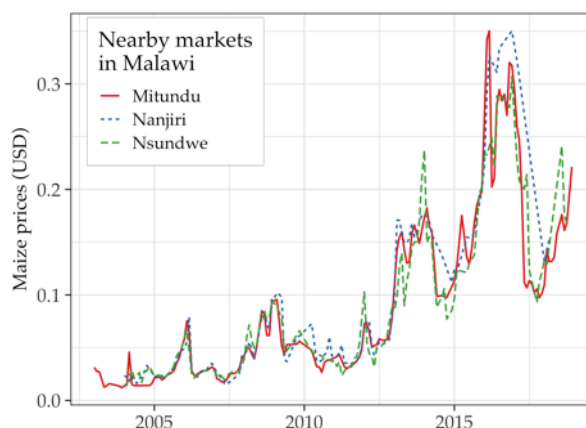
⁷⁰Importantly, idiosyncratic shocks to prices – such as weather shocks – are accounted for, but with the underlying assumption that they are normally distributed and have expectation equal to zero (in the error term $\varepsilon_{j,t}^k$) at the $j \times k$ level.

Figure B.2: WFP-VAM raw data, matching to grid cells, and price decomposition

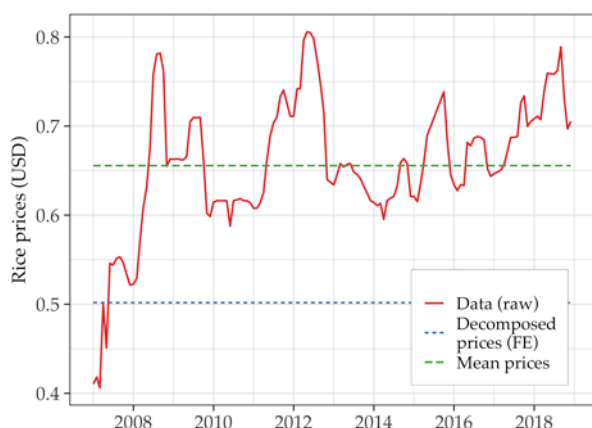
Panel A: Markets in the same grid cell in Mali



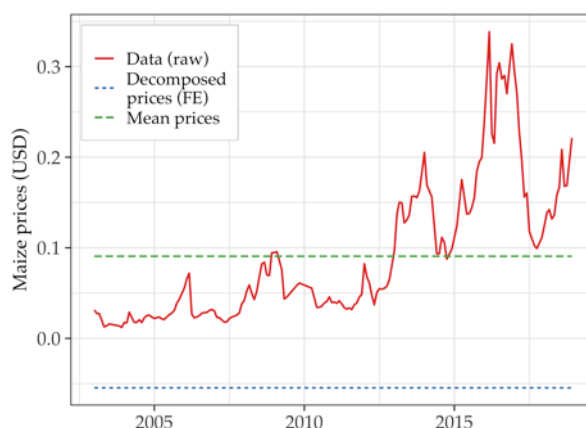
Panel B: Markets in the same grid cell in Malawi



Panel C: Decomposed cell-level average prices



Panel D: Decomposed cell-level average prices



Notes: Panels A and B plot two samples of crop prices in markets within common grid cells (in Mali and Malawi, respectively). Panels C and D show how the grid cell-level average (i.e., across markets within grid cells over time) crop prices are decomposed into a location-crop time invariant component $\bar{c}_j^k \equiv P_j^k$ and contrasts it to the unconditional mean along each $j \times k$ time series (“Mean prices”).

B.8 Discussion of the parameters taken from the literature

Lower CES tier. The values taken for $\{\eta_k\}_k$ come from [Costinot et al. \(2016\)](#) and [Bernard et al. \(2003\)](#) for crops and non-agriculture, respectively. These values are widely used in other applications in the literature (e.g. [Desmet et al., 2018](#), for η_K). They nevertheless are estimated in global (or cross-country) settings. Assuming different values for $\{\eta_k\}_k$ (say, substitution of varieties within countries being more intense than across countries) would mainly affect the model-generated trade flows, and consequently the levels of the parameters associated to trade frictions.

Middle CES tier. The value $\gamma_a = 2.5$ comes from [Sotelo \(2020\)](#), who studies rural Peru by early 2000s and focus on intranational trade in that country. Thus, it stands for a context similar to rural SSA as of 2000.

Upper CES tier (and Ω_k shifters). The values for $\{\varepsilon_k\}$ and σ come from the global estimation of [Comin et al. \(2021\)](#) (and are particularly close to [Nath \(2022\)](#)'s estimates). These values therefore reflect preferences between agricultural and non-agricultural goods from a global representative consumer. Thus, the values can underestimate the subsistency aspect of agricultural goods in SSA, where the negative slope of the Engel curve could be steeper vis-à-vis the rest of the world. If so, then, my results would underestimate the welfare losses associated to that mechanism. In fact, the estimated $\{\Omega_k\}_{a,K}$ reflects that: I quantify a relative Ω_a/Ω_K that is about twice the estimates from [Nath \(2022\)](#) for the global economy, reflecting that expenditures in agriculture are much more pronounced in SSA vis-à-vis the global economy.⁷¹

B.9 Discussion of the estimated trade and migration frictions

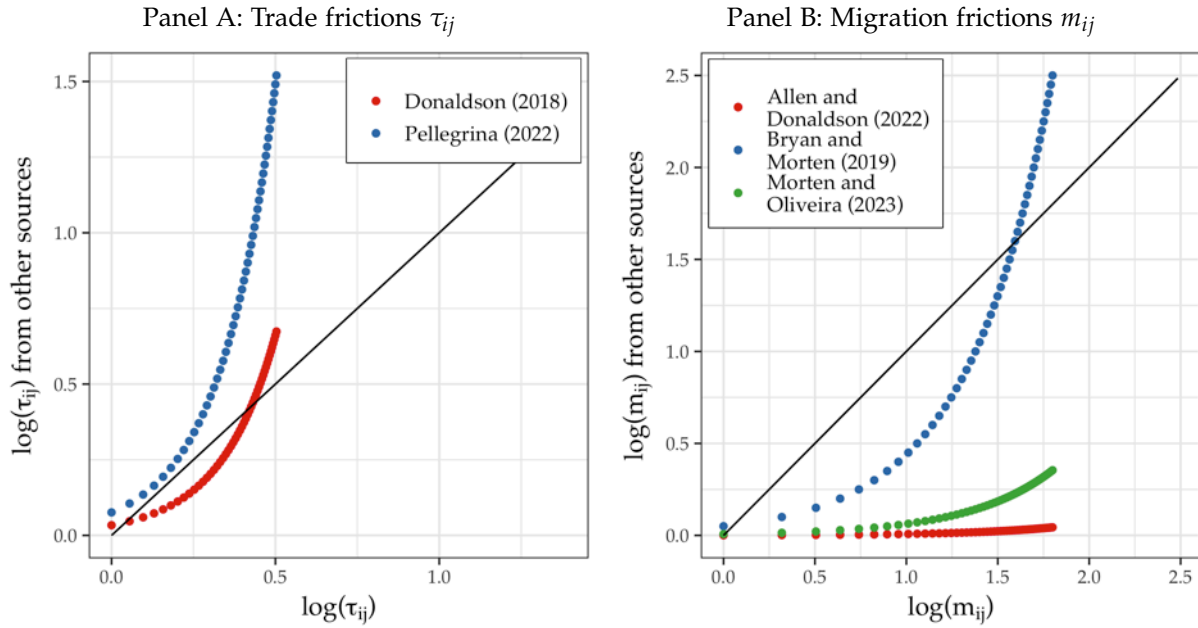
In what follows, I benchmark trade and migration frictions quantified in Section 5 with estimates from related literature. This exercise is relevant due to the different approaches from these studies (in terms of functional format or units of distance), which hinders a direct comparison between their estimates and mine. When comparing them, I also stress the reasons and advantages of my modeling choices.

Trade frictions. Many studies estimate the relationship between distance and trade frictions for developing contexts (e.g. [Donaldson, 2018](#); [Sotelo, 2020](#); [Pellegrina and Sotelo, 2021](#); [Pellegrina, 2022](#)). Importantly, most of these parametrize trade costs with an exponential format; e.g., $\log(\tau_{ij}) = \delta \times \text{dist}(i, j)$. Moreover, some use different distance metric – such as travel time. Hence, to compare my trade costs estimates to related studies, I use the functional formats and estimates from [Donaldson \(2018\)](#) and [Pellegrina \(2022\)](#) (for India and Brazil, respectively) to calculate and benchmark their resulting τ_{ij} to mine (i.e., with $\text{dist}(i, j)^{0.156}$). Figure B.3 Panel A documents their differences visually. It shows that, for small distances, my estimated τ_{ij} lie between Indian and Brazilian estimates. However, as distances increase, these estimates (exponentially) exceed mine. In fact, for extremely large distances (between, say, the North-South extremes of SSA), the resulting τ_{ij} becomes unreasonably large (which generates numerical problems, such as close-to-infinite prices in the economy). My functional format, instead, is tailored for continental empirical settings like mine, conveying reasonable values τ_{ij} for small (i.e., within country) distances that smoothly increase with (large) distances.

Migration costs. I analogously benchmark my estimated $m_{ij} = \text{dist}(i, j)^{0.47}$ to values from Indonesia, Brazil, and the US (from [Bryan and Morten, 2019](#); [Morten and](#)

⁷¹In particular, I quantify $\Omega_a/\Omega_K = 1/0.16 = 6.25$, while [Nath \(2022\)](#) estimates a relative agriculture and manufacturing shifters for the global economy of $11.73/3.7 = 3.2$.

Figure B.3: Equivalence between the quantified (trade and migration) frictions and related estimates from the literature.



Notes: Scatter plots of the estimated trade (Panel A) and migration (Panel B) costs from Section 5 against estimates from the literature.

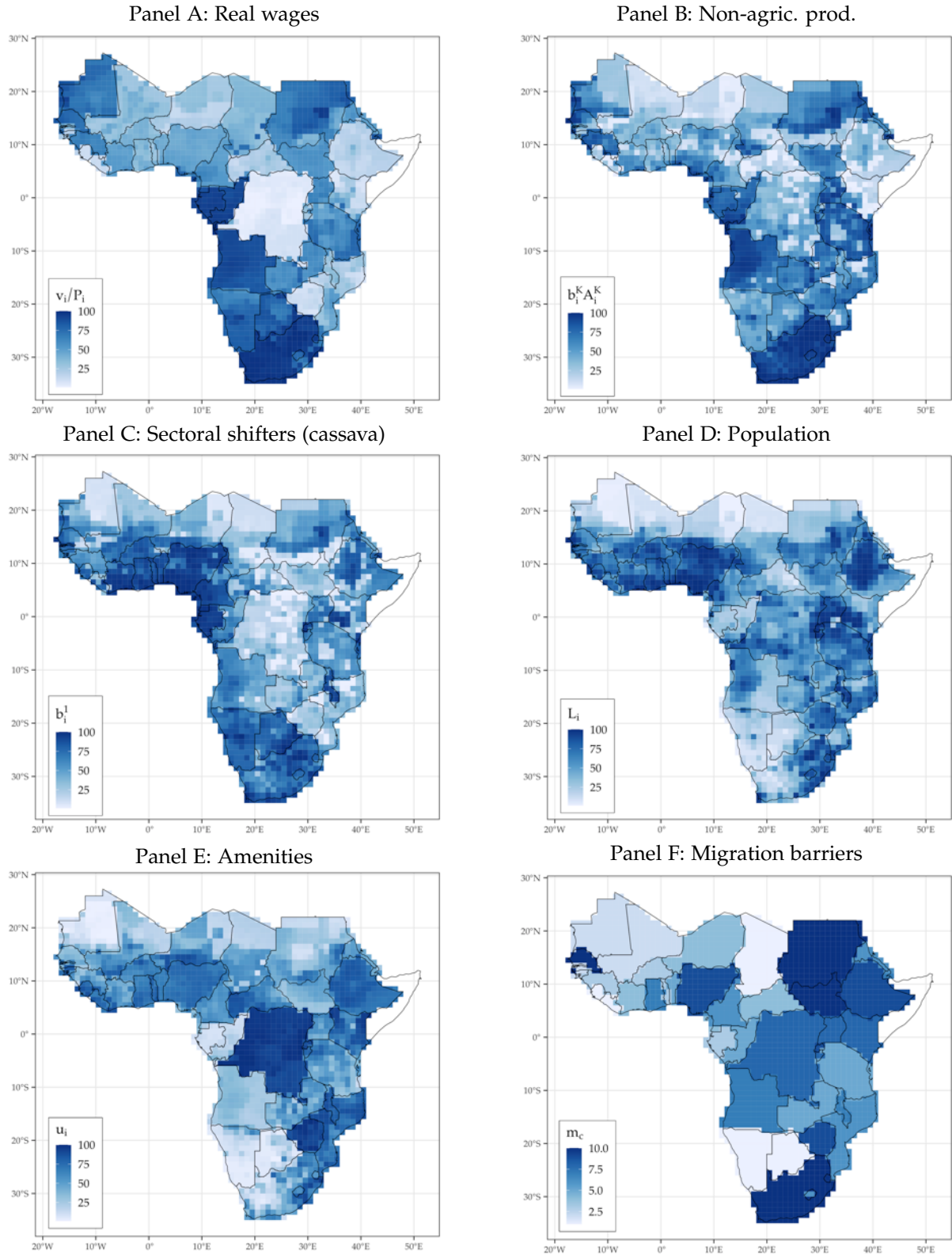
Oliveira, 2018; Allen and Donaldson, 2022, respectively). Figure B.3 Panel B shows the results: my median SSA estimates are about 20 percent larger than the median estimates for Indonesia, and about three to four times larger than those for Brazil and the US, respectively. Moreover, the (exponential) increase in the migration costs for larger distances is also visible, though not as pronounced as for trade costs (however, these patterns hold for continental distances between geographical extremes of SSA).

B.10 Discussion of the inversion results

Figure B.4 illustrates the spatial distribution of some of the quantified fundamentals. Panel A and B show that more productive locations (which have higher real wages) have higher fundamental productivities in the K^{th} sector. Thus, the model rationalizes that, net of the variation in the $K - 1$ sectors, locations with a high level of economic activity must be very productive in non-agriculture. This pattern stands out in some capitals and in high-GDP countries, such as South Africa. Panel C illustrates an analogous aspect of the quantified sectoral shifters of cassava. There are high $\{b_i^k\}_i$ values for locations in countries that are large cassava producers, such as Nigeria.

Moreover, Panel D and E show that high-amenity locations have relatively high population density and very low real wages. DR Congo and Zimbabwe are two examples. Their higher amenities are utility compensations that explain why individuals are not living somewhere else in SSA. Intuitively, this captures local cultural or

Figure B.4: Comparison between the calibrated fundamentals and the observed endogenous variables



Notes: Each panel plots the spatial distribution of the quantified fundamentals as explained in sections 5.3 and 5.4 in percentiles (or deciles for F), where 100 (or 10) stands top percentile.

institutional characteristics that work as pull factors (which will be kept constant in the counterfactuals).

However, these characteristics do not include migration frictions, since they are accounted for separately in my framework. To illustrate, Panel F plots the distribution of the quantified country-level migration barriers, i.e. $\{m_c\}_c$. High-barrier countries display two characteristics: higher income differentials relative to neighboring countries and relatively low inflows of migrants. Sudan and South Africa (which are geographically close to DR Congo and Zimbabwe, respectively) illustrate this. Their relative income differences (with respect to their surrounding countries) are disproportionately larger than the observed total flow of immigrants, which implies higher migration barriers.⁷²

B.11 Details on the backcasting exercise for 1975

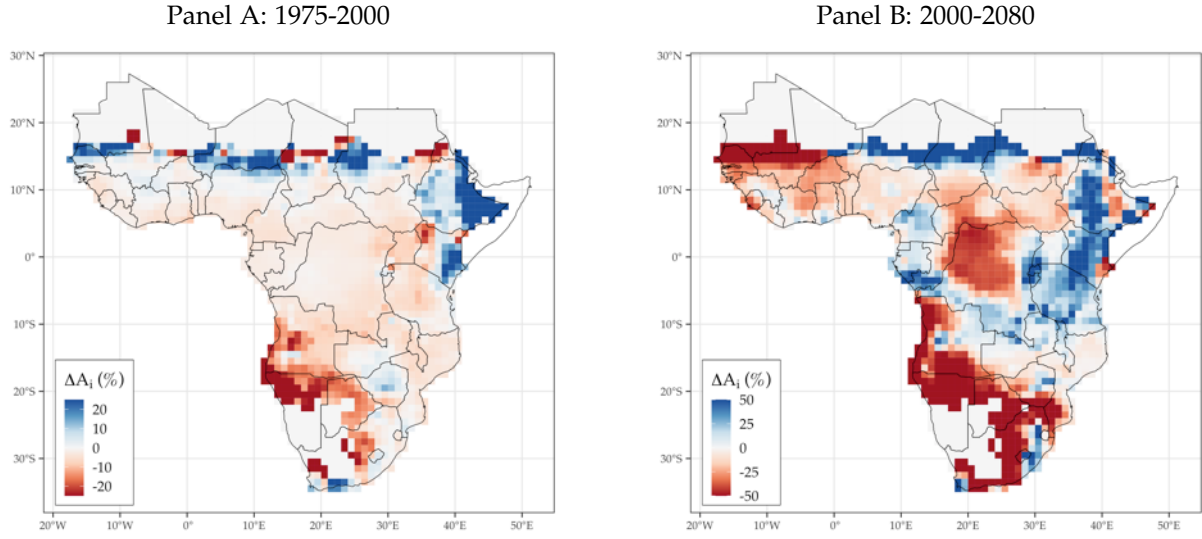
The backcasting exercise consists of solving for the spatial equilibrium of the SSA in 1975. In particular, it uses the calibrated model for 2000 and replaces two fundamentals that reflect the reality of the economy in 1975:

Population. I calculate and estimate of the initial population in 1975 by projecting the distribution of the observed population in 2000 into the levels of the SSA population in 1975. The reversibility of the spatial equilibrium follows [Desmet et al. \(2018\)](#), who characterize the possibility of backcasting exercises such as mine (i.e. validating spatial models calibrated in a cross section).

Crop yields. I replace the fundamental productivities $\{A_j^k\}_{k \neq K}$ used in the calibration with the values of 1975. Importantly, during the period there was already climate-driven changes in these productivities so that the model can generate climate migration (Figure B.5 illustrates that). Finally, the validating exercises consists of comparing the model outcomes with observed population data for 1975. Because the data source of the latter (GHSP, [Florczyk et al., 2019](#)) differs from the source of population data used in the calibration (G-Econ, [Nordhaus et al., 2006](#)), I check the consistency of these two datasets for the period of 2000 (for which data in both sources is available) in terms of grid cell- and country-level population correlation in Figure B.6.

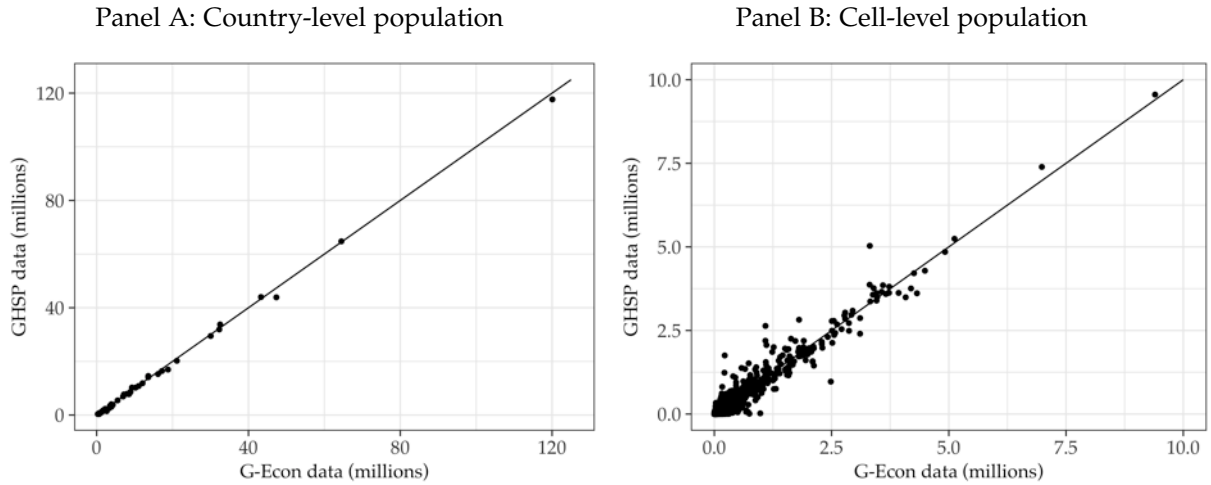
⁷²A second mechanism explaining the variation in country barriers is the absolute variation in migration flows. Countries with low migration flows, even if at the left of the real wage distribution, must have, at least to some extent, relatively high migration barriers. The reason for this is the idiosyncratic component of workers' preferences, which generates some migration that must somehow be rationalized.

Figure B.5: Percentual changes in average crop potential yields within locations in the past and estimates for the future



Notes: Panel A: Within grid cell changes (%) in crop suitabilities between 1975 and 2000. Panel B: Analogous changes between 2000 and 2080 (under climate change). Note that the scale between Panels A and B are different to facilitate visualization (they imply that the effects between 1975 and 2000 are much less pronounced than the expected future effects).

Figure B.6: Correlations between G–Econ and GHSP datasets for the year of 2000



Notes: Panel A (B): Country (grid cell)-level population counts in SSA from G-Econ and GHSP.

B.12 Details on the calibration with EU data

I take the model to EU data so to retrieve the levels of the tariffs and country barriers parameters τ_{ij}^F and $\{m_c\}_c$. To do that, I build a likewise rich spatial dataset for the EU. I use the same sources described in Section 2, as all of them have a global coverage. Subsequently, I link that data to my model with the procedure described in Section 5. Importantly, when doing so, I use the same preference parameters and elasticities to bilateral distance, δ and ϕ . Thus, my quantification for the EU embeds the differences between cross country trade (or migration) in EU and SSA in the policy parameters

τ_{ij}^F (or $\{m_c\}_c$).

Finally, when replacing the EU policy parameters into the SSA counterfactual, I must match the country level EU parameters $\{m_c\}_c$ to SSA countries. I do that by quantiles. That is, I assign the country barrier value for the bottom decile of the EU sample to the countries in the bottom decile of the SSA county barrier distribution, as so forth for the other deciles. Importantly, to make the levels of $\{m_c\}_c$ comparable across EU and SSA, I normalize the former as a ratio with the minimum. Thus, I in practice simply scale SSA's country barriers in relatives (e.g. the ratio between the least and most strict country) so to reflect the relative ratios of the EU barriers.

C Alternative models

C.1 Agriculture as a unique crop

The model with a unique crop is identical to the model of Section 4. However, by assuming a unique crop ($K = 2$), there is no substitution within agriculture, so that the middle CES tier vanishes (i.e. $\Xi_j^1 = 1$ and $P_j^a = P_j^1$ for all j). To take this model to the data, I model the unique crop as an aggregate of the 6 crops. In particular, the agricultural fundamental productivity $\{A_j^k\}_{k \neq K}$ is a cross-crop average of the within grid cell productivities (and likewise for the 2080 estimates). Moreover, the crop expenditures used in the baseline quantification are the sum of the single-crop case.

C.2 Extension with the rest of the World

I allow for trade and migration between SSA and the ROW by modeling the latter as a single, representative location R . As such, I use the same data sources and methods in Sections 2 and 5 to link this extended model to global data and perform counterfactuals as in Section 6, but assuming that the ROW is unaffected by the climate.^{73,74}

Assuming so facilitates remarkably the quantification of this extended setting. The reason is that it rules out the necessity of separating shifters $\{b_R^k\}_k$ and fundamental productivities $\{A_R^k\}_k$ for the ROW (as they will be all kept fixed in the counterfactuals). Hence, the quantification normalizes $b_R^k A_R^k = 1$ for all k and pins down $\{b_j^k\}_{j \neq R, k}$ in relative terms to the ROW. In terms of trade frictions, I assume $\text{dist}(i, R)$ as the distance to the nearest port and, for simplicity, $\delta = 0.156$ and $\tau_{iR}^F = \tau^F = 8.2$. For

⁷³In terms of data, the process is simple. For instance, land endowments (or population) for R are simply the sum of the land area (or population from G-Econ) in all locations but the SSA grid cells.

⁷⁴The reasoning behind this assumption is that, over the course of the decades until the end of the century, the ROW could be able to adapt to the agricultural productivity shocks from GAEZ such that, on average, its productivity would be unaffected.

migration costs, I also use the port distances and the quantified ϕ . However, to keep a consistent quantification of country migration barriers $\{m_c\}_c$, I aggregate all gross migration flows from SSA to the ROW to pin down m_R .⁷⁵

C.3 Homothetic preferences

I simulate the climate change effects in SSA with homothetic preferences by setting $\sigma = 4$ (as in Bernard et al., 2003) and $\epsilon_k = 1 - \sigma$ for all $k \in \{a, K\}$. As such, the income effect on Equation (13) cancels out and only relative sectoral prices matters for sectoral expenditures. That is, Equation (13) becomes isomorphic to (9). I link this model to the data with the same procedure as in Section 5 and, with the quantified model in hand, perform a counterfactual as in the baseline of Section 6.

C.4 Endogenous fertility

I endogenize fertility, with respect to climate change, with a simple damage function that assumes that the projected grid-cell-level initial population for 2080 is affected by the average change in local crop yields. Formally:

$$\hat{L}_j^0 = (\iota \times \Delta A_j) \times L_j^0,$$

where ΔA_j is the average crop yield change in j (as in Section 3) and ι a shifter that maps the latter into fertility changes. When doing so, the initial population of SSA \mathcal{L} reduces if compared to the baseline case. In particular, it decreases more in the locations and countries that are most affected by climate change. Thus, in distributional terms, the initial population of SSA starts slightly better distributed, which leads to lower climate migration flows. However, these level differences are not too strike; hence, the aggregate effects of climate change are not stark vis-à-vis the baseline. The fertility robustness results of Table 6 use \hat{L}_j^0 and $\iota = .5$ in the climate change simulations. As of completeness, Table C.1 below document how these results are sensitive to the choice of ι .

C.5 Economic growth

I account for economic growth in my simulations by scaling up the non-agricultural productivities $\{b_j^K A_j^K\}_j$ with country-level projections of GDP growth. For that, I first

⁷⁵The quantified $\{m_c\}_c$ with the ROW illustrates the degree of real income spatial disparities between SSA and the global economy. Specifically, the quantified m_R is thousands of times larger than the maximum of $\{m_c\}_{c \neq R}$, reflecting that, through the lens of the model, these barriers must be substantial to explain the observed migration choices conditional on real income differences.

Table C.1: Robustness of the endogenous fertility exercise with respect to ι

	(1)	(2)	(3)
	Climate migration (million individuals)	Δ GDP per capita (%)	Δ Non-agricultural employment (%)
Endogenous fertility $\iota = 0.1$	14.06	-0.07	-0.10
Endogenous fertility $\iota = 0.25$	13.98	-0.07	-0.10
Endogenous fertility $\iota = 0.5$	13.80	-0.08	-0.10

retrieve the GDP growth rates at the country level between 1980 and 2020 from the World Bank Development Indicators. Next, I calculate the country-level cumulative rate in this 40-years interval and use its square as the 80-years projected rate for each country. Figure C.1 Panel A shows the results. Most countries experience a two- to fourfold increase in productivity (and some up to a tenfold increase).

Importantly, Figure C.1 Panel B shows that the $\{b_j^K A_j^K\}_j$ distribution in the two cases barely changes. This is due to the large spatial level differences in the quantified $\{b_j^K A_j^K\}_j$, some in the order of millions.⁷⁶ Hence, even if accounting for tenfold growth in some countries, the $\{b_j^K A_j^K\}_j$ distribution, as well as the climate change simulation results in Section 6.4, remain little affected.

C.6 Climate damage on non-agriculture

I consider climate change productivity effects on non-agriculture by scaling $\{b_j^K A_j^K\}_j$ with a damage function that maps climate conditions to the latter. For that, I borrow the non-agricultural $g^K(T_j)$ damage function from Conte et al. (2021). It is a bell-shaped function, quantified at a global scale, that maps local temperature, in Celsius, into a shifter between zero and one. I collect temperatures by the early 2000s and estimates for the end of the century, also from Conte et al. (2021), to calculate a $\Delta g^K(T_j)$. I use the latter as the non-agriculture damage function that scales $\{b_j^K A_j^K\}_j$. Figure C.1 shows the result: there are large spatial differences in the expected changes in non-agricultural productivities (Panel C) but, for the same reason as in Appendix C.5, that does not affect drastically the relative productivities across space (Panel D) and, likewise, the climate change results.

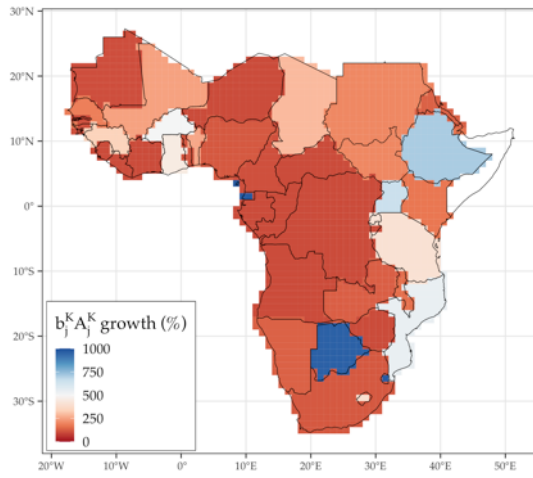
C.7 Climate damage on amenities

I allow for climate change impacts in life quality through a damage function that affects amenities $\{u_j\}_j$. For that, I borrow the amenity damage function $\Lambda^b(T_j)$ from

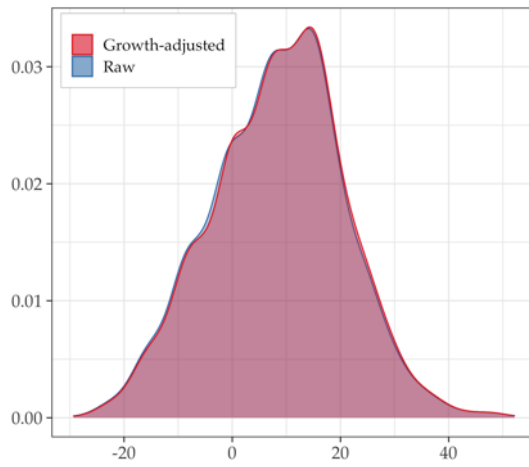
⁷⁶That is so due to the likewise large differences in real income per capita across SSA, that my quantification method (conditional on crop productivities and production) interprets as large differences in fundamental non-agricultural productivities $\{b_j^K A_j^K\}_j$.

Figure C.1: Changes in the fundamentals for robustness checks

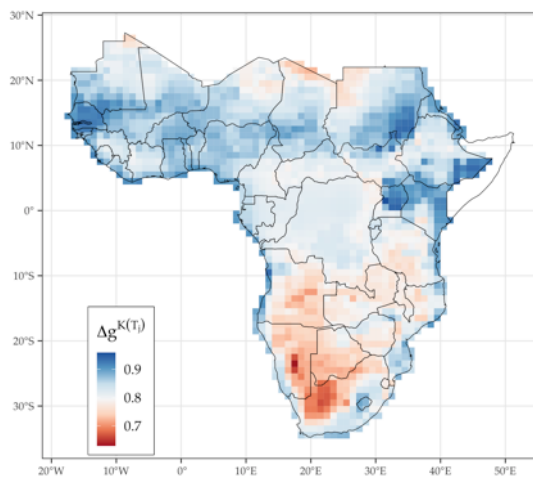
Panel A: Country-level GDP growth



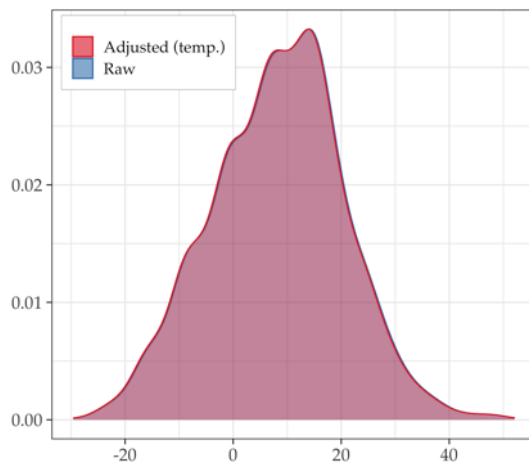
Panel B: $\log(b_j^K A_j^K)$ distribution, in logs



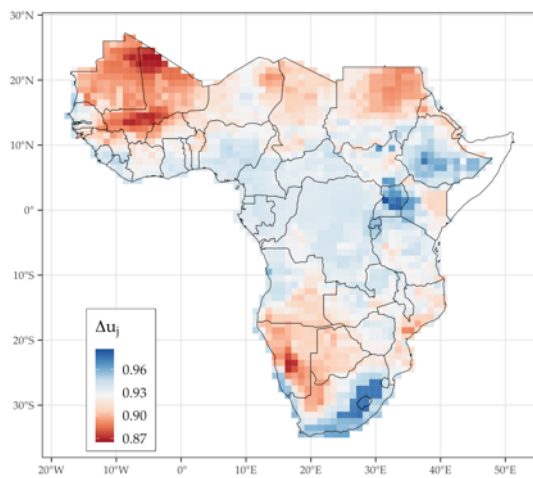
Panel C: Non-agric. damage function $\Delta g^K(T_i)$



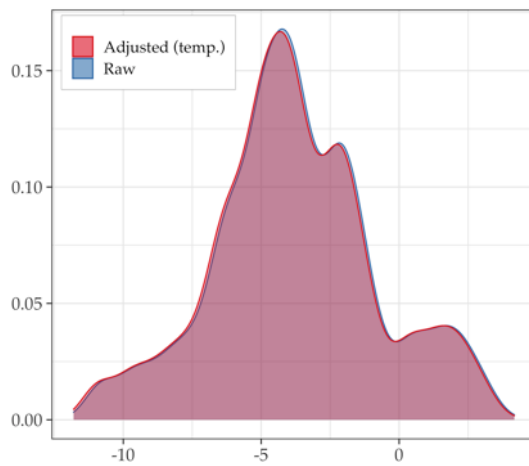
Panel D: $\log(b_j^K A_j^K)$ distribution, in logs



Panel E: Amenity damage function Δu_j



Panel F: $\log(u_j)$ distribution, in logs



Cruz and Rossi-Hansberg (2023). It provides a non-linear relationship between temperature changes and amenities, quantified for the global economy. I combined it with the expected temperature changes previously calculated (appendix C.6) to retrieve these changes, illustrated in Figure C.1 Panel F. Similarly to Appendices C.5 and C.6, that barely affects the distribution of amenities across SSA, and hence the result of the simulations in this setting.

D Additional results

D.1 Motivating facts: additional results and details

The following provides formal support for the Facts 2 and 3 of Section 3 on the correlations between potential crop yields and production, trade, and migration.

Country-level production. I investigate the relationship between country-level crop production and crop yields estimated with:

$$\log(\text{crop production}_i^k) = \alpha \times \log(A_i^k) + a_i + b^k + \varepsilon_i^k, \quad (\text{D.1})$$

where A_i^k is the country i average yields of crop k . Including country a_i and crop b^k fixed effects implies that the variation that identifies α , the parameter of interest, is at the country-crop level. Hence, a positive $\hat{\alpha}$ is evidence of specialization in production across countries, i.e., countries producing the crops that they are, on average, more suitable for, according to the GAEZ potential estimates. Table D.1 Column 1 shows that this is the case, as in Figure 3 Panel A: a 10 percent increase in average country-crop potential yields is associated with a 7 percent larger production of that crop.⁷⁷

Within-country specialization. Table D.1 Column 2 provides additional evidence of specialization in production, but within countries. That is, it shows the regression results of Equation (D.2) on grid cell-level crop production and potential yields. Important, this setting allows for country-crop fixed effects. As a consequence, the variation that identifies α is within-countries: grid cells producing the crops that they are more productive at vis-à-vis other locations within the same country. The results in Column 2 corroborate this hypothesis, with an estimated within country elasticity of production of about 4.5 percent.

⁷⁷Importantly, the effective production data is retrieved from national statistics (FAOSTAT). Hence, I exclude an eventual mechanical correlation between production and potential yields that could arise if building country-level production data by aggregating cell-level data from GAEZ.

Table D.1: Correlational results between potential crop yields (changes) and production, trade, and migration

	log(production ^k)		log(bilateral trade ^k _{cc'})			Internal mig _{ij}		International mig _{cc'}	
	(1)	(2)	(3)	(4)	(5)	(6)	(7)	(8)	(9)
log(potential yields ^k)	0.735** (0.339)	0.044** (0.019)							
log(relative yields ^k _{cc'})			0.433** (0.183)	0.300* (0.154)	0.317* (0.166)				
Δ relative yields (%)						1.859 (6.550)	2.562 (6.537)	3.664 (47.624)	6.151 (83.191)
Bilateral distance					-0.001*** (0.0001)		-0.012*** (0.004)		-0.805** (0.336)
Country FE	Yes	No	No	No	No	Yes	Yes	No	No
Crop FE	Yes	No	Yes	Yes	Yes	No	No	No	No
Country-crop FE	No	Yes	No	No	No	No	No	No	No
Origin-destination FE	No	No	Yes	No	No	No	No	No	No
Origin FE	No	No	No	Yes	Yes	No	No	No	No
Destination FE	No	No	No	Yes	Yes	No	No	Yes	Yes
Observations	194	8,136	352	352	352	4,913	4,913	324	324
R ²	0.521	0.876	0.840	0.538	0.589	0.361	0.367	0.074	0.236

Notes: *p<0.1; **p<0.05; ***p<0.01.

Bilateral crop trade. I verify the hypothesis of specialization in trade by estimating:

$$\log(X_{cc'}^k) = \alpha \times \log(A_c^k/A_{c'}^k) + a_{cc'} + b^k + \varepsilon_{cc'}^k, \quad (\text{D.2})$$

where $X_{cc'}^k$ is the bilateral crop k trade flows from country c to c' from the ITPD-E trade data by the early 21st century. Moreover, $A_c^k/A_{c'}^k$ are the exporter-importer relative crop k potential yields calculated from the GAEZ estimates in 2000. By introducing importer-exporter fixed effects, I absorb all fixed characteristics at this dimension – including bilateral trade resistance elements such as bilateral tariffs – and exploit variation at the country pair-crop level. The positive α (Table D.1 Column 3) implies that, conditional on a importer-exporter pair, a 10 percent increase in the relative (exporter over importer) average yields of a specific crop is associated with four percent higher exports of that crop. Consistent with Figure 3 Panel A, this elasticity is about 40 percent lower than the one of specialization of production (Column 1).

Subsequently, I use this framework to investigate the role of geographical distance as a bilateral trade resistance. Specifically, I replace the $a_{cc'}$ fixed effects with a set of separate importer and exporter fixed effects in Equation (D.2). The results (Table D.1 Column 4) are much less precise, but close to the former estimate in magnitude. I then add to this model (column 5) covariates at the importer-exporter level: bilateral distances (between capitals). The α estimate remains considerably stable, suggesting that non-tariffs trade barriers, such as distances, might not be as strict, as bilateral resistance between countries, if compared to tariffs.

Internal migration flows. I then verify whether changes in crop potential yields, over time, associate with observed internal migration flows. For that, I estimate

$$L_{ij} = \alpha \times \Delta \text{relative yields}_{ij} + a_{c(i,j)} + \text{population}_i + \varepsilon_{ij}, \quad (\text{D.3})$$

where L_{ij} is the total number of migrants between subnational region i to j observed in the IPUMS data (that is, from the early 1970s to early 2010s). Along the same lines, $\Delta \text{relative yields}_{ij}$ is the percentual change in the relative (destination over origin) average yields between 1975 and 2000 from GAEZ. Equation (D.3) also controls for population at origin and country fixed effects.⁷⁸

The results in Table D.1 Column 6 provide evidence of relative potential yields as a push factor of migration (i.e., $\hat{\alpha} > 0$). The point estimate has little power and small magnitude.⁷⁹ However, adding origin-destination bilateral distances as a covariate (Column 7) improves that and delivers an economically meaningful message. The $\hat{\alpha}$ estimate increases in magnitude by about 40 percent, suggesting that geographical distances are an important aspect underlying migration choices within countries. Moreover, the precisely estimated negative coefficient of distance aligns with the idea that internal migration becomes more costly for destinations that are further away.

International migration flows. I conclude with an analogous investigation for international migration with:

$$L_{cc'} = \alpha \times \Delta \text{relative yields}_{cc'} + a'_c + \text{population}_c + \varepsilon_{cc'}, \quad (\text{D.4})$$

where $L_{cc'}$ stand for thousands of migrants from country c to country c' . The results (Columns 8 and 9) convey a similar message: international migration in SSA did respond to changes in crop yields in the past decades, and more so for the countries that are geographically close by.

⁷⁸Ultimately, I control for population at origin by using migration flows per thousand inhabitants at origin in the regressions.

⁷⁹This is not surprising given the high urbanization rates experienced in SSA (which does not need to be necessarily driven by changes in relative yields at destination but rather other forces driving structural change).

D.2 Additional figures and tables

Table D.2: Share of grain crop production (in tonnes) over total production of the main staple and cash crops in SSA.

Grain crop	Share	Cash crop	Share
Cassava	56.65%	Coffee	1.13%
Maize	11.75%	Cotton	1.14%
Millet	4.59%	Groundnut	2.72%
Rice	2.18%	Palm oil	4.93%
Sorghum	6.15%	Soybean	0.33%
Wheat	1.13%	Sugarcane	7.31%
<i>Total:</i>	82.45%	<i>Total:</i>	17,55%

Source: GAEZ production data for 2000 aggregated in over all countries of my empirical setup. SSA includes all sub-Saharan African countries but Somalia.

Table D.3: Climate migration results for country capitals

Country	Capital	ΔL_i (K)	Country	Capital	ΔL_i (K)
Angola	Luanda	-77.31	Lesotho	Maseru	28.01
Burundi	Bujumbura	1,839.29	Mali	Bamako	68.85
Benin	Cotonou	15.74	Mozambique	Maputo	-229.99
Burkina Faso	Ouagadougou	27.09	Mauritania	Nouakchott	90.89
Botswana	Gaborone	-371.03	Malawi	Lilongwe	11.93
Central African Republic	Bangui	83.96	Namibia	Windhoek	289.60
Ivory Coast	Abidjan	50.70	Niger	Niamey	-2.02
Cameroon	Yaounde	38.32	Nigeria	Abuja	35.68
Congo (Kinshasa)	Kinshasa	573.44	Rwanda	Kigali	182.53
Congo (Brazzaville)	Pointe-Noire	218.07	Sudan	Khartoum	25.29
Djibouti	Djibouti	16.28	Senegal	Dakar	86.57
Eritrea	Asmara	9.32	Sierra Leone	Freetown	-70.91
Ethiopia	Addis Ababa	31.01	Swaziland	Mbabane	52.77
Gabon	Libreville	633.11	Chad	Ndjamena	-10.66
Ghana	Accra	20.50	Togo	Lome	46.51
Guinea	Conakry	-80.86	Tanzania	Dar es Salaam	-12.17
The Gambia	Banjul	98.73	Uganda	Kampala	37.28
Guinea Bissau	Bissau	17.78	South Africa	Johannesburg	163.78
Equatorial Guinea	Malabo	146.15	Zambia	Lusaka	-38.52
Kenya	Nairobi	-59.89	Zimbabwe	Harare	-4.74
Liberia	Monrovia	119.74			